

IMPROVING SELECTIVITY IN OLEFIN  
METATHESIS FOR SMALL MOLECULE  
SYNTHESIS AND MATERIALS  
APPLICATIONS

Thesis by

Jean Li

In Partial Fulfillment of the Requirements for the

Degree of

Doctor of Philosophy

CALIFORNIA INSTITUTE OF TECHNOLOGY

Pasadena, California

2012

(Defended July 25, 2011)

© 2012

Jean Li

All Rights Reserved

*aut viam inveniam aut faciam*

## ACKNOWLEDGEMENTS

My first thanks go to **Bob**, for guidance, mentorship and creating a workspace to cultivate creativity and independence. It is a true testament to his kindness, intelligence and work ethic that the Grubbs lab has not only produced many great scientists, but also, simply put, many great people. In fact, I am going to go ahead and thank the entire **Grubbs Clan**, including **Helen**, **Brendan**, **Katie** and **Barney** for being like a second family to us Grubbs Groupies.

Amongst those I have been fortunate to work alongside and get to know, I have to begin by highlighting **Erin Guidry** and **Jacob Berlin**, my first two mentors who got me hooked on this thing called olefin metathesis. Not only did they patiently teach me much of what I know now, they also welcomed me with open arms into the group and became great friends. **WWJ&ED** is still a motto that hangs over my hood. After all, **Erin** was my SURF mentor for the summer of 2005, arguably my most productive summer in the Grubbs group! And **Jacob** patiently taught me how to use the glovebox, how to make my first catalyst, how to hit a baseball and how to stay up all night in Vegas. All skills I have put to good use in the last five years.

As long as we are talking about people who inspired me in my early days, I also have to thank **Silas Cook**, **John Hendrix**, **Eric McArthur**, **Marcos Arribas-Layton**, **BJ Wright** and **Jeremiah Johnson** for putting up with “that loud Asian undergrad.”

While working downstairs in 119 Church, a very unique setting, I was also able to garner guidance from a bevy of experienced postdoctoral students, including **Ian Stewart**, **Daryl Allen**, **Patricio Romero** and **Anna Wenzel**, who have all gone on to make their own mark on the world of chemistry. As postdocs leave in the blink of an eye (you cannot get too attached, they are like goldfish in their tenure in the Grubbs group), I chose to move upstairs, to spend more time with the new young set, forming our very own “Brain Trust” with my enantiomer, **Chris Daeffler** (remember the possum?), my new Texan baymate **Gumby** (ooops, I mean **Keith Keitz**), and his diastereomer, **Matthew Van Wingerden**. Late night Jack-in-the-Box trips, milkshake taste tests, polymerizing bugs and planning our Grubbs Group Attack-Downhill-Ski-Paintball Team – all things that show off our Brain-Trust Brilliance. And yes, we executed that paintball thing quite nicely.

Notables that came and went and dispensed some valuable advice along the way include **AJ Boydston** and his science brood, **Kayla** and **Jack Jack**, **Vlad Iluc** and our many photo-trips, **Paul Clark** (**Paul** gets special thanks for answering my panicked “how do I get a job,” “how do I write proposals” and “how do I write a thesis” emails in the past couple months!), **John “Beef” Matson** (eight hugs a day keeps the clinical depression at bay!), **Andy Hejl** (drafting fruit! drafting chemists! drafting anything!), **Donde Anderson**, **Kevin Kuhn**, and **Yan Xia** (let’s hang out in the motherland again). In the last couple months I have been fortunate enough to work closely with **Jeremiah Johnson** (Vegas! Pedicures! Say hi to Mark for me!), **Rose Conrad**, and **Alan Burts** (GPC! GPC! GPC!) who have patiently taught me about polymer chemistry. **JJ** gets special thanks for reading

through and discussing all my proposals, papers and this thesis; without him I probably would not be graduating!

Hopefully I was able to “pay it forward” and teach a thing or two to my undergrads, **Ray Weitekamp** and **Sam Elder**. I know I certainly learned a lot from them, ranging from inventing column templates to how to fix a roof leak with a bucket, a funnel and some tubing (and Beef’s bike helmet). They were certainly both fun to work with and I know you two are going on to your own greatness!

Speaking of new kids, now there is a brand new gang to carry on the legacy of the Grubbs Group, the Softball Team (Go Imperial Palace!), and the late night milkshake runs, including **Ray, Renee Thomas, Myles Herbert, Benjamin Sveinbjornsson, Zach Wickens, and Brendan Quigley**. It looks like some new traditions are getting started as I am packing up to leave and I will surely miss Tuesday Night Poker! Oh, I probably should have said this sooner, but the following people were forced into slogging through multiple rounds of edits for this thesis and/or frantic pleas for help with Word/Chemdraw/Excel: **Josh Palmer, Alexey Federov, Pinky Patel, Jeremiah Johnson, Keith Keitz, Matthew Van Wingerden, Chris Daeffler, Myles Herbert, Zach Wickens, Brendan Quigley and Ben Sveinbjornsson**. I was told this is unusual or does not happen in many other groups, so I guess I got pretty lucky with the Grubbs Group!

Since mentors come in all shapes and sizes, I want to also thank **Sabina Weber** and **Cybelle Greenman** for teaching me strength, peace and keeping an open heart (and for keeping me sane).

When I was looking for an escape from the second floor of Church, I was lucky enough to have **Bonnie Gurry** (where are your keys??), **Mike Krout**, **JT Mohr**, **Angela Blum**, **Erin Lamb** (Pool dates and bike shopping dates), **Young In Oh** (Pho-Phora Dates), **Narae Park** (hikes, bikes and dinner and a movie), **Chithra Krishnamurthy** (yogadates), **Jessica Pfeilsticker** (too many costume parties to even count Jess-bunny), **Lexi Gounalis** (VEGAS!) and **Kiki Zheng** to call upon and talk about, well, anything that was not olefin metathesis! **Mike** gets a special shoutout for being an inspiration; I do not know anyone who holds themselves to a higher standard as a chemist and a friend. Particular gratitude also goes to **Christian Sjulsen** for being my BFF, and a beacon and a escape in WeHo for the better part of two years. Break out the Veuve, I am finally coming home!

Going back in time, I have to thank **Alec Durrell** (remember the possum?) and **Dan Bower** for being great roommates and embarking on more than one culinary adventure with me. My newest roommate, **G**, prefers not to get his paws dirty.

I want to thank my thesis committee members for all their excellent advice and for reading through all the proposals and thesis chapters I have generated, my chair, **Dave Tirrell**, along with **John Bercaw** and my newest member, **Brian Stoltz**. I have to say, most of the chemistry in this thesis could not have been accomplished without the talented help of **David Vandervelde**, **Mona Shahgholi**, **Scott Virgil**, **Rick Gerhart**, **Larry Henling**, **Joe Drew** and **Linda Syme**. I have to embarrass Larry for a moment here and remind him that every single crystal I have ever brought him has been on the “poor side of average” but that said, Larry certainly went out of his way to help me with everything I had to do that is X-

ray related, even patiently teaching me the rudiments of Diamond 3 not once, but twice. He exemplifies the fact that the true heart of this department lies with those that go above and beyond, to teach and to engender the educational process. I have always been impressed by the people here at Caltech who not only do their job, but do it really freaking well, and with a smile.

I now also have to thank **Ryan Zeidan** and **Amy Greenwood**, two Caltech Alums, without whom I would not have an amazing job to start in the fall. Let us not forget **Rishi Kant**, **Andy Lin**, **Cathal McCarthy** and **Halvar Trodahl** for, well, general awesomeness. Onward, and upward, kiddos.

Finally, last, but certainly not least, I have to thank my family, **my mom** and **my dad**, who have dealt with more than one long, confusing rant about enantioselectivity over cross-country phone calls, and patiently reminded me that yes, life will go on, even if it is not  $C_2$ -symmetric. Thanks for always supporting me; I get the feeling the adventure is just beginning.

## ABSTRACT

The olefin metathesis reaction has been studied extensively from the perspective of catalyst design and synthesis, as well as from that of reaction control and application in a variety of fields. Beginning with the design of enantioselective catalysts based on the “geared”  $C_2$ -symmetric *N*-heterocyclic carbene (NHC) containing ruthenium catalysts, architectural modifications were envisioned and implemented in order to control the *N*-bound arene tilt angle (Chapter 2). From there, the asymmetric class of olefin metathesis reactions were explored and trends in enantioselectivities were obtained and reapplied in the further design of novel, chiral catalysts. These asymmetric catalysts were developed not only for their useful application in a range of asymmetric metathesis reactions, but also to provide insight into the spatial arrangement of the NHC ligand during the catalytic cycle.

Amidst this overall cyclical process, mechanistic understandings of the ruthenium-based olefin metathesis catalysts were garnered and integrated; and the concept of a covalently-linked NHC ligand was born. In Chapter 3, both the *cis*-fused and *trans*-fused versions of this linked NHC were constructed, with each independent synthesis hinging on a key ring-closing metathesis reaction mediated by ruthenium catalysts. These novel NHCs were then translated into rhodium-bound complexes and their unique structural conformations were studied with X-Ray crystallography.

Chapter 4 explores the forefront of control and selectivity in olefin metathesis, specifically, in the selective reactivity of dienes in cross-metathesis reactions. The desire to synthesize



conjugated dienes, thus limiting reactivity to one of two potentially reactive olefins, is both mechanistically intriguing and contains practical applications for the synthesis of linear pheromone natural products. These pheromones show great utility as a green, biorational pesticide with few ecological and biological side-effects. Thus, exploration of the general diene cross-metathesis reaction was focused on the actual synthesis of codlemone, one of the world's most sought-after insecticides.

The potential of the olefin metathesis reaction for biomedical applications was further explored in the application of peptide-containing polynorbornenes formed from ring-opening metathesis polymerization (ROMP). In order to apply synthetic materials made from ROMP in biological applications, a route towards ruthenium removal to the FDA-approved levels of 10 parts per million (ppm) was developed. Once low ppm remnant ruthenium content was obtained, the synthesis of varying monomers for crosslinking to bulk materials was explored.

## TABLE OF CONTENTS

Acknowledgements .....	iii
Abstract.....	vii
Table of Contents .....	ix
List of Figures.....	xi
List of Tables .....	xiii
List of Schemes .....	xiv
List of Abbreviations.....	xvi
Chapter I: Introduction to Olefin Metathesis.....	1
Historical Perspective on Olefin Metathesis.....	2
Olefin Metathesis Reactions .....	4
Ruthenium Olefin Metathesis Catalysts .....	5
Future Outlook and Prospectus.....	6
References and Notes.....	8
Chapter II: Asymmetric Olefin Metathesis Catalysts.....	11
Introduction .....	12
Halogenated Chiral Catalyst .....	17
Backbone Modified Chiral Catalysts.....	22
Conclusions .....	28
Experimental Methods .....	29
References and Notes.....	41

Chapter III: Fused <i>N</i> -Heterocyclic Carbenes.....	44
Introduction .....	45
Synthesis of Fused NHCs .....	47
Synthesis of Rhodium Complexes.....	49
Conclusions .....	54
Experimental Methods .....	55
References and Notes.....	63
Chapter IV: Selective Diene Metathesis .....	65
Introduction .....	66
Model System for Diene Selectivity.....	69
Applications in Pheromone Synthesis .....	76
Conclusions .....	77
Experimental Methods .....	78
References and Notes.....	81
Chapter V: RGD Polymers and Ruthenium Removal.....	83
Introduction .....	84
Ruthenium Removal in Polynorbornenes.....	86
Novel Thiol-Monomers for Hydrogel Formation .....	92
Conclusions .....	97
Experimental Methods .....	98
References and Notes.....	104
Appendix A: Bimetallic Ruthenium Fischer-Carbene Complexes .....	107

Introduction .....	108
Crystal Structure of Bimetallic Ruthenium Species.....	111
Conclusions .....	115
Appendix B: Crystallographic Data.....	119

## LIST OF FIGURES

**Chapter 1**

Figure 1.1. Mechanism of Olefin Metathesis by Chauvin.....	3
Figure 1.2. Early and Late Transition Metal Catalysts.....	3
Figure 1.3. Classifications of Olefin Metathesis Reactions.....	4
Figure 1.4. Progression of Ruthenium-Based Olefin Metathesis Catalysts.....	5

**Chapter 2**

Figure 2.1. Commercially Available Ruthenium Catalysts.....	12
Figure 2.2. Chiral Ru-Based and Mo-Based Olefin Metathesis Catalysts.....	13
Figure 2.3. “Gearing” Motif for Chiral Ruthenium Catalysts.....	14
Figure 2.4. Transition State for Origin of Enantioselectivity in ARCM.....	15
Figure 2.5. Structural Modifications for Increasing Arene Tilt Angle.....	16
Figure 2.6. Novel Chiral Ruthenium Olefin Metathesis Catalysts.....	17
Figure 2.7. Tetrahalogenated Achiral Ruthenium Catalysts .....	18
Figure 2.8. Preferred Geometry of Various NHC Catalysts.....	18
Figure 2.9. Kinetics for Ring-Closing of DEDAM .....	20
Figure 2.10. Competing Mode of Olefin Binding .....	25
Figure 2.11. Crystal Structure of Catalyst 2.14 .....	27

**Chapter 3**

Figure 3.1. NHCs Utilized in Metal-Mediated Catalysis .....	45
Figure 3.2. Design of Rotationally Locked NHCs .....	46

Figure 3.3. ORTEP Diagram of 3.17 with 50% Probability Ellipsoids .....	50
Figure 3.4. ORTEP Diagram of 3.18 with 50% Probability Ellipsoids .....	52
Figure 3.5. Side-View of Structures 3.17 and 3.18 .....	54

## **Chapter 4**

Figure 4.1. Selectivity in Diene Cross-Metathesis .....	66
Figure 4.2. Electronic Manipulation of Diene Selectivity in CM .....	67
Figure 4.3. Substrates Screened for Electronic and Steric Deactivation.....	67
Figure 4.4. Known Insect Pheromones .....	68
Figure 4.5. Desired Reaction Pathway.....	70
Figure 4.6. Undesired Reaction Pathway.....	70
Figure 4.7. Formation of Desired Diene at Room Temperature .....	72
Figure 4.8. Formation of Undesired Olefin at Room Temperature.....	73
Figure 4.9. Formation of Desired Diene at 40 °C .....	74
Figure 4.10. Formation of Undesired Olefin at 40 °C .....	74

## **Chapter 5**

Figure 5.1. Polynorbornenes Containing Peptidic Side Chains .....	84
Figure 5.2. Cell Adhesion and Cell Survival.....	85
Figure 5.3. Schematic for Desired RGD-Polymer.....	86
Figure 5.4. Remnant Ruthenium Content At 70 °C and 23 °C.....	90
Figure 5.5. Polymer Samples Without Versus With Ruthenium Removal.....	90
Figure 5.6. Remnant Ruthenium Content at 70 °C for 20:1 Ratio .....	91
Figure 5.7. Remnant Ruthenium Content at 70 °C with TBP .....	92

Figure 5.8. Uncontrolled Crosslinking of Polymer 5.11 .....	94
---	----

Figure 5.9. Attempted Crosslinkers for Free Thiol.....	95
--	----

## **Appendix A**

Figure A.1. Commercially Available Ruthenium Catalysts .....	108
--	-----

Figure A.2. Phosphonium Alkylidene and Potential Intermediates .....	109
--	-----

Figure A.3. Crystal Structure of Bimetallic Species A.11.....	112
---	-----

Figure A.4. Trimetallic Ruthenium Complex.....	113
--	-----

Figure A.4. Crystal Structure of Trimetallic Species A.12 .....	114
---	-----

## LIST OF TABLES

**Chapter 2**

Table 2.1. ARCM Reactions with Chlorinated Chiral Catalysts.....21

Table 2.2. AROCM Reactions with Chlorinated Chiral Catalysts.....22

Table 2.3. ARCM Reactions with Backbone Modified Chiral Catalysts .....24

Table 2.4. AROCM Reactions with Backbone Modified Chiral Catalysts .....26

**Chapter 3**Table 3.1. Selected Bond Lengths [ $\text{\AA}$ ] and Angles [ $^{\circ}$ ] for 3.17 .....51Table 3.2. Selected Bond Lengths [ $\text{\AA}$ ] and Angles [ $^{\circ}$ ] for 3.18 .....53**Chapter 3**

Table 4.1. Initial Screening Conditions for Model System.....71

Table 4.2. Selectivity of Desired Diene Over Undesired Olefin.....75

**Appendix A**Table A.1. Selected Bond Lengths [ $\text{\AA}$ ] and Angles [ $^{\circ}$ ] for A.11 .....112



## LIST OF SCHEMES

**Chapter 2**

Scheme 2.1. Representative Asymmetric Olefin Metathesis Reactions .....	13
Scheme 2.2. Synthesis of Chlorinated Catalyst.....	19
Scheme 2.3. Ring-Closing of DEDAM .....	20
Scheme 2.4. Synthesis of Enantiopure Diamines 2.35a and 2.35b .....	23
Scheme 2.5. Synthesis of Backbone Functionalized Chiral Catalysts .....	23

**Chapter 3**

Scheme 3.1. Synthesis of <i>Cis</i> -Carbene Precursor 11.....	47
Scheme 3.2. Synthesis of <i>Trans</i> -Carbene Precursor 16.....	48
Scheme 3.3. Synthesis of Rhodium Complexes.....	49

**Chapter 4**

Scheme 4.1. Attempts at Pheromone Synthesis.....	76
Scheme 4.2. Further Attempts at Pheromone Synthesis.....	76

**Chapter 5**

Scheme 5.1. Initial Polymer Designed for Hydrogel Formation.....	88
Scheme 5.2. Synthesis of Monomer 5.1 .....	88
Scheme 5.3. Synthesis of Monomers 5.2 and 5.3.....	89
Scheme 5.4. Polymer with Protected Thiol Monomer for Crosslinking .....	93
Scheme 5.5. Synthesis of Protected Cysteine Monomer.....	95
Scheme 5.6. Synthesis of NBz-Protected Cysteine Monomer 5.18.....	96

Scheme 5.7. Incorporation of NBz-Cysteine Monomer into Polymer 5.19.....	96
--	----

## **Appendix A**

Scheme A.1. Initial Steps of Olefin Metathesis Mechanism.....	108
---	-----

Scheme A.2. Initiation Study with Butyl Vinyl Ether.....	110
--	-----

Scheme A.3. Addition of Ethyl Vinyl Ether to A.9.....	110
---	-----

Scheme A.4. Addition of Ethyl Vinyl Ether to A.2b.....	111
--	-----

Scheme A.5. Attempts at Bimetallic Crystallization of A.13 and A.15.....	115
--	-----

## List of abbreviations

<b>ADMET</b>	acyclic diene metathesis
<b>Boc</b>	<i>tert</i> -butyl carbamate
<b>br</b>	broad
<b>CM</b>	cross-metathesis
<b>COD</b>	1,5-cyclooctadiene
<b>DMAP</b>	4-(N,N-dimethylamino)pyridine
<b>DMSO</b>	dimethylsulfoxide
<b>e.e.</b>	enantiomeric excess
<b>EDC</b>	1-ethyl-3-(3-dimethylaminopropyl)carbodiimide
<b>EtOAc</b>	ethyl acetate
<b>FAB</b>	fast atom bombardment
<b>GC</b>	gas chromatography
<b>GPC</b>	gel permeation chromatography
<b>HPLC</b>	high pressure liquid chromatography

<b>HRMS</b>	high resolution-mass spectrometry	xx
<b>Mn</b>	number average molecular weight	
<b>MsCl</b>	methanesulfonyl chloride	
<b>NBz</b>	nitrobenzyl	
<b>NHC</b>	<i>N</i> -Heterocyclic carbene	
<b>NMR</b>	Nuclear Magnetic Resonance	
<b>ORTEP</b>	Oak Ridge Thermal Ellipsoid Plot	
<b>PCy<sub>3</sub></b>	tricyclohexylphosphine	
<b>PDI</b>	polydispersity index	
<b>PPh<sub>3</sub></b>	triphenylphosphine	
<b>ppm</b>	parts per million	
<b>RCM</b>	ring-closing metathesis	
<b>REMP</b>	ring-expansion metathesis polymerization	
<b>ROMP</b>	ring-opening metathesis polymerization	
<b>r.b.</b>	round-bottom	

**r.t.**

room temperature

**TBP**tris(*n*-butyl)phosphine**TFA**

trifluoroacetic acid

**THF**

tetrahydrofuran

**THMP**

tris(hydroxymethyl)phosphine

*Chapter 1*

## INTRODUCTION TO OLEFIN METATHESIS

## HISTORICAL PERSPECTIVE ON OLEFIN METATHESIS

From bulletproof vests to insect pheromones, the introduction of olefin metathesis into the lexicon of synthetic organic transformations has transformed the utility of organic chemistry in a global society. The olefin metathesis reaction mediates the scission and rearrangement of carbon–carbon double bonds and has engendered much development in biomedical applications, materials applications, and industrial applications. Wherever a C–C double bond can be found, olefin metathesis has effected change.<sup>1</sup> Only in the past decades has the true power of this seemingly trivial reaction been realized. However, one cannot discuss the forefront of metathesis research without first understanding its development.

In the burgeoning days of organometallic chemistry, metathesis was a phenomenon observed when olefin feed stocks were passed over ill-defined mixtures of metal coordination complexes such as  $\text{Mo(CO)}_6/\text{alumina}$ ,  $\text{WCl}_6/\text{Bu}_4\text{Sn}$ ,  $\text{MoO}_3/\text{SiO}_2$  and  $\text{WOCl}_4/\text{EtAlCl}_2$ .<sup>2</sup> Industrially, the process was of great interest and was considered as commercially relevant as the Shell Higher Olefin Process (SHOP). Early players such as The Goodyear Tire and Rubber Company and Dow Chemical Corporation reported the disproportionation of 2-pentene to mixtures of higher- and lower- order olefins, eventually terming the observed phenomenon “olefin metathesis” in 1967.<sup>2</sup> By then, increased industrial interest in the process had led several academic chemists to investigate the reaction and posit theories about the reaction mechanism.<sup>3-6</sup>

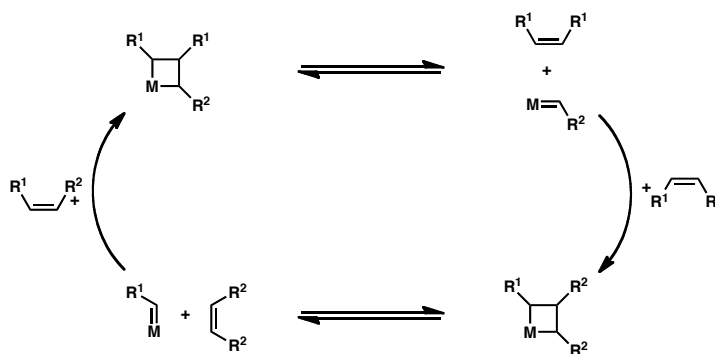


Figure 1.1. Mechanism of Olefin Metathesis By Chauvin.<sup>4</sup>

It was not until Chauvin's seminal mechanistic postulation in 1971, envisioning a metallacyclobutane intermediate, that the true nature of olefin metathesis was unraveled (figure 1.1).<sup>4</sup> Understanding that metal alkylidenes played a crucial role in the reaction mechanism opened the door for progress in catalyst design. Elucidation of a reaction's mechanism often informs the development of more efficient catalysts; reports of well-defined early and late transition metal alkylidenes as metathesis catalysts began to appear in the literature, once the scientific community accepted and confirmed Chauvin's mechanism (figure 1.2).<sup>7,8</sup> Unlike the mixtures used in industry, the molybdenum, tungsten and ruthenium catalysts did not require nearly as harsh conditions or high temperatures.

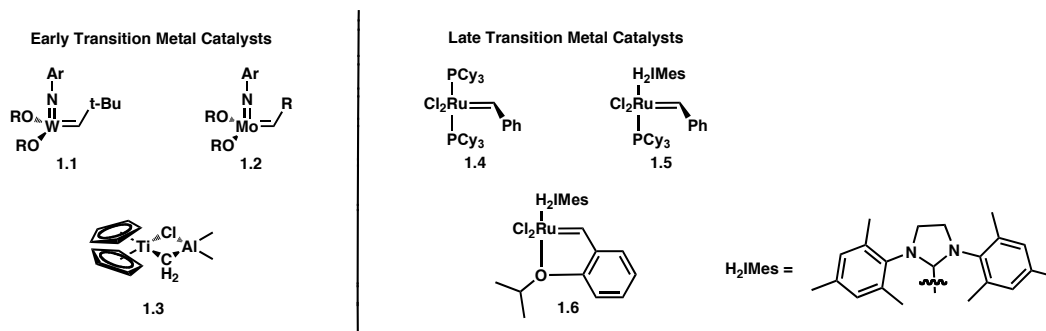
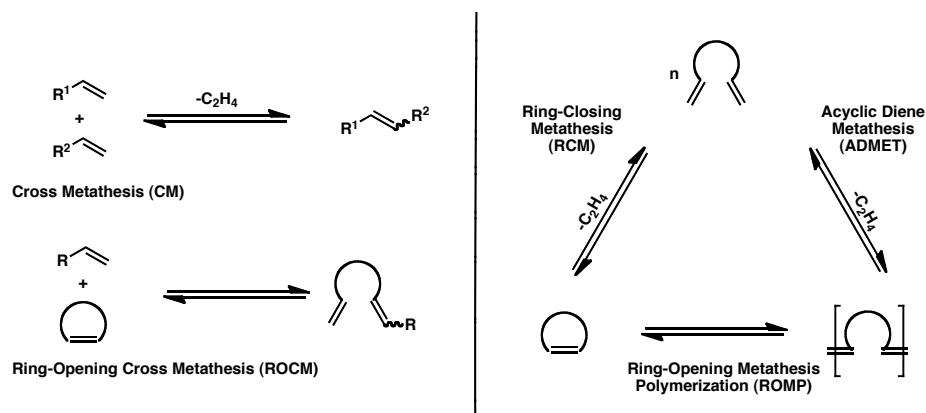


Figure 1.2. Early and Late Transition Metal Catalysts.<sup>7,8</sup>



## OLEFIN METATHESIS REACTIONS

With the advent of well-defined catalysts, olefin metathesis transcended its strictly limited applicability; research began categorizing the differing ways olefin metathesis could be conducted to give various desirable products (figure 1.3).<sup>9</sup>



**Figure 1.3. Classifications of Olefin Metathesis Reactions.**<sup>9</sup>

Intermolecular reactions such as cross metathesis (CM) and ring-opening cross metathesis (ROCM) yield valuable and novel olefins. Diene-containing reactions such as acyclic diene metathesis (ADMET), ring-closing metathesis (RCM) and ring-opening metathesis polymerization (ROMP) allow for the facile interconversion of individual dienes to cyclic structures and olefin-containing polymers.<sup>10</sup> The aforementioned reactions operate under thermodynamic control, requiring a driving force such as concomitant release of a small molecule like ethylene, or the release of ring strain in ROMP. In order to produce even more new and value-added product olefins in high selectivity and controlled conditions, the development of novel catalysts has been extensively investigated.

## RUTHENIUM OLEFIN METATHESIS CATALYSTS

During the course of developing olefin metathesis catalysts, the ruthenium-based catalysts have, in particular, stood out in terms of stability and functional-group tolerance.<sup>10a</sup> Moreover, recent advances in ligand design based on mechanistic discoveries providing a textured understanding of the catalyst have engendered new levels of selectivity and efficiency.<sup>11</sup> Shown in figure 1.4 is a historical progression of ruthenium-based catalysts: the newest catalysts showing great promise in specific applications such as tetrasubstituted cross-metathesis (catalysts **1.11** and **1.12**), the asymmetric variants of ring-closing and ring-opening metathesis (catalyst **1.9**), the formation of cyclic polymers (catalyst **1.10**) and Z-selective metathesis (catalyst **1.13**).<sup>8,12</sup>

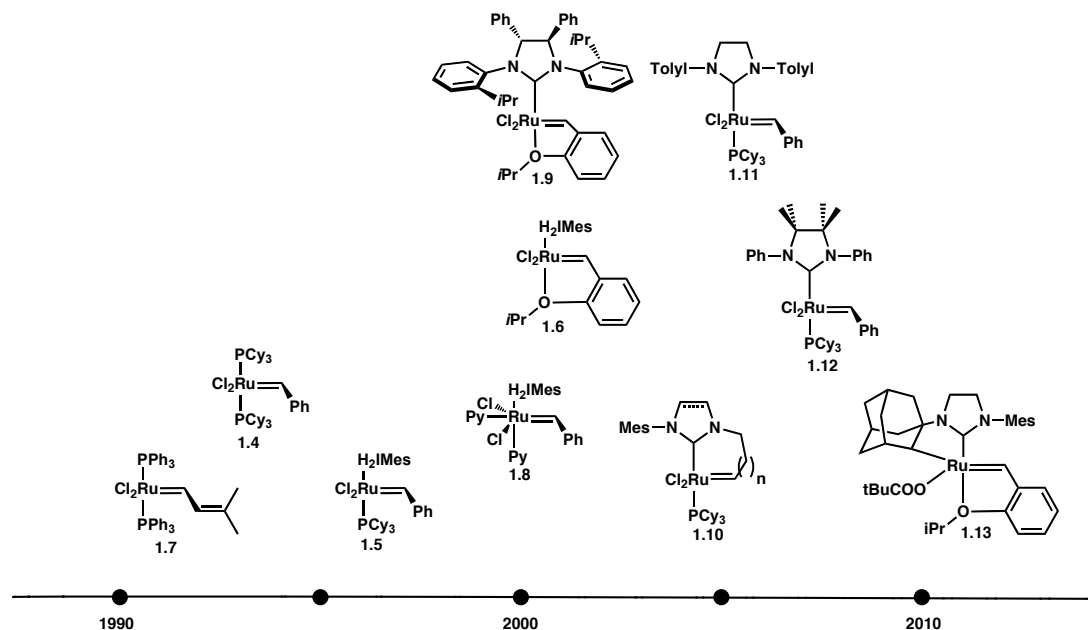


Figure 1.4. Progression of Ruthenium-Based Olefin Metathesis Catalysts.<sup>8,12</sup>

All of the ruthenium-based catalysts are designed about a core architectural motif, with a parent catalyst of structure  $X_2L_2Ru=CHR$ . The first stable, well-defined ruthenium alkylidene, **1.7**, was synthesized and isolated by Nguyen in 1992.<sup>8a</sup> Shortly

afterwards, what is generally considered Grubbs first generation catalyst (G1) was developed, replacing the triphenylphosphine ligands with tricyclohexylphosphine and the vinyl alkylidene with a benzyldiene to give catalyst **1.4**.<sup>8b</sup>

It was the discovery of catalyst **1.5** in 1999 that propelled the ruthenium-based catalyst into the limelight, and into the hands of most synthetic organic chemists.<sup>8d</sup> This complex, known as Grubbs second generation (G2), incorporated a novel *N*-heterocyclic carbene (NHC) ligand, which has since become a general ligand of great focus in the organometallic community. The activity of catalyst **1.5** was shown to rival early transition metal catalysts, which, though highly active, are not as air or water stable as ruthenium-based complexes. Moreover, the unique structure and low lability of the NHC ligand has allowed for multiple points of modification and functionalization, as illustrated by the many novel catalysts based on its structure that have been developed since.<sup>12</sup>

Other notable historical developments include the introduction of Hoveyda's chelating isopropoxybenzyldiene in catalyst **1.6** (G2-Hov), which has allowed for even superior stability, and the design of the fast initiating bipyridine catalyst **1.8**, which has greatly benefited polymer synthesis in materials applications.<sup>8e,12a</sup>

## FUTURE OUTLOOK AND PROSPECTUS

Although much progress has been made in understanding the subtle aspects driving the olefin metathesis reaction, there are still many problems left unsolved. In order to tackle the moving target of control in a reaction as complex as olefin metathesis, further exploration of reaction intermediates and mechanism must be undertaken. Questions such as what influences the geometry of olefin association and subsequent

metallacyclobutane formation must be addressed in order to build improved stereoselective catalysts.<sup>13</sup> Better understanding of the resting state of the catalyst, as well as the propagating species, could allow for the elucidation of degenerate metathesis as well as the general metathesis mechanism.<sup>14</sup> And finally, analyzing the modes of decomposition for ruthenium-based catalysts in a variety of circumstances could expand the materials applications of ROMP and ring-expansion metathesis polymerization (REMP), especially for promising biomedical applications.<sup>15</sup>

## REFERENCES AND NOTES

- (1) (a) Grubbs, R. H. *Handbook of Metathesis*; Germany, Wiley-VCH: Weinheim, **2003** and references cited therein. (b) Ivin, K. J.; Mol, J. C. *Olefin Metathesis and Metathesis Polymerization*; Academic Press: San Diego, CA. **1997** and references cited therein. (c) Noels, A. F.; Demonceau, A. *J. Phys. Org. Chem.* **1998**, *11*, 602–609. (d) Grubbs, R. H. *Tetrahedron*, **2004**, *60*, 7117–7140. (e) Grubbs, R. H. *Angew. Chem. Int. Ed.* **2006**, *45*, 3760–3765. (f) Schrock, R. R. *Angew. Chem. Int. Ed.* **2006**, *45*, 3748–3759.
- (2) Calderon, N.; Chen, H. Y.; Scott, K. W. *Tet. Lett.* **1967**, *34*, 3327–3329.
- (3) Calderon, N.; Ofstead, E. A.; Ward, J. P.; Judy, W. A.; Scott, K. W. *J. Am. Chem. Soc.* **1968**, *90*, 4133–4140.
- (4) Herisson, J.-L.; Chauvin, Y. *Makromol. Chem.* **1971**, *141*, 161–176.
- (5) Lewandos, G. S.; Pettit, R. *J. Am. Chem. Soc.* **1971**, *93*, 7087–7088.
- (6) Grubbs, R. H.; Brunck, T. K. *J. Am. Chem. Soc.* **1971**, *94*, 2538–2540.
- (7) Early Transition Metal Catalysts: (a) Schrock, R. R. *J. Am. Chem. Soc.* **1974**, *96*, 6796–6797. (b) Schrock, R. R.; Rocklage, S.; Wengrovius J.; Rupprecht, G.; Fellman, J. *J. Mol. Cat.* **1980**, *8*, 73–83. (c) Schrock, R. R.; DePue, R. T.; Feldman, J.; Schaverien, C. J.; Dewan, J. C.; Liu, A. H. *J. Am. Chem. Soc.* **1988**, *110*, 1423–1435. (d) Schrock, R. R.; Murdzek, J. S.; Bazan, G. C.; Robbins, J.; DiMare, M.; O'Regan, M. *J. Am. Chem. Soc.* **1990**, *112*, 3875–3886. (e) Bazan, G. C.; Oskam, J. H.; Cho, H.-N.; Park, L. Y.; *J. Am. Chem. Soc.* **1991**, *113*, 6899–6907.

- (8) Late Transition Metal Catalysts: (a) Nguyen, S. T.; Johnson, L. K.; Grubbs, R. H. *J. Am. Chem. Soc.* **1992**, *114*, 3974–3975. (b) Schwab, P.; France, M. B.; Ziller, J. W.; Grubbs, R. H. *Angew. Chem. Int. Ed.* **1995**, *34*, 2039–2040. (c) Scholl, M.; Trnka, T. M.; Morgan, J. P.; Grubbs, R. H. *Tetrahedron Lett.* **1999**, *40*, 2247–2250. (d) Scholl, M.; Ding, S.; Lee, C. W.; Grubbs, R. H. *Org. Lett.* **1999**, *1*, 953–956. (e) Garber, S. B.; Kingsbury, J. S.; Gray, B. L.; Hoveyda, A. H. *J. Am. Chem. Soc.* **2000**, *122*, 8168–8179.
- (9) Trnka, T. M.; Grubbs, R. H. *Acc. Chem. Res.* **2001**, *34*, 18–29.
- (10) (a) Chatterjee, A. K.; Choi, T.-L.; Sanders, D. P.; Grubbs, R. H. *J. Am. Chem. Soc.* **2003**, *125*, 11360–11370. (b) Fu, G. C.; Nguyen, S. T.; Grubbs, R. H. *J. Am. Chem. Soc.* **1993**, *115*, 9856–9857. (c) Chatterjee, A. K.; Morgan, J. P.; Scholl, M.; Grubbs, R. H. *J. Am. Chem. Soc.* **2000**, *122*, 3783–3784. (d) Bielawski, C. W.; Grubbs, R. H. *Angew. Chem. Int. Ed.* **2000**, *39*, 2903–2906.
- (11) (a) Dias, E. L.; Nguyen, S. T.; Grubbs, R. H. *J. Am. Chem. Soc.* **1997**, *119*, 3887–3897. (b) Sanford, M. S.; Ulman, M.; Grubbs, R. H. *J. Am. Chem. Soc.* **2001**, *123*, 749–750. (c) Sanford, M. S.; Love, J. A.; Grubbs, R. H. *J. Am. Chem. Soc.* **2001**, *123*, 6543–6554. (d) Kuhn, K. M.; Bourg, J.-B.; Chung, C. K.; Virgil, S. C.; Grubbs, R. H. *J. Am. Chem. Soc.* **2009**, *131*, 5313–5320.
- (12) (a) Sanford, M. S.; Love, J. A.; Grubbs, R. H. *Organometallics*, **2001**, *20*, 5314–5318. (b) Stewart, I. C.; Ung, T.; Pletnov, A. A.; Berlin, J. M.; Grubbs, R. H.; Schrodi, Y. *Org. Lett.* **2007**, *9*, 1589–1592. (c) Chung, C. K.; Grubbs, R. H. *Org. Lett.* **2008**, *10*, 2693–2696. (d) Seiders, T. J.; Ward, D. W.; Grubbs, R. H. *Org. Lett.* **2001**, *3*, 3225–3228. (e) Bielawski, C. W.; Benitez, D.; Grubbs, R. H.

- Science*, **2002**, 297, 2041–2043 (f) Endo, K.; Grubbs, R. H. *J. Am. Chem. Soc.* **2011**, 133, 8525–8527. (g) Keitz, B. K.; Endo, K.; Herbert, M. B.; Grubbs, R. H. *J. Am. Chem. Soc.* **2011**, 133, 9686–9688.
- (13) (a) Wenzel, A. G.; Grubbs, R. H. *J. Am. Chem. Soc.* **2006**, 128, 16048–16049. (b) Wenzel, A. G.; Blake, G.; VanderVelde, D. G.; Grubbs, R. H. *J. Am. Chem. Soc.* **2011**, 133, 6429–6439. (c) Romero, P. E.; Piers, W. E. *J. Am. Chem. Soc.* **2007**, 129, 1698–1704. (d) Romero, P. E.; Pier, W. E. *J. Am. Chem. Soc.* **2005**, 127, 5032–5033. (e) van der Eide, E. F.; Romero, P. E.; Piers, W. E. *J. Am. Chem. Soc.* **2008**, 130, 4485–4491. (f) Leitao, E. M.; van der Eide, E. F.; Romero, P. E.; Piers, W. E.; McDonald, R. *J. Am. Chem. Soc.* **2010**, 132, 2784–2794. (g) Rowley, C. N.; van der Eide, E. F.; Piers, W. E.; Woo, T. K. *Organometallics*, **2008**, 27, 6043–6045. (h) Anderson, D. A.; Hickstein, D. D.; O’Leary, D. J.; Grubbs, R. H. *J. Am. Chem. Soc.* **2006**, 128, 8386–8387.
- (14) Stewart, I. C.; Keitz, B. K.; Kuhn, K. M.; Thomas, R. M.; Grubbs, R. H. *J. Am. Chem. Soc.* **2010**, 132, 8534–8535.
- (15) (a) Hong, S. H.; Wenzel, A. G.; Salguero, T. T.; Day, M. W.; Grubbs, R. H. *J. Am. Chem. Soc.* **2007**, 129, 7961–7968. (b) Hong, S. H.; Chlenov, A.; Day, M. W.; Grubbs, R. H. *Angew. Chem. Int. Ed.* **2007**, 46, 5148–5151.

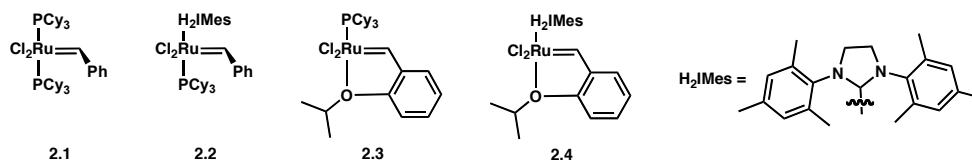
*Chapter 2*

## ASYMMETRIC OLEFIN METATHESIS



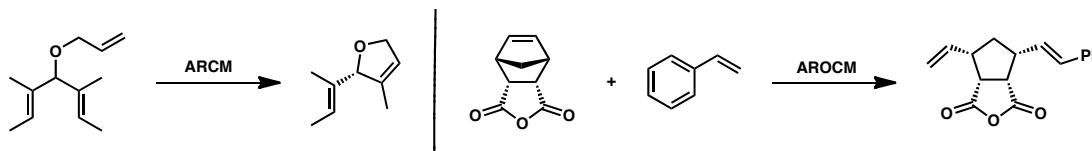
## INTRODUCTION

Olefin metathesis is a powerful methodology for the construction of carbon-carbon double bonds.<sup>1</sup> There are now a large number of transition metal olefin metathesis catalysts, many of which are commercially available, that allow for control over one or more of the various olefin metathesis parameters: there are catalysts that provide high *Z*-selectivity, allow for enantioselective metathesis in various settings, generate high activity and tolerate a wide range of functional groups.<sup>2,3</sup> Ruthenium-based catalysts (figure 2.1), in particular, have seen widespread use due to their functional-group tolerance and high activity; advances in the synthesis of stereoselective Ru-based catalysts have lagged behind other systems, though important recent progress has been reported.<sup>4</sup>

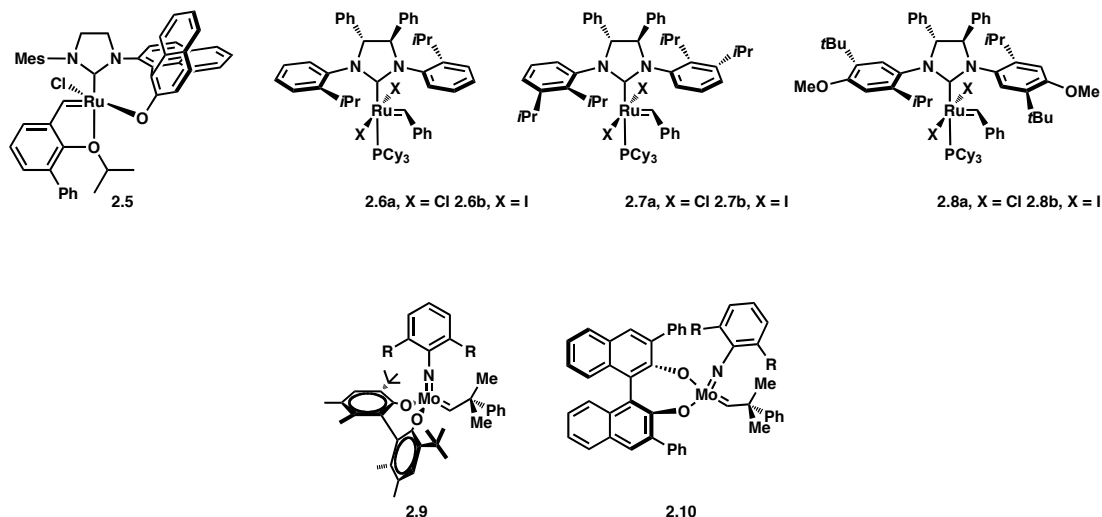


**Figure 2.1. Commercially Available Ruthenium Catalysts.**

Within the broader context of stereoselective olefin metathesis resides the issue of enantioselective reactions. Not only is enantioselective olefin metathesis an interesting and important hurdle within organic synthesis, but historically, the study of the asymmetric aspects of olefin metathesis has often led to seminal advances for the field as a whole.<sup>2e</sup> Enantioselective olefin metathesis encompasses three classes of reactions, asymmetric ring-closing metathesis (ARCM), asymmetric ring-opening cross-metathesis (AROCM) and asymmetric cross-metathesis (ACM). Representative ARCM and AROCM reactions are shown in scheme 2.1.<sup>3</sup>

Scheme 2.1. Representative Asymmetric Olefin Metathesis Reactions.<sup>3</sup>

The most common approach to the design of enantioselective olefin metathesis catalysts involves exchanging ligands on commercially available Mo- or Ru-catalysts with chiral ligands. Currently, Mo-based systems such as complexes **2.9** and **2.10** in figure 2.2, have shown the highest enantioselectivities in AROCM reactions.<sup>5</sup> In these Mo complexes, the chirality of the rigid bis-phenolate ligand, which drives enantioselectivity, lies in very close proximity to the metal center.<sup>5</sup> In Ru-based systems, the most common approach to generate chiral complexes involves installation of a chiral *N*-heterocyclic carbene (NHC) ligand.<sup>3</sup>

Figure 2.2. Chiral Ru-Based and Mo-Based Olefin Metathesis Catalysts.<sup>2,3</sup>

Using this approach, several chiral Ru-complexes based on commercially available catalysts (figure 2.1) have been designed and synthesized such as the BINOL-bound ruthenium complex, **2.5** (figure 2.2).<sup>2,3</sup> Though these catalysts still maintain the

high functional-group tolerance of ruthenium systems, they have not yet reached the high enantioselectivities of the Mo-based systems. This is most likely due to the increased distances between the ligand chiral centers and the metal center in several of the chiral-NHC Ru-based catalysts.

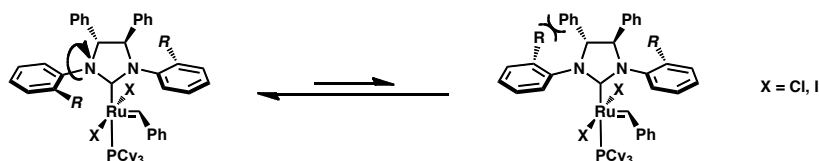


**Figure 2.3. “Gearing” Motif for Chiral Ruthenium Catalysts.<sup>3</sup>**

Previous work from our group has elucidated a mechanism for chiral induction wherein monodentate NHC ligands relay chirality from the carbene backbone toward the metal center via unsymmetrical *N*-aryl substituents (figure 2.3).<sup>3</sup> This structural motif is termed the “gearing effect,” and a series of chiral ruthenium catalysts, **2.6**, **2.7**, and **2.8**, have been synthesized based on this principal, which are shown in figure 2.2.<sup>3</sup> These catalysts have been applied successfully in ARCM, AROCM and ACM reactions with enantiomeric excesses (e.e.) up to 92% and conversions reaching up to 98%.

Modifications of the “geared” NHC have thus far been limited to the *N*-bound aryl group, with increased enantioselectivities achieved with increased steric bulk at specific positions about the arene.<sup>3b,3c</sup> The proposed transition state, shown in figure 2.4, for the selectivity of the catalyst in ARCM reactions, was developed based on a bottom-bound olefin intermediate.<sup>3b</sup> In recent years, experimental data and calculations have provided evidence for both a bottom-bound and a side-bound olefin adduct; however, the prevailing mechanistic postulation involves a bottom-bound olefin adduct and a bottom-bound ruthenacyclobutane.<sup>6,7</sup>

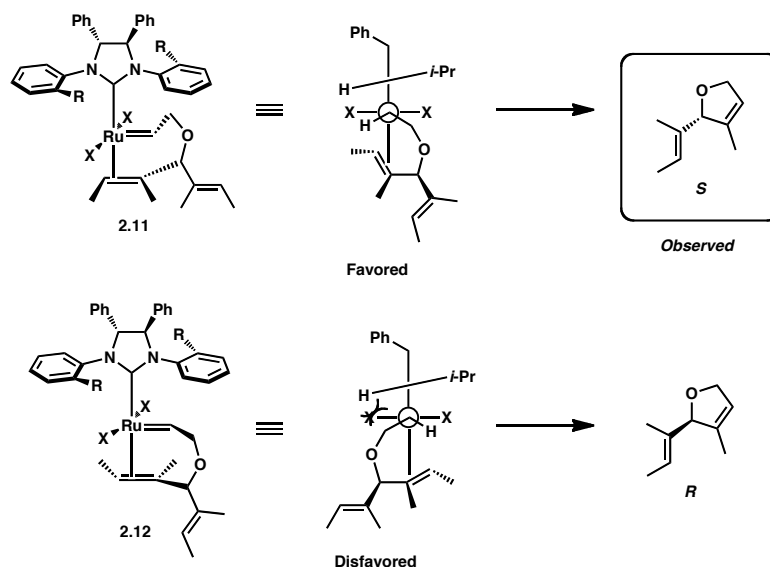


**Figure 2.4. Transition State for Origin of Enantioselectivity in ARCM.**

Note that in Figure 2.4, the presence of the phenyl substituents on the NHC backbone imparts a tilt to the *N*-bound arenes that is not present in achiral Grubbs-type catalysts. In the achiral variants, the *N*-bound arene is orthogonal to the plane of the NHC ligand. In the chiral, “geared” catalysts, the tilt of the arene out of the horizontal plane desymmetrizes the quadrants beneath the aryl ring, with the larger quadrant beneath the *ortho*-substituent. In the bottom-bound olefin adduct **2.11**, the alkylidene is positioned in the larger quadrant, minimizing unfavorable steric interactions between the pendant olefin and the arene, thus leading to the favored and observed enantiomer. It is important to note that many factors may drive the arene tilt angle, which in turn defines the resting position of the alkylidene and subsequently the selection of the *S* enantiomer over the *R* enantiomer.

Thus, the parent catalyst **2.6a**, which was the first ruthenium-based catalyst to utilize this geared motif, has managed to achieve good levels of enantioselectivity for ARCM and moderate enantioselectivities for AROCM.<sup>3a</sup> Further exploration of this motif

yielded catalysts **2.7** and **2.8** (figure 2.2), which showed that increasing bulk on one side of the arene ring is one factor which can increase the arene tilt angle, thus increasing enantioselectivities in asymmetric metathesis reactions.<sup>3b,3c</sup> A substantial halide effect was noted in both the parent chiral catalyst and the more bulky *N*-arenyl chiral catalysts. Substitution of the X-type ligands from chlorides to iodides produced a pronounced increase in e.e. for both ARCM and AROCM.

Although the proposed transition state does not account for this increase in e.e., it has been noted that in exchanging the X-type ligand, the catalyst's electronic structure is altered and overall catalyst reactivity is lowered. This lower reactivity leads to a late, product-like transition state where the negative steric interactions are amplified and thus higher e.e. is obtained.<sup>8</sup>

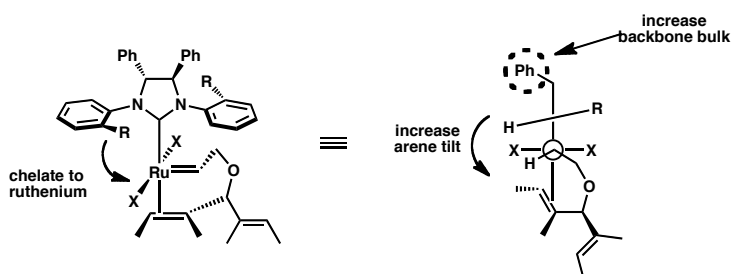


**Figure 2.5. Structural Modifications for Increasing Arene Tilt Angle.**

In order to further increase e.e., other points of modification centered around the goal of increasing the arene tilt angle. This can be accomplished a number of ways, the most readily available being either linking the NHC to the metal center or increasing the backbone bulk (figure 2.5). We report herein the synthesis and evaluation of three chiral ruthenium olefin metathesis catalysts in an effort to explore the electronic and steric effects of differential substitution about the NHC ligand (figure 2.6). These catalysts bear the stabilizing isopropoxybenzylidene ligand.

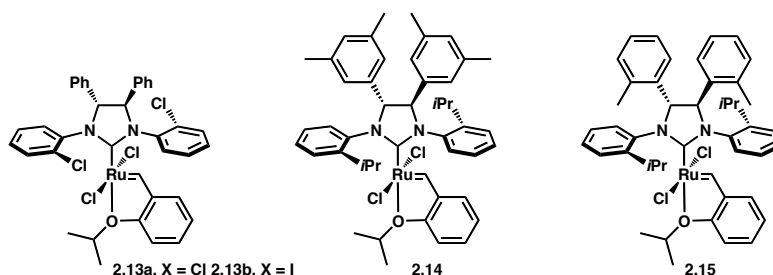


**Figure 2.6. Novel Chiral Ruthenium Olefin Metathesis Catalysts.**

We designed catalyst **2.13** to probe the potential of a halogen-ruthenium interaction, which may lead to an increased arene-tilt, as previously reported by Ritter et al. and will be discussed further.<sup>9</sup> We designed catalysts **2.14** and **2.15** to investigate the effect of increasing the tilt of the *N*-bound arene via increasing the steric bulk of the chiral NHC backbone. These catalysts were evaluated in a variety of ARCM and AROCM reactions and benchmarked against the parent chiral catalyst **2.6**.

## HALOGENATED CHIRAL CATALYST

In 2006, Ritter and Grubbs observed a unique halogen-ruthenium interaction observed in the solid-state structures of tetrahalogenated ruthenium catalysts **2.16** and **2.17** (figure 2.7).<sup>9</sup> A nonbonded distance of 3.23 Å was found in the X-ray structure of the fluorinated catalyst **2.16**, and an average nonbonded distance of 3.02 Å was found in the X-ray structure of the chlorinated catalyst **2.17**. Both chlorinated catalysts **2.17** and **2.19** unfortunately were much less stable than the corresponding fluoro-counterparts and thus were not suitable for metathesis.

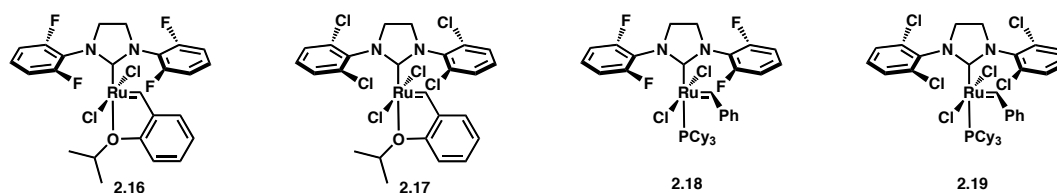


**Figure 2.7. Tetrahalogenated Achiral Ruthenium Catalysts.<sup>9</sup>**

The phosphine-bound catalyst **2.18** also showed a unique halogen-ruthenium interaction in solution, with a significant rate acceleration in olefin metathesis.<sup>9</sup> In catalyst **2.16** and **2.17**, the tetrahalogenated NHC ligand is forced to adopt an unusual and unexpected geometry in order to accommodate the observed halogen-ruthenium interaction from the solid-state. This torque and unusual alignment of the NHC is reminiscent of that invoked in the transition-state of the  $C_2$ -symmetric chiral catalyst.

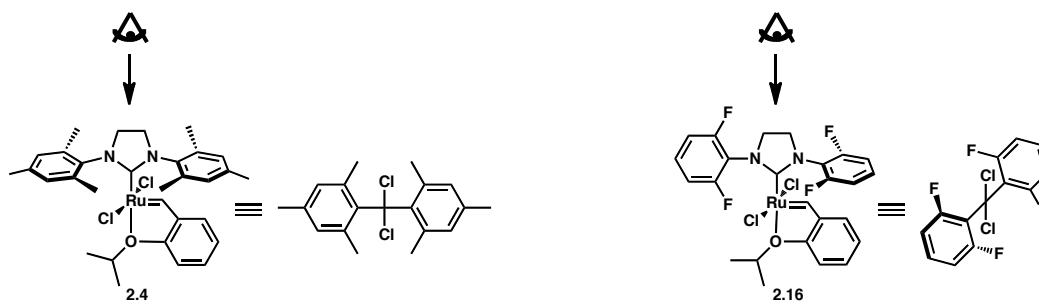


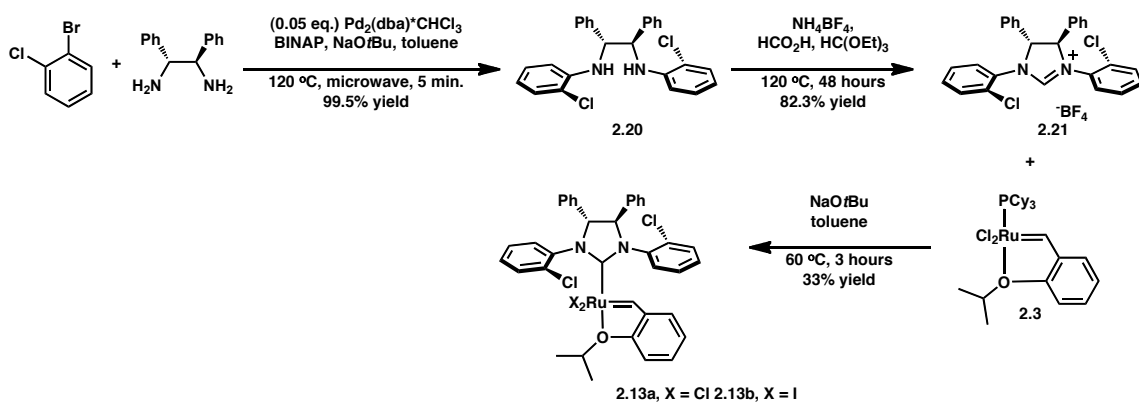
**Figure 2.8. Preferred Geometry of Various NHC Catalysts.**

As viewed down the backbone of the NHC, nonhalogenated Grubbs-type catalyst **2.4** positions the plane of the NHC ligand over and in the plane of the alkylidene (figure 2.8). The NHC effectively bisects the Cl-Ru-Cl angle. Both *N*-bound arenes are thus orthogonal to that plane and create a horizontal. As previously discussed, addition of a chiral 1,2-diphenyl backbone in the NHC ligand imposes an arene tilt that desymmetrizes these arenes out of the horizontal plane. As shown in figure 2.8, the tetrafluorinated catalyst **2.16** exhibits a similar tilt of one of the two *N*-bound arenes. Additionally, the

entire NHC ligand rotates out of the plane of the alkylidene and thus no longer bisects the Cl-Ru-Cl angle.

We report herein the synthesis of a novel chiral ruthenium olefin metathesis catalyst, **2.13**, bearing *N*-2-Cl-phenyl substituents (scheme 2.2). In designing this catalyst, we hoped to exploit the potential NHC-halogen-ruthenium interaction in the NHC to increase enantioselectivity in ARCM and AROCM reactions. Moreover, theoretical studies have predicted that electronegative halogens on the NHC ligand would decrease catalyst activity, which would be expected to further increase e.e. due to a late-transition state.<sup>7,8</sup>

**Scheme 2.2. Synthesis of Chlorinated Catalyst.**



Ligand synthesis began with microwave-assisted Buchwald-Hartwig coupling of commercially available 1,2-bromochlorobenzene and (1*R*, 2*R*)-diphenylethylenediamine to form diamine **2.20**, which was then cyclized with triethylorthoformate to form imidazolinium salt **2.21**. Catalyst **2.13a** was obtained in 33% yield by addition of the imidazolinium salt to ruthenium precursor **2.3** in the presence of sodium tert-butoxide.



Scheme 2.3. Ring Closing of DEDAM.

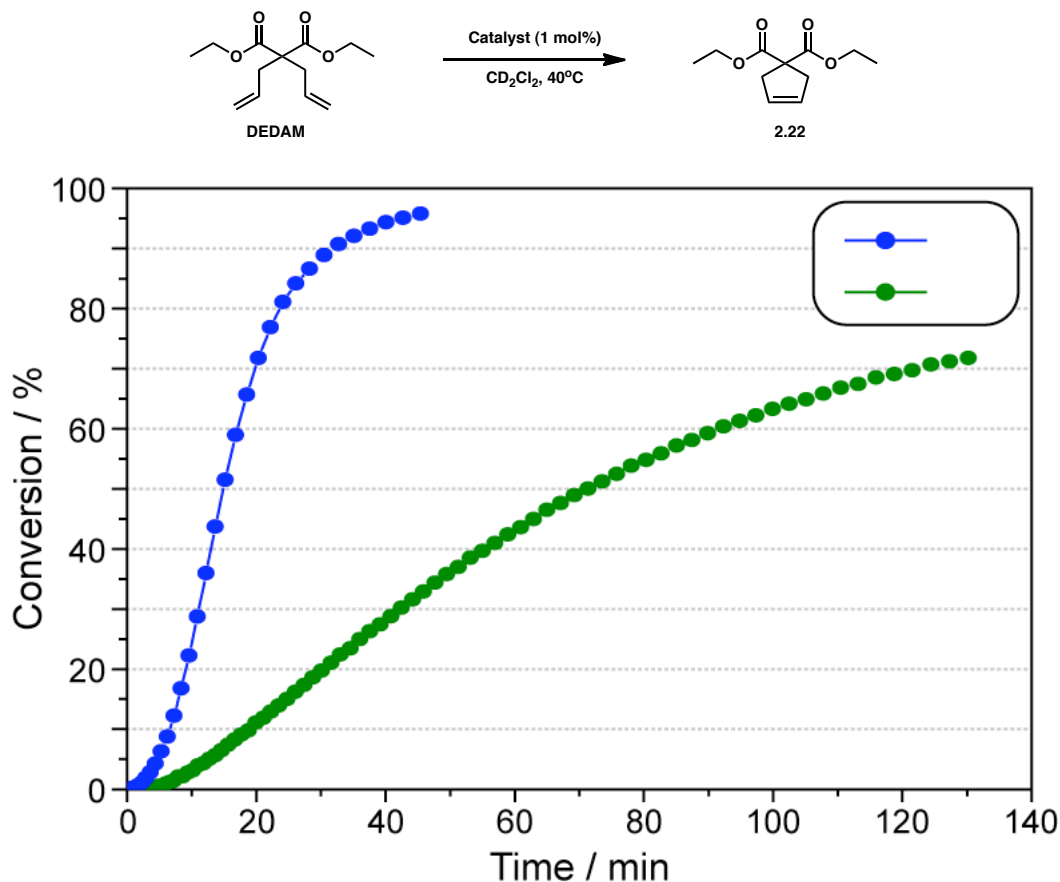
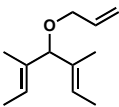
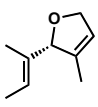
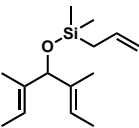
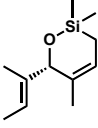
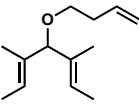
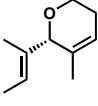
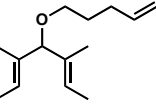
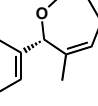


Figure 2.9. Kinetics for Ring Closing of DEDAM.

In order to explore the reactivity of catalyst **2.13a**, an initiation array was conducted (figure 2.9). Under modified ( $40^\circ\text{C}$ ) standard conditions, the ring closing of diethyl diallylmalonate (DEDAM) was monitored via  $^1\text{H}$ -NMR (scheme 2.3).<sup>10</sup> The decreased reaction rate of catalyst **2.13a** is not unexpected, as Ritter and Grubbs observed an analogous rate decrease for the phosphine-free tetrachlorinated catalyst.<sup>9</sup> It was predicted, however, that lowering the reactivity could potentially lead to higher e.e. Thus, with these results in hand, we chose to explore ARCM of several trienes with higher catalyst loadings and at longer reaction times than previous studies of ARCM.

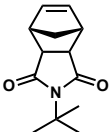
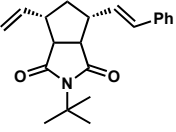
All ARCM reactions were conducted at 5 mol% and for 3 hours. Catalyst **2.13b** was formed *in situ* with sodium iodide. A moderate halide effect, subdued in comparison to previously published results, was observed.<sup>3</sup>

**Table 2.1. ARCM Reactions with Chlorinated Chiral Catalysts**

triene	product	catalyst	e.e.	conversion
 2.23	 2.24	<b>2.6a</b>	35%	98%
		<b>2.6b</b>	90%	98%
		<b>2.13a</b>	67%	66%
		<b>2.13b</b>	87%	60%
 2.25	 2.26	<b>2.6a</b>	83%	98%
		<b>2.6b</b>	86%	68%
		<b>2.13a</b>	90%	40%
		<b>2.14b</b>	90%	10%
 2.27	 2.28	<b>2.6a</b>	NA	NA
		<b>2.6b</b>	90%	98%
		<b>2.13a</b>	82%	63%
		<b>2.14b</b>	NA	NA
 2.29	 2.30	<b>2.6a</b>	NA	NA
		<b>2.6b</b>	85%	5%
		<b>2.13a</b>	79%	30%
		<b>2.13b</b>	NA	NA

Shown in table 2.1 are the enantioselectivities obtained with novel catalysts **2.13a** and **2.13b** compared to the published catalysts **2.6a** and **2.6b**. In comparing the parent chiral catalyst **2.6a** to the novel chlorinated **2.13a**, note that despite the smaller size of the chlorine compared to the isopropyl moiety, the e.e. for the ring-closed product is substantially higher, going from 35% e.e. to 67% e.e. A nonsteric rationale for the increased enantioselectivity must rely either on a canted geometry in the transition state or an electronic interaction between the chlorine and the ruthenium, thus reaffirming the halogen-ruthenium affinity as shown by Ritter.

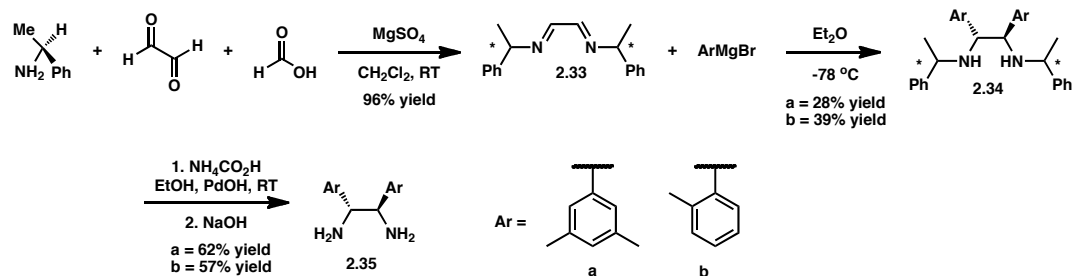
Table 2.2. AROCM Reactions with Chlorinated Chiral Catalysts

norbornene	product	catalyst	e.e. ( <i>cis</i> )	e.e. ( <i>trans</i> )
 2.31	 2.32	2.8a	38%	57%
		2.8b	50%	75%
		2.13a	7%	38%

With the increased e.e. in hand, we had hoped to show an analogous increase in enantioselectivity in AROCM, a reaction that, to date, has shown room for improvement with chiral ruthenium catalysts. Surprisingly, the novel catalyst **2.13a** showed a decrease in enantioselectivity when screened against the standard AROCM substrate shown in table 2.2 compared to published catalyst **2.8a** and **2.8b**. This is however, still intriguing, as it lends insight into the differences between the ARCM and AROCM reaction mechanisms.

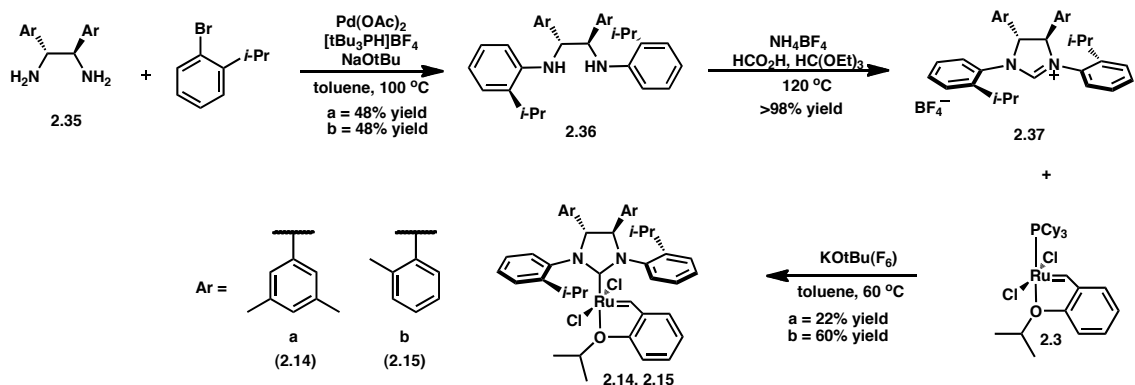
## BACKBONE-MODIFIED CHIRAL CATALYSTS

Next we chose to explore further bulk on the chiral backbone of the NHC ligand. It was proposed that increasing the bulk of the aryl substituents in the backbone of the ligand should increase enantioselectivities. We began the catalyst synthesis with the synthesis of the enantiopure diamines **2.35a** and **2.35b** (scheme 2.4). Commercially available (*S*)-1-phenylethanamine was condensed with glyoxal and formic acid to form the known bisimine **2.33**.<sup>11</sup> Slow addition of the aryl Grignard reagent is diastereoselective and cleavage of the chiral auxiliary under hydrogenolysis conditions gives the (*R,R*) enantiomer of **2.35a** and **2.35b**.<sup>11</sup>

Scheme 2.4. Synthesis of Enantiopure Diamines **2.35a** and **2.35b**.

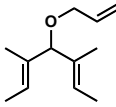
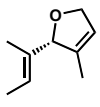
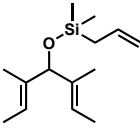
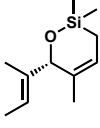
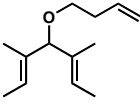
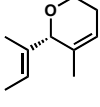
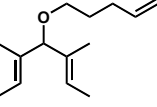
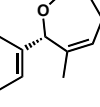
Enantiopure diamines **2.35a** and **2.35b** were further elaborated to the corresponding imidazolium salts (scheme 2.5). As seen previously, Buchwald-Hartwig coupling proceeded with moderate yields and subsequent condensation in triethylorthoformate was robust and quantitative in conversion. The yield obtained from catalyst formation by way of ligand exchange with ruthenium precursor **2.3** proved sensitive to salt purity.

Scheme 2.5. Synthesis of Backbone Functionalized Chiral Catalysts.



As with the chlorinated chiral catalyst, novel catalysts **2.14** and **2.15** were evaluated in ARCM and AROCM. ARCM reactions were conducted at 5 mol% of ruthenium catalyst and for 3 hours. Shown in table 2.3 are the enantioselectivities obtained in ARCM for catalysts **2.14** and **2.15**, again, benchmarked against the parent catalyst **2.6a**.

Table 2.3. ARCM Reactions with Backbone-Modified Chiral Catalysts

triene	product	catalyst	e.e.
 2.23	 2.24	2.6a	35%
		2.14	38%
		2.15	40%
 2.25	 2.26	2.6a	83%
		2.14	94%
		2.15	92%
 2.27	 2.28	2.6a	NA
		2.14	76%
		2.15	74%
 2.29	 2.30	2.6a	NA
		2.14	71%
		2.15	28%

Both backbone-modified catalysts showed marked increases in enantioselectivity when compared to the parent chiral catalyst. However, from simple molecular models, it was predicted that the NHC ligand of catalyst **2.15** would experience a greater tilt of the *N*-bound arene rings than the NHC of catalyst **2.14**. This should lead to a consistently higher e.e. obtained for catalyst **2.15** versus catalyst **2.14**, with both expected to yield higher e.e. than the parent. Note that, in the table, formation of **2.24** follows the expected trend. Formation of **2.26** and **2.28** however, begin to invert the expected trend between catalysts **2.15** and **2.14**. And finally, for the large ring formation of **2.30** there is a marked decrease in e.e. for catalyst **2.15**, substantially below that obtained by catalyst **2.14**.

One potential explanation for the inversion in expected trend is that as the arene tilt angle is significantly increased, the transition state in ARCM is forced to adopt an alternate conformation, and as a result, is forced into an overall different mechanism for olefin binding and metallacycle formation.

Therefore we propose the following competing transition state, which may account for the erosion in e.e. as the alkyl chain in the terminal olefin group is extended (figure 2.10). Under conditions of mild to moderate arene tilt, the triene, regardless of alkyl chain length, may adopt the *trans*-binding mode for the incoming olefin, as depicted in the original transition state (Figure 2.4).

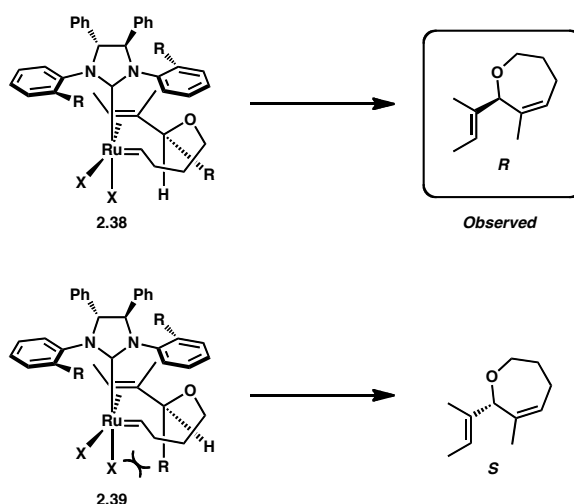


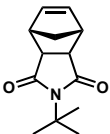
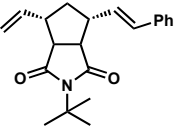
**Figure 2.10. Competing Mode of Olefin Binding.**

When arene tilt is substantially increased however, and the triene has increased flexibility in binding, as potentially imparted by a longer alkyl chain, *i.e.* substrate **2.29**, the quadrants beneath the tilted arene are sufficiently different in spatial allotment such that the reacting olefin may choose to adopt a conformation equivalent to a side-bound olefin. The alkylidene of **2.38** still rests under the “roomier” quadrant, but unlike the original transition state, in this competing mode the incoming olefin would then approach

from the opposite face to yield the *R* enantiomer, in order to avoid unfavorable steric interactions between the X-type ligand and the R-group of transition state **2.39** (Figure 2.10). Further study of olefin binding modes are necessary to begin to understand this intriguing mechanistic puzzle.

In the meantime, we continued benchmarking the novel backbone modified chiral catalysts in AROCM. Unlike for ARCM, the AROCM reaction mechanism is notably less well understood, due to the introduction of new degrees of freedom not present in ring closing. We observed that the e.e. for AROCM with these catalysts did not erode over time and no secondary cross-metathesis was present. Analysis of AROCM results did not, however, elucidate whether the arene tilt angle of catalysts **2.14** and **2.15** were truly increased or followed the computationally predicted trend (table 2.4). We instead observed a much higher e.e. for catalyst **2.14**, the predicted “less arene-tilted” of the two catalysts.

**Table 2.4. AROCM Reactions with Backbone Modified Chiral Catalysts**

norbornene	product	catalyst	e.e. ( <i>cis</i> )	e.e. ( <i>trans</i> )
 <b>2.31</b>	 <b>2.32</b>	<b>2.8a</b>	38%	57%
		<b>2.14</b>	63%	66%
		<b>2.15</b>	12%	24%

It was at this point that we chose to begin solid-state analysis of these two catalysts. Unfortunately, catalyst **2.15** proved relatively unstable and a solid state crystal structure was not obtained. However, we did manage to obtain a basic structure for catalyst **2.14** showing connectivity and conformation, which proved somewhat surprising (figure 2.11).

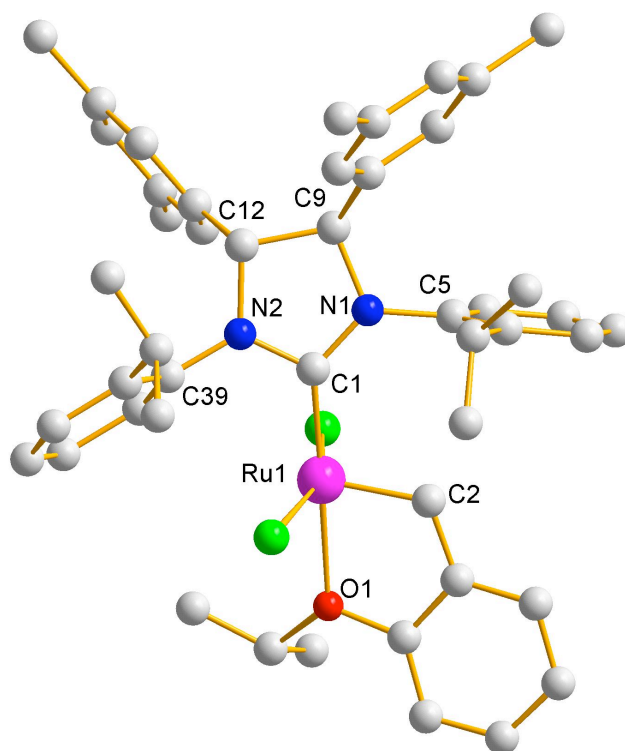


**Figure 2.11. Crystal Structure of Catalyst 2.14.**

Most unusual in this crystal structure was the *syn*-conformation of the *ortho*-isopropyl substituents, a conformation that is not  $C_2$ -symmetric as was expected for all geared chiral catalysts. This discovery, however, fits well with the proposed competing transition state for olefin binding and enantioselectivity. In the crystal structure, one can see that not only are both arenes tilted in the same direction, one *N*-bound arene is substantially tilted upwards. It is likely the alkylidene rests underneath this quadrant, and the other side is left relatively empty, thus allowing the incoming olefin to easily form a side-bound olefin adduct. Further exploration of chiral NHC catalysts and olefin binding modes in both ARCM and AROCM are therefore necessary and ongoing in our lab.



## CONCLUSIONS

In conclusion, differential substitution about the chiral NHC ligand was explored in order to identify electronic and steric effects on the enantioselectivity and reactivity of ruthenium catalysts in asymmetric metathesis. Catalyst **2.13**, which bears halogenated *N*-bound aryl rings, along with backbone-modified catalysts **2.14** and **2.15**, were synthesized and characterized. These catalysts were also evaluated in an array of ARCM reactions and one AROCM reaction. A notable decrease in reactivity of the halogenated catalyst was observed. Unexpectedly, the trend between predicted arene-tilt angle and e.e. was not uniform. A competing mode of olefin binding and catalyst conformation was proposed and reaffirmed by an observed crystal structure of catalyst **2.14**.

## EXPERIMENTAL METHODS

### Materials and Methods

NMR spectra were measured on an Oxford 300 MHz spectrometer running Varian VNMR software unless otherwise noted. Resonances for NMR spectra are reported relative to Me<sub>4</sub>Si ( $\delta$  0.0) for <sup>1</sup>H and <sup>13</sup>C. Spectra are reported as follows: chemical shift ( $\delta$  ppm), multiplicity, coupling constant (Hz) and integration. High Resolution Mass Spectroscopy (HRMS) was obtained by the California Institute of Technology MS Facility. Enantiomeric excess values were determined by chiral GC (Chiraldex G-TA, 30mx0.25mm) and chiral HPLC (Chiracel AD, OD-H, AS) and were compared to racemic samples. Air-sensitive metal-containing complexes were handled in a dry box under nitrogen or via standard Schlenk techniques under argon. Flash chromatography was conducted using silica gel 60 with the exception of ruthenium-containing complexes, which was conducted using TSI Scientific silica. Solvents were purified by passage through alumina.<sup>1</sup> Ruthenium starting materials were provided by Materia, Inc. All other reagents were purchased from Aldrich and used without prior purification.

### Catalysts Synthesis.

**Synthesis of (1*R*,2*R*)-*N*1,*N*2-bis(2-chlorophenyl)-1,2-diphenylethane-1,2-diamine (2.20):** A solution of the bromochlorobenzene (1.8 g, 9.4 mmol) in toluene (15 mL) was loaded into a sealable microwave vial. (1*R*,2*R*)-1,2-diphenylethane-1,2-diamine (1 g, 4.7 mmol), Pd<sub>2</sub>(dba)<sub>3</sub>•CHCl<sub>3</sub> (0.22 g, 0.21 mmol) and (+/ –)-BINAP (0.32 g, 0.51 mmol) were then added in a single portion. The solution was briefly evacuated and backfilled,

---

<sup>1</sup> Pangborn, A. B.; Giardello, M. A.; Grubbs, R. H.; Rosen, R. K.; Timmers, F. J. *Organometallics* **1996**, *15*, 1518–1520.

then NaOt-Bu (1.23 g, 12.8 mmol) was added. The reaction was sealed and heated to 120°C for 5 minutes. The diamine was purified by flash chromatography (1% MeOH in CH<sub>2</sub>Cl<sub>2</sub>) and gave pure product in 99% yield. <sup>1</sup>H NMR (300 MHz, CDCl<sub>3</sub>): δ 7.35 – 7.31 (m, 4H), 7.27 – 7.25 (m, 2H), 6.99 (t, J = 7.7 Hz, 1H), 6.66 (t, J = 7.6 Hz, 1H), 6.48 (d, J = 8.15, 1H), 5.34 (s, 1H), 4.85 (s, 1H). <sup>13</sup>C NMR (75 MHz, CDCl<sub>3</sub>) δ 143.2, 139.1, 138.2, 129.6, 129.0, 128.7, 128.1, 128.0, 125.9, 120.6, 118.6, 113.6, 63.5. HRMS (FAB+) *m/z* calc for C<sub>26</sub>H<sub>22</sub>Cl<sub>2</sub>N<sub>2</sub>; 432.1210, found 432.1190.

**Synthesis of (4*R*,5*R*)-1,3-bis(2-chlorophenyl)-4,5-diphenyl-4,5-dihydro-1*H*-imidazol-3-ium (2.20):** The diamine, **2.20** (0.51 g, 1.18 mmol), was dissolved in HC(OEt)<sub>3</sub> (1.38 mL, 11.78 mmol) and NH<sub>4</sub>BF<sub>4</sub> (0.175 g, 1.18 mmol) was added along with a catalytic amount of formic acid. The reaction was heated to 120°C and stirred for 48 hours. Upon cooling to room temperature, the reaction mixture was diluted with Et<sub>2</sub>O and purified by flash chromatography (3% MeOH in CH<sub>2</sub>Cl<sub>2</sub>). <sup>1</sup>H NMR (500 MHz, C<sub>6</sub>D<sub>6</sub>): δ 8.04 (dd, J = 1.5 Hz, 8.0 Hz, 2H), 7.82 (s, 1H), 7.38 (d, J = 7.2 Hz, 4H), 6.95 (t, J = 7.8 Hz, 4H), 6.83 (t, J = 7.5 Hz, 2H), 6.76 (dd, J = 8.0 Hz, 15.2 Hz, 4H), 6.50 (t, J = 8 Hz, 2H), 6.10 (s, 2H). <sup>13</sup>C NMR (125 MHz, CDCl<sub>3</sub>) δ 158.9, 132.4, 131.3, 130.8, 130.1, 129.6, 129.3, 128.9, 128.6, 128.0, 127.8, 127.6, 76.1. HRMS (FAB+) *m/z* calc for C<sub>27</sub>H<sub>21</sub>Cl<sub>2</sub>N<sub>2</sub>; 443.1082, found 443.107.

**Synthesis of Ruthenium Complex (2.13a):** Potassium hexafluoro-*t*-butoxide (10.4 mg, 0.0472 mmol), imidazolium salt **2.21** (25 mg, 0.0472 mmol), and ruthenium precursor **2.3** (28.3 mg, 0.0472 mmol) were suspended in toluene (5 mL). The flask was sealed with a

septum and heavy parafilm, removed from the glove box, and stirred at 60°C for 4 hours. The reaction mixture was concentrated and purified by flash chromatography using TSI silica gel (5%, 50% Et<sub>2</sub>O in pentane) and lyophilized from benzene. <sup>1</sup>H NMR (500 MHz, C<sub>6</sub>D<sub>6</sub>): δ 16.46 (s, 1H), 7.89 – 6.10 (m, 22H), 4.45 (m, 1H), 3.99 (m, 2H), 1.44 (m, 6H). <sup>13</sup>C NMR (125 MHz, CDCl<sub>3</sub>) Only diagnostic peaks reported: δ 214.7. HRMS (FAB+) *m/z* calc for C<sub>37</sub>H<sub>32</sub>N<sub>2</sub>ORuCl<sub>2</sub>; 764.0323, found 764.0308.

**General Procedure for Synthesis of Chiral Diamines:** A flame-dried 50 mL round-bottom flask was charged with commercially available anhydrous MgSO<sub>4</sub> (4 g), CH<sub>2</sub>Cl<sub>2</sub> (0.32 M in amine), and (*S*)-1-phenylethylamine (2.06 mL, 16 mmol). A 40% by weight solution of glyoxal (1.13 mL, 7.9 mmol) was then added, along with a catalytic amount of formic acid. The mixture was stirred for 1 hour at room temperature. The reaction mixture was then filtered through Celite and the solvent was evaporated to yield known bisimine **2.33**. To a dry-ice-cooled solution of bisimine in Et<sub>2</sub>O was added dropwise (2.5-4 equiv.) a solution of arylmagnesium bromide at –78°C. The solution was allowed to slowly warm to room temperature and then quenched with NH<sub>4</sub>Cl. The aqueous layer was separated and extracted with ether. The combined organic layers were washed with brine, dried over Na<sub>2</sub>SO<sub>4</sub>, filtered and concentrated to afford the crude secondary diamines which were purified by flash chromatography (2% EtOAc in hexanes). Separate hydrogenolysis procedures were then followed for **2.34a** and **2.34b**.

**(1*R*,2*R*)-1,2-bis(3,5-dimethylphenyl)-*N*1,*N*2-bis((*S*)-1-phenylethyl)ethane-1,-diamine (2.34a):** To a dry-ice-cooled solution of **2.33** (15.5 mmol) in Et<sub>2</sub>O was added dropwise

(2.5 equiv.) a solution of (3,5-dimethylphenyl)magnesium bromide (32 mL, 1.25 M, 40 mmol) at  $-78^{\circ}\text{C}$ . The solution was allowed to slowly warm to room temperature over 2 hours and then quenched with  $\text{NH}_4\text{Cl}$ . The aqueous layer was separated and extracted three times (50 mL) with ether. The combined organic layers were washed with brine, dried over  $\text{Na}_2\text{SO}_4$ , filtered and concentrated to afford the crude secondary diamine which was purified by flash chromatography (2% EtOAc in hexanes).  $^1\text{H}$  NMR (300 MHz,  $\text{CDCl}_3$ ):  $\delta$  7.16 – 7.14 (m, 6H), 6.85 (s, 2H), 6.79 – 6.78 (m, 4H), 6.73 (s, 4H), 3.45 – 3.43 (q,  $J$  = 6.6 Hz, 2H), 3.33 (s, 2H), 2.25 (s, 12 H), 1.26 – 1.23 (d,  $J$  = 6.6 Hz, 6H).

**(1*R*,2*R*)-1,2-bis(3,5-dimethylphenyl)ethane-1,2-diamine (2.35a):** To a solution of **2.34a** (0.36 g, 0.756 mmol) in EtOH (10mL) were added  $\text{Pd}(\text{OH})_2\text{-C}$  20% (0.05 g) by weight and anhydrous ammonium formate (0.285 g, 4.5 mmol). The mixture was refluxed for 4 hours and then filtered over Celite and concentrated. The crude residue was redissolved in  $\text{Et}_2\text{O}$  and saturated  $\text{K}_2\text{CO}_3$ . The organic layer was separated and dried over  $\text{Na}_2\text{SO}_4$  to yield crude diamine, which was purified by flash chromatography (4:1 EtOAc/MeOH).  $^1\text{H}$  NMR (300 MHz,  $\text{CDCl}_3$ ):  $\delta$  6.99 (s, 4H), 6.91 (s, 2H), 4.11 (s, 2H), 2.34 (s, 12H), 1.62 (br s, 2H).

**(1*R*,2*R*)-*N*1,*N*2-bis((*S*)-1-phenylethyl)-1,2-di*o*-tolylethane-1,2-diamine (2.34b):** To a dry-ice-cooled solution of **2.33** (9.5 mmol) in  $\text{Et}_2\text{O}$  was added dropwise (4 equiv.) a solution of *o*-tolylmagnesium bromide (45 mL, 0.83 M, 37.4 mmol) at  $-78^{\circ}\text{C}$ . The solution was allowed to slowly warm to room temperature over 6 hours and then quenched with  $\text{NH}_4\text{Cl}$ . The aqueous layer was separated and extracted three times

(50mL) with ether. The combined organic layers were washed with brine, dried over  $\text{Na}_2\text{SO}_4$ , filtered and concentrated to afford the crude secondary diamine which was purified by flash chromatography (2% EtOAc in hexane) and recrystallized out of pentane.  $^1\text{H}$  NMR (300 MHz,  $\text{CDCl}_3$ ):  $\delta$  7.51 – 7.49 (d,  $J$  = 7.5 Hz, 2H), 7.38 – 7.06 (m, 14H), 6.89 – 6.87 (d,  $J$  = 7.5 Hz, 2H), 3.68 (s, 2H), 3.35 – 3.33 (q,  $J$  = 6.9 Hz, 2H), 1.67 (br s, 2H), 1.44 (s, 6H), 1.26 – 1.24 (d,  $J$  = 6.9Hz, 6H).

**(1*R*,2*R*)-1,2-dio-tolyethane-1,2-diamine (2.35b):** To a solution of **2.34b** (0.1 g, 0.23 mmol) in EtOH (3 mL) were added Pd–C 5% (0.36 g) by weight and a 10% solution of HCl. The solution was degassed by bubbling through with dry argon followed by dry hydrogen gas. A balloon of hydrogen gas was allowed to hydrogenate the solution over 48 hours. After absorption of hydrogen was shown to be complete, the solution was filtered through Celite and concentrated. The residue was redissolved in  $\text{CH}_2\text{Cl}_2$  and basified with a saturated solution of  $\text{NaHCO}_3$ . The aqueous layer was then separated and extracted three times with  $\text{CH}_2\text{Cl}_2$  (50 mL). The combined organic layers were dried over  $\text{Na}_2\text{SO}_4$ , filtered and concentrated to yield crude diamine, which was used in the next step unpurified. The chiral diamine proved sensitive toward attempts at flash chromatography.  $^1\text{H}$  NMR (300 MHz,  $\text{CDCl}_3$ ):  $\delta$  7.59 – 7.57 (d,  $J$  = 7.5 Hz, 2H), 7.20 – 7.17 (t,  $J$  = 7.8 Hz, 2H), 7.10 – 7.08 (t,  $J$  = 7.5 Hz, 2H), 7.03 – 7.00 (d,  $J$  = 7.5 Hz, 2H), 4.35 (s, 2H), 2.12 (s, 6H), 1.68 (br s, 2 H).

**(1*R*,2*R*)-1,2-bis(3,5-dimethylphenyl)-*N*1,*N*2-bis(2-isopropylphenyl)ethane-1,2-diamine (2.36a):** A flame-dried Schlenk flask equipped with stir bar was charged with

Pd(OAc)<sub>2</sub> (0.026 g, 2.62 mmol), [*t*-Bu<sub>3</sub>PH]BF<sub>4</sub> (0.034 g, 0.118 mmol), and NaO*t*-Bu (0.38 g, 3.94 mmol). The reaction vessel was evacuated and backfilled twice with dry argon. Toluene (15 mL) was added and the solution was subsequently degassed by bubbling through with dry argon for 30 minutes. 1-bromo-2-isopropylbenzene (0.34 mL, 2.62 mmol) was added, followed by chiral diamine **2.35a** (0.352 g, 1.31 mmol). The Schlenk flask was then sealed and heated to 100°C for 18 hours. The reaction mixture was quenched with NH<sub>4</sub>Cl while under dry argon. The organic layer was then washed twice with NH<sub>4</sub>Cl and dried over Na<sub>2</sub>SO<sub>4</sub> and the diamine used immediately without purification.

**(4*R*,5*R*)-4,5-bis(3,5-dimethylphenyl)-1,3-bis(2-isopropylphenyl)-4,5-dihydro-1*H*-imidazol-3-ium (2.37a):** The general procedure for imidazolium salt preparation was followed. **2.36a** (0.317 g, 0.63 mmol) was dissolved in HC(OEt)<sub>3</sub> (0.74 mL, 6.3 mmol) and NH<sub>4</sub>BF<sub>4</sub> (0.093 g, 0.63 mmol) was added along with a catalytic amount of formic acid. The reaction was heated to 120°C and stirred for 18 hours. Upon cooling to room temperature, the reaction mixture was diluted with Et<sub>2</sub>O and purified by flash chromatography (5% MeOH in CH<sub>2</sub>Cl<sub>2</sub>). <sup>1</sup>H NMR (300 MHz, CDCl<sub>3</sub>): δ 8.31 (s, 1H), 7.53 – 7.51 (m, 2H), 7.35 – 7.21 (m, 6H), 7.03 (s, 4H), 7.00 (s, 2H), 5.59 (s, 2H), 3.20 – 3.15 (m, 2H), 2.30 (s, 12H), 1.35 – 1.32 (d, *J* = 6.9 Hz, 6H), 1.21 – 1.19 (d, *J* = 6.9 Hz, 6H). HRMS (FAB+) *m/z* calc for C<sub>37</sub>H<sub>43</sub>N<sub>2</sub>; 515.3426, found 515.3404.

**(1*R*,2*R*)-*N*1,*N*2-bis(2-isopropylphenyl)-1,2-di*o*-tolylethane-1,2-diamine (2.36b):** A flame-dried Schlenk flask equipped with stir bar was charged with Pd(OAc)<sub>2</sub> (0.012 g,

0.018 mmol), [*t*-Bu<sub>3</sub>PH]BF<sub>4</sub> (0.015 g, 0.053 mmol), and NaO*t*-Bu (0.17 g, 1.77 mmol).

The reaction vessel was evacuated and backfilled twice with dry argon. Toluene (8 mL) was added and the solution was subsequently degassed by bubbling through with dry argon for 30 minutes. 1-bromo-2-isopropylbenzene was added, followed by chiral diamine **2.35b** (0.158 g, 1.18 mmol). The Schlenk flask was then sealed and heated to 100°C for 18 hours. The reaction mixture was quenched with NH<sub>4</sub>Cl while under dry argon. The organic layer was then washed twice with NH<sub>4</sub>Cl and dried over Na<sub>2</sub>SO<sub>4</sub> and used immediately. <sup>1</sup>H NMR (300 MHz, CDCl<sub>3</sub>): δ 7.62 – 7.59 (d, *J* = 8.7 Hz, 2H), 7.2 – 7.06 (m, 10 H), 6.91 – 6.85 (t, *J* = 7.8 Hz, 2H), 6.71 – 6.66 (t, *J* = 7.2 Hz, 2H), 6.19 – 6.16 (d, *J* = 9 Hz, 2H), 4.94 (s, 2H), 4.78 (s, 2H), 2.89 – 2.85 (m, 2H), 2.17 (s, 6H), 1.30 – 1.27 (d, *J* = 6.9 Hz, 6H), 1.15 – 1.12 (d, *J* = 6.9 Hz, 6H).

**(4*R*,5*R*)-1,3-bis(2-isopropylphenyl)-4,5-dio-tolyl-4,5-dihydro-1*H*-imidazol-3-ium**

**(2.37b):** The general procedure for imidazolium salt preparation was followed. **2.36b** (0.445 g, 0.935 mmol) was dissolved in HC(OEt)<sub>3</sub> (1 mL, 9.35 mmol) and NH<sub>4</sub>BF<sub>4</sub> (0.139 g, 0.935 mmol) was added along with a catalytic amount of formic acid. The reaction was heated to 120°C and stirred for 18 hours. Upon cooling to room temperature, the reaction mixture was diluted with Et<sub>2</sub>O and purified by flash chromatography (2% MeOH in CH<sub>2</sub>Cl<sub>2</sub>). <sup>1</sup>H NMR (300 MHz, CDCl<sub>3</sub>): δ 8.27 (s, 1H), 8.02 – 7.99 (d, *J* = 7.5 Hz, 2H), 7.58 – 7.56 (d, *J* = 7.5 Hz, 2H), 7.47 – 7.45 (t, *J* = 7.8 Hz, 2H), 7.37 – 7.19 (m, 8H), 7.02 – 7.00 (d, *J* = 7.5 Hz, 2H), 6.20 (s, 2H), 3.27 – 3.18 (m, 2H), 1.81 (s, 6H), 1.37 – 1.31 (m, 6H), 1.28 – 1.24 (m, 6H). HRMS (FAB+) *m/z* calc for C<sub>35</sub>H<sub>39</sub>N<sub>2</sub>; 487.3113, found 487.3119.



**Ruthenium Complex (2.14):** Following the general procedure, potassium hexamethyldisilazane (8.3 mg, 0.0415 mmol), imidazolium salt **2.37a** (25 mg, 0.0415 mmol), and ruthenium precursor (25 mg, 0.0415 mmol) were suspended in toluene (5 mL). The flask was sealed with a septum and heavy parafilm, removed from the glove box, and stirred at 60°C for 4 hours. The reaction mixture was concentrated and purified by flash chromatography (5%, 50% Et<sub>2</sub>O in pentane) and lyophilized from benzene. HRMS (FAB+) *m/z* calc for C<sub>47</sub>H<sub>54</sub>N<sub>2</sub>ORuCl<sub>2</sub>; 834.2657, found 834.2675.

**Ruthenium Complex (2.15):** Following a modified procedure, potassium hexamethyldisilazane (5.9 mg, 0.02995 mmol), imidazolium salt **2.37b** (14.3 mg, 0.02495 mmol), and ruthenium precursor (10 mg, 0.0166 mmol) were suspended in toluene (5 mL). The flask was sealed with a septum and heavy parafilm, removed from the glovebox, and stirred at 60°C for 1 hour. The reaction mixture was concentrated and purified by flash chromatography (5%, 50% Et<sub>2</sub>O in pentane) and lyophilized from benzene. HRMS (FAB+) *m/z* calc for C<sub>45</sub>H<sub>51</sub>N<sub>2</sub>ORuCl<sub>2</sub>; 806.2344, found 806.2329.

### **ARCM and AROCM.**

**General Procedure A for ARCM:** A flame-dried 10 mL two-neck round-bottom flask with a magnetic stir bar and condenser was charged with dichloride catalyst (5mol%) in CH<sub>2</sub>Cl<sub>2</sub> (0.002 M). Triene substrate was then injected and the reaction vessel was heated to 40°C for 3 hours. The solvent was then evaporated and the residue was purified by flash chromatography to yield ring-closed diene.

**General Procedure B for ARCM (2.13b Generated In Situ):** A flame-dried 10 mL two-neck round-bottom flask with a magnetic stir bar and condenser was charged with dichloride catalyst (5mol %) in THF (0.002 M). A solution of NaI (25 equivalents to catalyst) was then added and the solution stirred for 1 hour. Triene substrate was injected and the reaction vessel was heated to 40°C for 3 hours. The solvent was then evaporated and the residue was purified by flash chromatography to yield ring-closed diene.

<sup>1</sup>H and <sup>13</sup>C NMR spectra and GC spectra of triene products matched previously reported spectra. Synthesis of substrates was conducted according to the published protocols.<sup>2</sup>

**(S,E)-2-(but-2-en-2-yl)-3-methyl-2,5-dihydrofuran (2.24):** General Procedure A was followed using **2.23** (42.5 mg, 0.24 mmol) and **2.13a** (10 mg, 0.012 mmol). After 3 hours the solvent was evaporated and the residue was purified by flash chromatography (5% Et<sub>2</sub>O in pentane). An isolated yield was not obtained. The e.e. was determined by chiral GC (60ISO60, ret. times: 28.6 [major] 30.7 [minor]). <sup>1</sup>H NMR (300 MHz, CDCl<sub>3</sub>) matched the known characterization spectra: δ 5.56 (quintet, J = 1.6Hz, 1H), 5.52 (quartet, J = 6.9Hz, 1H), 4.88 (broad singlet, 1H), 4.53 – 4.68 (multiplet, 2H), 1.64 (doublet of quint, J = 6.9Hz, 3H), 1.56 (quint, J = 1.4 Hz, 3H), 1.47 (quint, J = 1.4 Hz, 3H).

---

<sup>2</sup> Funk, T. W.; Berlin, J. M.; Grubbs, R. H. *J. Am. Chem. Soc.*, **2006**, 128, 1840-1846.

**(*S,E*)-6-(but-2-en-2-yl)-2,2,5-trimethyl-3,6-dihydro-2*H*-1,2-oxasiline (2.26):**

General Procedure A was followed using **2.25** (62.4 mg, 0.262 mmol) and **2.13a** (10 mg, 0.0131 mmol). After 3 hours the solvent was evaporated and the residue was purified by flash chromatography (5% EtOAc in hexanes). An isolated yield was not obtained. The e.e. was determined by chiral GC (60ISO60, ret. times: 42.4 [major] 41.0 [minor]). <sup>1</sup>H NMR (300 MHz, CDCl<sub>3</sub>) matched the known characterization spectra: δ 5.69 (dq, *J* = 7.7, 1.4 Hz, 1H), 5.49 (q, *J* = 6.6 Hz, 1H), 4.54 (s, 1H), 1.63 (dd, *J* = 6.6, 1.1 Hz, 3H), 1.51 (s, 3H), 1.29 – 1.39 (m, 1H), 1.12 – 1.21 (m, 1H), 0.19 (s, 3H).

**(*S,E*)-6-(but-2-en-2-yl)-5-methyl-3,6-dihydro-2*H*-pyran (2.28):** General Procedure A was followed using **2.27** (25.5 mg, 0.131 mmol) and **2.13a** (5 mg, 0.00655 mmol). After 3 hours the solvent was evaporated and the residue was purified by flash chromatography (3% EtOAc in hexanes). An isolated yield was not obtained. The e.e. was determined by chiral GC (60ISO60, ret. times: 28.6 [major] 30.7 [minor]). <sup>1</sup>H NMR (300 MHz, CDCl<sub>3</sub>) matched the known characterization spectra: δ 5.56 – 5.68 (m, 1H), 5.53 (q, *J* = 6.6 Hz, 1H), 4.29 (s, 1H), 3.88 – 3.94 (m, 1H), 3.53 – 3.61 (m, 1H), 2.19 – 2.32 (m, 1H), 1.85 – 1.96 (m, 1H), 1.64 (dd, *J* = 6.6, 1.1 Hz, 3H), 1.54 (t, *J* = 1.4 Hz, 3H), 1.47 (q, *J* = 1.4 Hz, 3H).

**(*S,Z*)-7-((*E*)-but-2-en-2-yl)-6-methyl-2,3,4,7-tetrahydrooxepine (2.30):** General Procedure A was followed using **2.29** (44 mg, 0.209 mmol) and **2.13a** (8 mg, 0.0105 mmol). After 3 hours the solvent was evaporated and the residue was purified by flash chromatography (4% EtOAc in hexanes). An isolated yield was not obtained. The e.e.

was determined by chiral GC (60ISO90, ret. times: 82.1 [major] 80.5 [minor]).  $^1\text{H}$  NMR (300 MHz,  $\text{CDCl}_3$ ) matched the known characterization spectra:  $\delta$  5.57 – 5.62 (m, 1H), 5.51 (q,  $J$  = 6.6 Hz, 1H), 4.26 (s, 1H), 3.85 – 3.92 (m, 1H), 3.57 – 3.66 (m, 1H), 2.48 – 2.59 (m, 1H), 1.87 – 2.03 (m, 2H), 1.67 – 1.80 (m, 1H) 1.67 (t,  $J$  = 2.2 Hz, 3H), 1.65 (d,  $J$  = 6.6 Hz, 3H), 1.50 (s, 3H).

**General Procedure for AROCM:** To a flame-dried 10 mL two-neck round-bottom flask was added norbornene, styrene,  $\text{CH}_2\text{Cl}_2$  and dichloride catalyst (1mol%). The reaction was stirred at room temperature for 1 hour, at which time the solvent was evaporated and the residue was purified by flash chromatography.

**(4*R*,6*S*)-2-*tert*-butyl-4-styryl-6-vinyltetrahydrocyclopenta[*c*]pyrrole-1,3(2*H*,3*aH*)-dione (2.32):** Following the general procedure, norbornene **2.31** (29 mg, 0.131 mmol), styrene (0.15 mL, 1.31 mmol),  $\text{CH}_2\text{Cl}_2$  (2 mL) and **2.13a** (1 mg, 0.00131 mmol) were added to the reaction vessel. The reaction was stirred at room temperature for 1 hour, the solvent was evaporated and the residue was purified by flash chromatography (30%  $\text{Et}_2\text{O}$  in hexanes). An isolated yield was not obtained. The e.e. was determined by chiral HPLC (3% IPA/Hex, 1 mL/min, *trans* ret. times: 36.7 [major] 30.1 [minor], *cis* ret. times: 11.7 [major] 10.0 [minor]).  $^1\text{H}$  NMR (300 MHz,  $\text{CDCl}_3$ ) matched the known characterization spectra: *trans*:  $\delta$  7.39 – 7.18 (m, 5H), 6.48 – 6.32 (m, 2H), 6.07 – 5.95 (m, 1H), 5.16 – 5.09 (m, 2H), 3.16 – 2.91 (m, 5H), 2.03 – 1.96 (m, 1H), 1.54 (s, 9H); *cis*:  $\delta$  7.37 – 7.23 (m, 5H), 6.65 (d,  $J$  = 11.1 Hz, 1H), 6.02 – 5.90 (m, 1H), 5.64 (dd,  $J$  = 11.7,

11.7 Hz, 1H), 5.12 – 5.04 (m, 2H), 3.37 – 3.25 (m, 1H), 3.10 – 3.01 (m, 2H), 2.90 – 2.79 (m, 1H), 1.94 – 1.86 (m, 1H), 1.59 (s, 9H).

## REFERENCES AND NOTES

- (1) (a) Grubbs, R. H. *Handbook of Metathesis*; Wiley-VCH: Weinheim, Germany, **2003** and references cited therein. (b) Ivin, K. J.; Mol, J. C. *Olefin Metathesis and Metathesis Polymerization*; Academic Press: San Diego, CA. **1997** and references cited therein. (c) Noels, A. F.; Demonceau, A. *J. Phys. Org. Chem.* **1998**, *11*, 602–609. (d) Grubbs, R. H. *Tetrahedron*, **2004**, *60*, 7117–7140. (d) Grubbs, R. H. *Angew. Chem. Int. Ed.* **2006**, *45*, 3760–3765. (e) Schrock, R. R. *Angew. Chem. Int. Ed.* **2006**, *45*, 3748–3759.
- (2) (a) Stewart, I. C.; Ung, T.; Pletnev, A. A.; Berlin, J. M.; Grubbs, R. H.; Schrodi, Y. *Org. Lett.* **2007**, *9*, 1589–1592. (b) Chatterjee, A. K.; Choi, T. L.; Sanders, D. P.; Grubbs, R. H. *J. Am. Chem. Soc.* **2003**, *125*, 11360–1170. (c) Sanford, M. S.; Love, J. A.; Grubbs, R. H. *J. Am. Chem. Soc.* **2001**, *123*, 6543–6554. (d) Sanford, M. S.; Ulman, M.; Grubbs, R. H. *J. Am. Chem. Soc.* **2001**, *123*, 749–750. (e) Scholl, M.; Ding, S.; Lee, C. W.; Grubbs, R. H. *Org. Lett.* **1999**, *1*, 953–956. (f) Dias, E. L.; Nguyen, S. T.; Grubbs, R. H. *J. Am. Chem. Soc.* **1997**, *119*, 3887–3897. (g) Meek, S. J.; O'Brien, R. V.; Llaveria, J.; Schrock, R. R.; Hoveyda, A. H. *Nature*, **2011**, 461–466. (h) Flook, M. M.; Jiang, A. J.; Schrock, R. R.; Muller, P.; Hoveyda, A. H. *J. Am. Chem. Soc.* **2009**, *131*, 7962–7963. (i) Garber, S. B.; Kingsbury, J. S.; Gray, B. L.; Hoveyda, A. H. *J. Am. Chem. Soc.* **2000**, *122*, 8168–8179. (j) Hoveyda, A. H.; Schrock, R. R.; *Chem. Eur. J.* **2001**, *7*, 945–950.
- (3) (a) Seiders, T. J.; Ward, D. W.; Grubbs, R. H. *Org. Lett.* **2001**, *3*, 3225–3228.

- (b) Funk, T. W.; Berlin, J. M.; Grubbs, R. H. *J. Am. Chem. Soc.* **2006**, *128*, 1840–1846. (c) Berlin, J. M.; Goldberg, S. D.; Grubbs, R. H. *J. Am. Chem. Soc.* **2006**, *45*, 7591–7595.
- (4) (a) Teo, P.; Grubbs, R. H.; *Organometallics*, **2010**, *29*, 6045–6050. (b) Endo, K.; Grubbs, R. H. *J. Am. Chem. Soc.* **2011**, *133*, 8525–8527.
- (5) (a) Cortez, G. A.; Baxter, C. A.; Schrock, R. R.; Hoveyda, A. H. *Org. Lett.* **2007**, *9*, 2871–2874. (b) Alexander, J. B.; La, D. S.; Cefalo, D. R.; Graf, D. D.; Hoveyda, A. H.; Schrock, R. R. *J. Am. Chem. Soc.* **1998**, *120*, 4041–4042. (c) La, D. S.; Alexander, J. B.; Cefalo, D. R.; Graf, D. D.; Hoveyda, A. H.; Schrock, R. R. *J. Am. Chem. Soc.* **1998**, *120*, 9720–9721. (d) La, D. S.; Sattely, E. S.; Ford, J. G.; Schrock, R. R.; Hoveyda, A. H. *J. Am. Chem. Soc.* **2001**, *123*, 7767–7778. (e) Zhu, S. S.; Cefalo, D. R.; La, D. S.; Jamieson, J. Y.; Davis, W. M.; Hoveyda, A. H.; Schrock, R. R. *J. Am. Chem. Soc.* **1999**, *121*, 8251–8259. (f) Alexander, J. B.; Schrock, R. R.; Davis, W. M.; Hultsch, K. C.; Hoveyda, A. H.; Houser, J. H. *Organometallics*, **2000**, *19*, 3700–3715. (g) Fujimura, O.; Grubbs, R. H. *J. Am. Chem. Soc.* **1996**, *118*, 2499–2500. (h) Fujimura, O.; Grubbs, R. H. *J. Org. Chem.* **1998**, *63*, 824–832.
- (6) (a) Wenzel, A. G.; Grubbs, R. H. *J. Am. Chem. Soc.* **2006**, *128*, 16048–16049. (b) Wenzel, A. G.; Blake, G.; VanderVelde, D. G.; Grubbs, R. H. *J. Am. Chem. Soc.* **2011**, *133*, 6429–6439. (c) Romero, P. E.; Piers, W. E. *J. Am. Chem. Soc.* **2007**, *129*, 1698–1704. (d) Romero, P. E.; Pier, W. E. *J. Am. Chem. Soc.* **2005**, *127*, 5032–5033. (e) van der Eide, E. F.; Romero, P. E.; Piers, W. E. *J. Am. Chem. Soc.* **2008**, *130*, 4485–4491. (f) Leitao, E. M.; van der Eide, E. F.;

- Romero, P. E.; Piers, W. E.; McDonald, R. *J. Am. Chem. Soc.* **2010**, *132*, 2784–2794. (g) Rowley, C. N.; van der Eide, E. F.; Piers, W. E.; Woo, T. K. *Organometallics*, **2008**, *27*, 6043–6045. (h) Anderson, D. A.; Hickstein, D. D.; O’Leary, D. J.; Grubbs, R. H. *J. Am. Chem. Soc.* **2006**, *128*, 8386–8387.
- (7) (a) Correa, A.; Cavallo, L. *J. Am. Chem. Soc.* **2006**, *128*, 13352–13353. (b) Adlhart, C.; Chen, P. *J. Am. Chem. Soc.* **2004**, *126*, 3496–3510.
- (8) Palucki, M.; Finney, N. S.; Pospisil, P. J.; Guler, M. L.; Ishida, T.; Jacobsen, E. N. *J. Am. Chem. Soc.* **1998**, *120*, 948–954.
- (9) Ritter, T.; Day, M. W.; Grubbs, R. H. *J. Am. Chem. Soc.* **2006**, *128*, 11768–11769.
- (10) Ritter, T.; Hejl, A.; Wenzel, A. G.; Funk, T. W.; Grubbs, R. H. *Organometallics* **2006**, *25*, 5740–5745.
- (11) (a) Anakabe, E.; Carrillo, L.; Badia, D.; Vicario, J. L.; Villegas, M. *Synthesis*, **2004**, 1093–1101. (b) Roland, S.; Mangeney, P. *Eur. J. Org. Chem.* **2000**, 611–616. (c) Roland, S.; Mangeney, P.; Alexakis, A. *Synthesis* **1999**, 228–230.



*Chapter 3*FUSED *N*-HETEROCYCLIC CARBENES

This chapter was taken in part from: Li, J.; Stewart, I. C.; Grubbs, R. H.

*Organometallics*, **2010**, 29, 3765-3768.

## INTRODUCTION

*N*-heterocyclic carbenes (NHCs), first isolated by Arduengo et al. in 1991, have become a well-studied and well-utilized class of ligands in the field of transition metal-catalyzed reactions.<sup>1a</sup> Their proficiency in catalysis, variable electronic properties, and ease of translation into complex architectural structures have allowed for the development of unique reactivity and targeted selectivity.<sup>1</sup> In the past 20 years, NHCs have been applied as ligands in reactions such as palladium catalyzed cross-coupling, olefin metathesis, asymmetric hydrosilylation and conjugate addition.<sup>2</sup> Free NHCs have also shown great efficacy as organocatalysts in a variety of reactions.<sup>3</sup> Exploration of novel structural motifs has enabled the development of novel applications for NHCs. As the synthetic and catalytic applications have grown, the array of structural motifs has grown in parallel (figure 3.1), illustrating the dynamic interchange between structure and function.<sup>1a,4,5</sup>

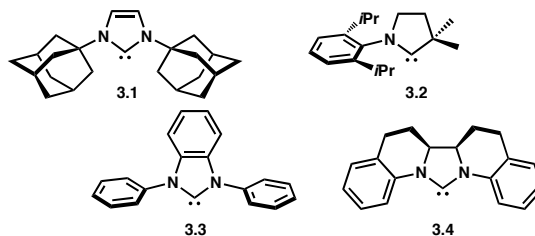


**Figure 3.1. NHCs Utilized in Metal-Mediated Catalysis.**

In particular, fused NHC structures are of interest, as it has been shown computationally that the rotational lability of the *N*-substituent on the carbene can greatly influence the behavior and dynamics of the NHC-bound metal complex.<sup>6</sup> In this study, the syntheses of fused carbenes **3.6** and **3.7** were designed to allow for control of stereochemistry at the backbone of the NHC as well as facile modification of the *N*-

bound arene fragment. A three-carbon chain from the backbone of the NHC to the arene was chosen to form the *cis*-fused **3.6** as well as the *trans*-fused **3.7** (figure 3.2). Independent synthesis of each carbene precursor allowed for separate *cis* and *trans* routes, bypassing a need to separate the meso from the racemic forms. Synthesis of the racemate could be easily modified to render the enantioenriched mixtures of the *trans*-species via resolution with inexpensive L-(+)-tartaric acid.<sup>7</sup>

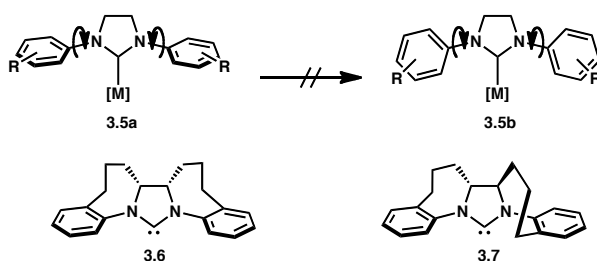


**Figure 3.2. Design of Rotationally Locked NHCs.**

Hermann and Blechert have synthesized similar NHC structures.<sup>5,8</sup> Carbene **3.4** was appended to ruthenium and shown to have limited metathesis activity.<sup>5</sup> Unfortunately, the synthesis of **3.4** yielded a 3:1 mixture of the meso and racemic forms, and only the meso form was isolated for study.<sup>5</sup> The crystal structure of carbene **3.4**, which contains a  $C_2$ -linkage, exhibited planarity of the *N*-bound arene with the heterocycle, thereby rendering the ruthenium species noncanonical with standard ruthenium-based catalysts.

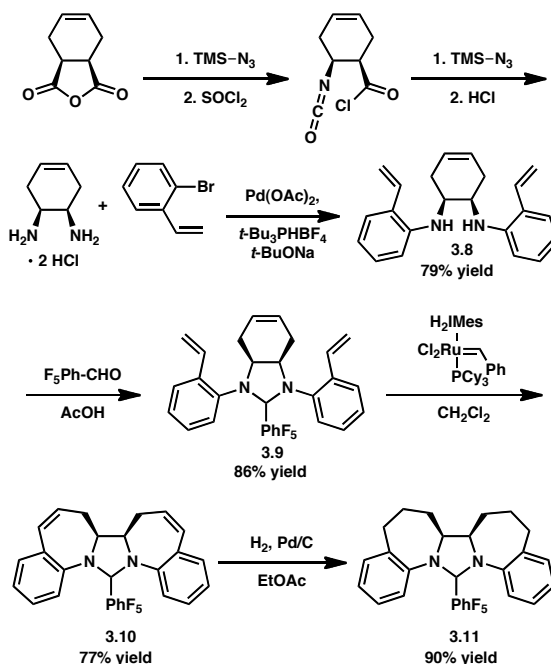
In designing both syntheses, we chose to utilize ring-closing metathesis as the key step in fusing the seven-membered ring fragment. Previous syntheses of fused NHC frameworks began from quinoline-type derivatives and were thus limited in both ring size and stereocontrol.<sup>5</sup> With intimate knowledge of the olefin metathesis reaction at hand, we

imagined separate syntheses hinging upon retention of the initially introduced backbone stereochemistry during ring closing metathesis (RCM).

## SYNTHESIS OF FUSED NHCS

The *cis*-cyclohexenyldiamine was synthesized by a known procedure.<sup>9</sup> Palladium catalyzed cross-coupling of the free diamine with *o*-bromostyrene yielded secondary diamine **3.8**. Attempts at ring-closing metathesis of **3.8** resulted in decomposition of both diamine and the ruthenium benzylidene species. In order to cloak the diamino functionality, **3.8** was condensed with pentafluorobenzaldehyde to form **3.9**, following a recent report.<sup>10</sup> Ring-closing with ruthenium catalyst provided *cis*-fused adduct **3.10** and hydrogenation gave the desired carbene precursor **3.11**.

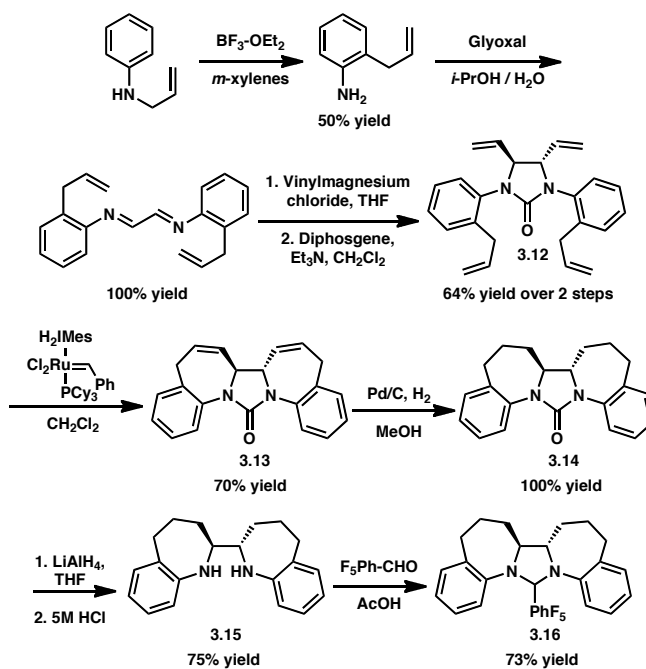
Scheme 3.1. Synthesis of *Cis*-Carbene Precursor 11.



Entry into the racemic *trans*-fused carbene began with *aza*-Claisen rearrangement of commercially available *N*-allylaniline. Condensation with glyoxal yielded the

bisimine, which was further functionalized via Grignard addition and *in situ* urea formation to give intermediate **3.12**. Although the pentafluorophenyl adduct could be introduced immediately succeeding addition of Grignard, the urea provided higher yields in the metathesis reaction, yielding ring-closed **3.13**.

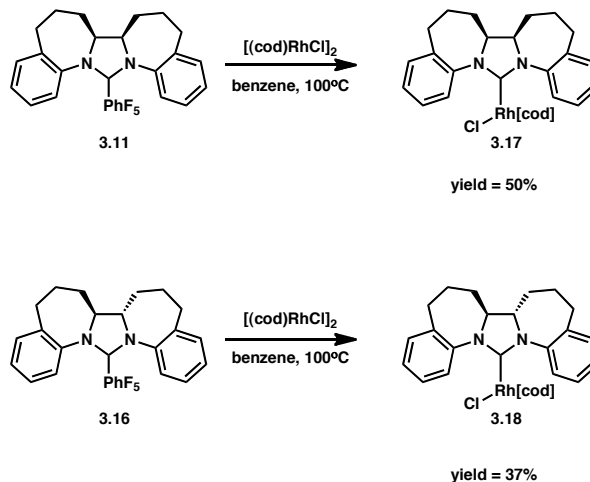
Scheme 3.2. Synthesis of *Trans*-Carbene Precursor **16**.



Hydrogenation with Pd/C at 1 atm gave the urea **3.14**, which was readily cleaved with lithium aluminum hydride to afford *trans*-fused diamine **3.15**. The free diamine was then condensed with pentafluorobenzaldehyde to provide the carbene precursor **3.16**. Multiple attempts at synthesizing and isolating the ruthenium olefin metathesis catalyst containing the *cis*- and *trans*-fused NHCs were conducted from a variety of masked carbene precursors including compounds **3.16** and **3.11** but were unsuccessful. A transient novel benzyldiene was observed with the decomposition of **3.16** with Grubbs first generation catalyst. However, it proved unstable to chromatography for isolation.

## SYNTHESIS OF RHODIUM COMPLEXES

Scheme 3.3. Synthesis of Rhodium Complexes.



Recently, we reported the facile decomposition of pentafluorophenyl adducts as NHC-precursors for ruthenium complexes.<sup>10</sup> We chose to isolate the masked carbene as pentafluorophenyl adducts rather than the traditional imidazolium salts in order to allow ligation onto metal fragments in the absence of a strong base. Thus, reaction of **3.11** or **3.16** with rhodium cyclooctadiene chloride dimer gave the corresponding rhodium complexes shown (scheme 3.3). Crystals suitable for X-ray diffraction studies were obtained as bright yellow blocks by vapor diffusion of pentane into a benzene solution of either **3.17** or **3.18**.

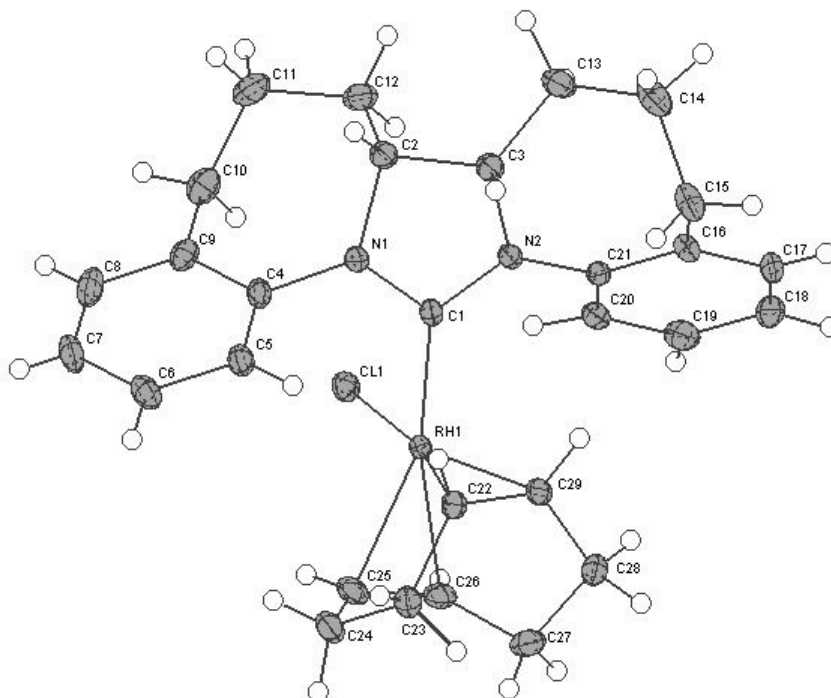


**Figure 3.3. ORTEP Diagram of 3.17 with 50% Probability Ellipsoids.**

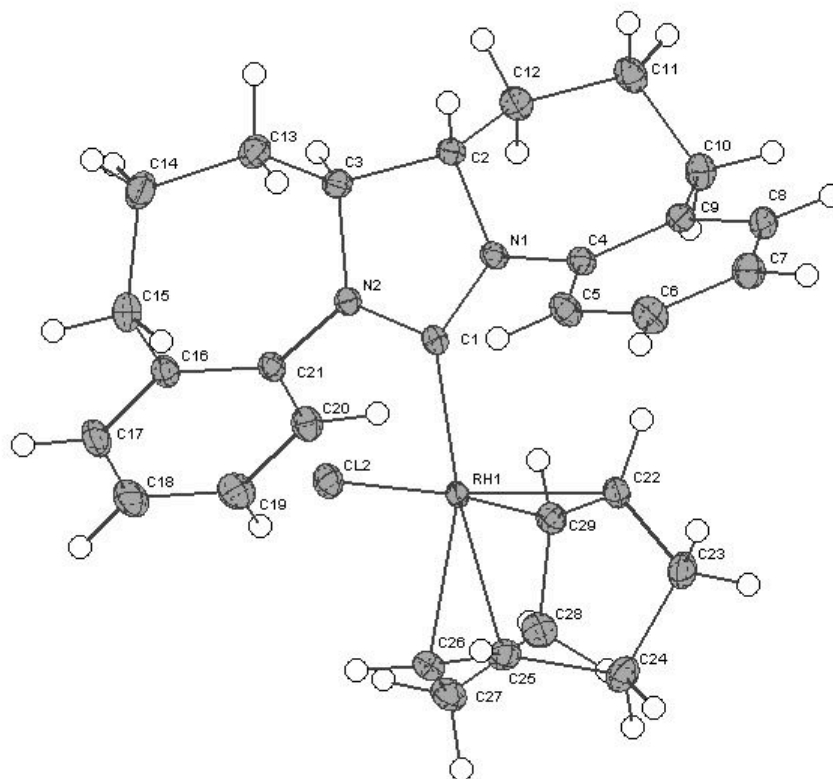
Figure 3.3 shows the ORTEP diagram of the *cis*-fused rhodium complex **3.17** obtained from X-ray diffraction. We were surprised to note that, although there exists a *cis*-orientation at the backbone of the NHC, a distortion in the carbene allows the two linkers to obtain a relative *trans*-configuration of the *N*-bound arenes. Note that the dihedral torsion angle between C(12)-C(2)-C(3)-C(13) at  $37.57^\circ$  confirms a *cis*-orientation (table 3.1). Neither arene is orthogonal to the plane of the NHC, containing dihedral angles at C(5)-C(4)-N(1)-C(1) of  $67.86^\circ$  and at C(20)-C(21)-N(2)-C(1) of  $31.84^\circ$ .

**Table 3.1. Selected Bond Lengths [Å] and Angles [°] for 3.17**

Rh(1)-C(1)	1.992(2)	C(1)-N(1)-C(2)	111.93(17)
Rh(1)-C(29)	2.105(2)	C(1)-N(2)-C(3)	110.99(17)
Rh(1)-C(22)	2.124(2)	N(1)-C(1)-N(2)	106.57(19)
Rh(1)-C(25)	2.207(2)	N(1)-C(1)-Rh(1)	124.58(14)
Rh(1)-C(26)	2.247(2)	N(2)-C(1)-Rh(1)	128.82(15)
Rh(1)-Cl(1)	2.4075(5)	N(1)-C(2)-C(3)	98.93(17)
		N(2)-C(3)-C(2)	100.04(18)
		C(12)-C(2)-C(3)-C(13)	37.57
		C(5)-C(4)- N(1)-C(1)	67.86
		C(20)-C(21)-N(2)-C(1)	31.84

X-ray crystal analysis of *trans*-fused **3.18** confirmed the expected *anti,anti*-relationship. Analogous to previously reported nonfused ligated NHCs, figure 3.4 shows the NHC to be planar, without the distortion noted in figure 3.3.





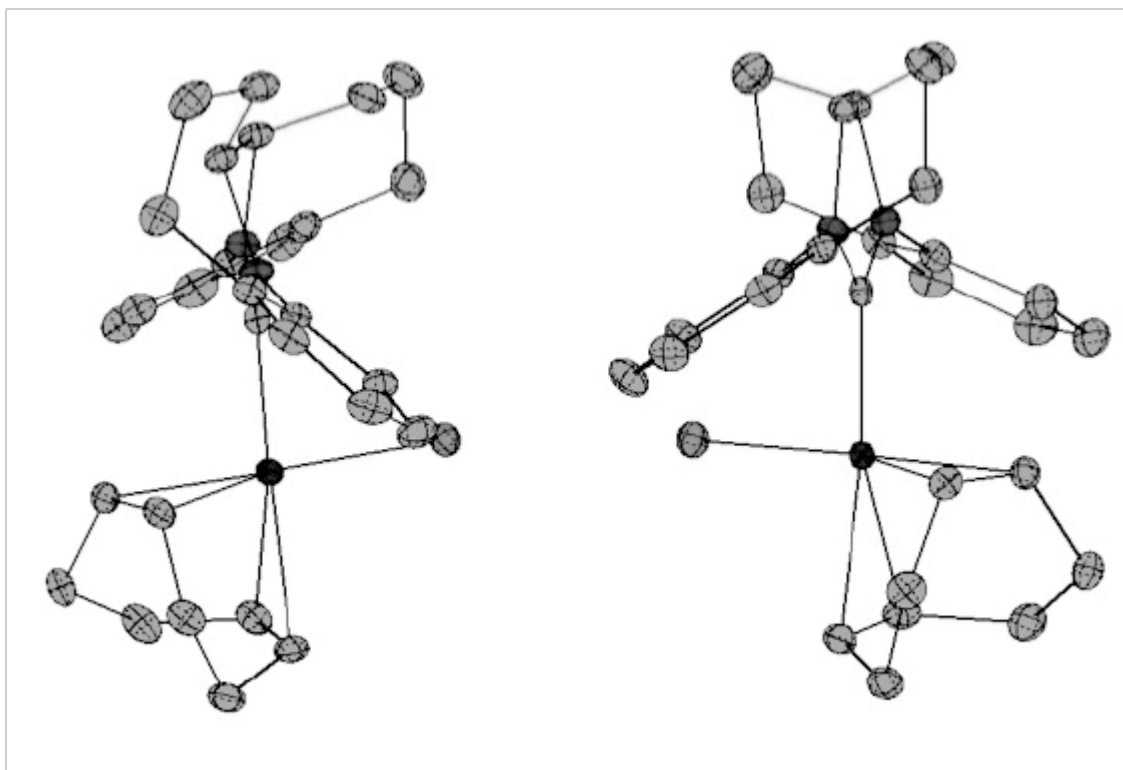
**Figure 3.4. ORTEP Diagram of 3.18 with 50% Probability Ellipsoids.**

Table 3.2 lists selected bond lengths and angles for **3.18**. Here the dihedral torsion angle at the backbone of the carbene is greater than  $90^\circ$ , with the angle at C(12)-C(2)-C(3)-C(13) of  $136.83^\circ$ . Again, neither arene ring is orthogonal or planar to the NHC, with dihedral angles at C(5)-C(4)-N(1)-C(1) of  $50.98^\circ$  and at C(20)-C(21)-N(2)-C(1) of  $62.57^\circ$ .

**Table 3.2. Selected Bond Lengths [Å] and Angles [°] for 3.18**

Rh(1)-C(1)	2.0032(7)	C(1)-N(1)-C(2)	113.12(5)
Rh(1)-C(22)	2.0969(7)	C(1)-N(2)-C(3)	113.17(5)
Rh(1)-C(29)	2.1263(8)	N(1)-C(1)-N(2)	107.40(6)
Rh(1)-C(26)	2.1847(8)	N(1)-C(1)-Rh(1)	123.40(5)
Rh(1)-C(25)	2.2169(8)	N(2)-C(1)-Rh(1)	129.10(5)
Rh(1)-Cl(1)	2.3896(2)	N(1)-C(2)-C(3)	101.40(6)
		N(2)-C(3)-C(2)	101.27(5)
		C(12)-C(2)-C(3)-C(13)	136.83
		C(5)-C(4)- N(1)-C(1)	50.98
		C(20)-C(21)-N(2)-C(1)	62.57

A simplified side view of both *cis*- and *trans*-fused Rh-species with hydrogens omitted for clarity is shown in figure 3.5. It is clear that the *cis*-linkage exists for complex **3.17**, however, the arenes are locked in a relative *trans*-conformation, similar to that of complex **3.18**, which shows a higher degree of overall symmetry.



**Figure 3.5. Side View of Structures 3.17 and 3.18.**

## CONCLUSIONS

In summary, we have developed the synthesis of stereochemically defined fused *N*-heterocyclic carbene structures that can be obtained in gram quantities either as the meso form or the racemate. X-ray crystallography data confirmed the covalent linkages. Attempts were made at synthesizing the ruthenium olefin metathesis catalysts bearing these novel NHC structures. However, the final metallated complexes proved transitory and unstable to isolation. Instead, rhodium complexes were formed and studied in the solid state for conformation and structure.

## EXPERIMENTAL METHODS

### Materials and Methods

All reactions involving metal complexes were conducted under nitrogen or argon atmospheres using standard glove box or standard Schlenk techniques. Solvents were purified by passage through alumina.<sup>1</sup> Resonances for NMR spectra are reported relative to Me<sub>4</sub>Si ( $\delta$  0.0) for <sup>1</sup>H and <sup>13</sup>C. Spectra are reported as follows: chemical shift ( $\delta$  ppm), integration, multiplicity and coupling constant (Hz). Ruthenium starting materials were provided by Materia, Inc. All other reagents were purchased from Aldrich and used without prior purification.

**Synthesis of cyclohex-4-ene-1,2-diamine hydrochloride salt:** For detailed procedures, see: Witiak, et al. *J. Med. Chem.* **1987**, *30*, 1327-1336.

**Synthesis of (3.8):** A flame-dried 50 mL 2-neck r.b. flask was charged with Pd(OAc)<sub>2</sub> (25 mg, 0.11 mmol), *t*Bu<sub>3</sub>PH<sup>+</sup>BF<sub>4</sub><sup>-</sup> (96 mg, 0.33 mmol), NaOtBu (0.62 g, 6.0 mmol) and a stirbar. Toluene (10 mL) was added via cannula and the suspension was stirred for 15 minutes at r.t. 2-Bromostyrene (0.34 mL, 2.7 mmol) was added via syringe, followed by the diamine (0.2 g, 1.08 mmol) via spatula. The suspension was heated to 100 °C and stirred for 18 h. After cooling to r.t., the suspension was filtered through a pad of Celite, which was then washed with additional toluene (100 mL). Concentration of the combined toluene solutions afforded a dark brown oil. The desired product was obtained

---

<sup>1</sup> Pangborn, A. B.; Giardello, M. A.; Grubbs, R. H.; Rosen, R. K.; Timmers, F. J. *Organometallics* **1996**, *15*, 1518–1520.

via silica gel chromatography (40:1 → 10:1 pentane:Et<sub>2</sub>O) as a pale beige oil. <sup>1</sup>H NMR (300 MHz, CDCl<sub>3</sub>) δ 7.23 (dd, J = 7.5, 1.7 Hz, 2H), 7.16 – 7.04 (m, 2H), 6.84 – 6.54 (m, 6H), 5.69 (t, J = 1.5 Hz, 2H), 5.52 (dd, J = 17.3, 1.6 Hz, 2H), 5.21 (dd, J = 11.0, 1.6 Hz, 2H), 4.13 (br s, 2H), 3.93 (t, J = 5.0 Hz, 2H), 2.53 (dd, J = 16.5, 3.9 Hz, 2H), 2.17 (dd, J = 16.6, 5.2 Hz, 2H). <sup>13</sup>C NMR (75 MHz, CDCl<sub>3</sub>) δ 144.7, 133.0, 130.4, 129.1, 127.9, 125.6, 125.2, 118.1, 116.6, 113.0, 50.9, 30.1. HR-MS (FAB+) Calculated for C<sub>22</sub>H<sub>25</sub>N<sub>2</sub>: 317.2018; found: 317.2032.

**Synthesis of (3.9):**<sup>3</sup> A procedure analogous to the formation of (3.16) was followed.

<sup>1</sup>H NMR (300 MHz, CDCl<sub>3</sub>) δ 18.79 (s, 1H), 7.97 (d, J = 4.2 Hz, 2H), 7.64 – 7.59 (m, 2H), 7.39 – 7.12 (m, 8H), 6.97 (d, J = 7.8 Hz, 2H), 4.38 – 3.93 (m, 4H), 2.49 (s, 2H), 2.28 (s, 2H). <sup>19</sup>F NMR (470 MHz, CDCl<sub>3</sub>) δ -137.35 (1F), -144.88 (1F), -154.52 (1F), -162.96 (1F), -163.60 (1F). HRMS (EI+) calculated 494.1781 found 494.1764.

**Synthesis of (3.10):** A procedure analogous to the formation of (3.13) was followed.

<sup>1</sup>H NMR (300 MHz, CDCl<sub>3</sub>) δ 7.13 (dd, J = 1.5, 7.8 Hz, 2H), 7.08 – 7.02 (m, 3H), 6.88 (dt, J = 1.5, 8.1 Hz, 2H), 6.67 (d, J = 3.3 Hz, 2H), 6.63 (s, 1H), 6.52 (dd, J = 2.1, 11.4 Hz, 2H), 6.29 – 5.99 (m, 2H), 4.26 – 4.00 (m, 2H), 2.94 – 2.36 (m, 2H), 1.55 (s, 1H). <sup>13</sup>C NMR (75 MHz, CDCl<sub>3</sub>) δ 147.8, 143.9, 132.3, 132.1, 128.8, 128.2, 127.5, 126.1, 120.5, 116.1, 72.5, 67.4, 31.1. HRMS (EI+) calculated 494.1781 found 494.1764.

**Synthesis of (3.11):** A procedure analogous to the formation of (3.14) was followed.

$^1\text{H}$  NMR (300 MHz,  $\text{CDCl}_3$ )  $\delta$  7.05 – 6.95 (m, 4H), 6.85 (dt,  $J$  = 1.2, 7.2 Hz, 2H), 6.64 (d,  $J$  = 8.4 Hz, 2H), 6.47 (s, 1H), 4.03 – 4.00 (m, 2H), 3.08 – 2.99 (m, 2H), 2.69 – 2.63 (m, 2H), 1.95 – 1.87 (m, 2H), 1.69 – 1.59 (m, 6H).  $^{19}\text{F}$  NMR (470 MHz,  $\text{CDCl}_3$ )  $\delta$  -146.51 (bs, 1F), -154.58 (t, 1F), -163.12 (bs, 2F). HRMS (FAB+) calculated for  $\text{C}_{27}\text{H}_{22}\text{N}_2\text{F}_5$  469.1703 found 469.1705.

**2-allylaniline:** To a r.t. solution of *N*-allylaniline (2.7 mL, 20 mmol) in *m*-xylene (40 mL) in a 200 mL round bottom flask with a teflon stopcock adapter was added  $\text{BF}_3 \cdot \text{Et}_2\text{O}$  (3 mL, 24 mmol) via syringe. The flask was sealed and the solution was heated at 150 °C for 18 h. After cooling to r.t., excess  $\text{BF}_3$  was quenched by careful addition of 15% NaOH. The resulting suspension was diluted with  $\text{Et}_2\text{O}$  (100 mL) and the organic layer was separated, and washed with brine. The aqueous layer was extracted with additional (100 mL)  $\text{Et}_2\text{O}$ . The combined organic layers were dried with  $\text{MgSO}_4$ , filtered and concentrated to afford a mixture of the starting material and product, which could be purified by fractional distillation.<sup>2</sup>

***N,N'*-(ethane-1,2-diylidene)bis(2-allylaniline):** A flask was charged with 2-allylaniline (0.79 g, 5.9 mmol), 2-propanol (6 mL), water (6 mL) and a stirbar. Glyoxal (0.31 mL, 2.7 mmol) was then added dropwise via syringe. After stirring at r.t. for 1 h, the bright yellow precipitate was collected via filtration using a C frit and washed sparingly with 2-propanol to afford the desired product.  $^1\text{H}$  NMR (300 MHz,  $\text{CDCl}_3$ )  $\delta$  8.30 (s, 2H), 7.34 – 7.17 (m, 4H), 7.08 – 6.94 (m, 2H), 6.07 – 5.87 (m, 2H), 5.09 – 4.92 (m, 4H), 3.57 (dt,  $J$

<sup>2</sup> Gagne, M. R.; Marks, T. J. *J. Am. Chem. Soc.*, **1989**, *111*, 4108-4109.

= 6.5, 1.4 Hz, 4H).  $^{13}\text{C}$  NMR (75 MHz,  $\text{CDCl}_3$ )  $\delta$  160.1, 149.2, 137.3, 134.9, 130.1, 127.8, 127.5, 117.6, 115.9, 35.9. HRMS (FAB+): Calculated for  $\text{C}_{20}\text{H}_{21}\text{N}_2$ : 289.1705; found: 289.1719.

**Synthesis of  $N^3,N^4$ -bis(2-allylphenyl)hexa-1,5-diene-3,4-diamine:** A flame-dried 50 mL 2-neck r.b. flask was charged with the diimine (1.0 g, 3.5 mmol) and a stirbar. Dry THF (15 mL) was added via cannula and the orange solution was cooled to  $-78^\circ\text{C}$ . Vinyl Grignard (13.9 mL, 1.0 M in  $\text{Et}_2\text{O}$ , Aldrich) was added dropwise via syringe, causing the orange solution to turn green. After stirring for 30 min at  $-78^\circ\text{C}$ , the solution was warmed to r.t. and stirred for an additional 2 h. After this time the solution was again clear and orange. Excess Grignard was quenched by careful addition of brine. The resulting suspension was diluted with  $\text{Et}_2\text{O}$  and washed with brine. The organic layer was dried with  $\text{Na}_2\text{SO}_4$  and concentrated to afford an orange solid (sometimes a reddish oil).  $^1\text{H}$  NMR (300 MHz,  $\text{CDCl}_3$ )  $\delta$  7.25 – 6.95 (m, 4H), 6.78 – 6.60 (m, 4H), 6.01 – 5.70 (m, 4H), 5.32 (dd,  $J$  = 16.9, 8.6 Hz, 4H), 5.09 (m, 4H), 4.12 (d,  $J$  = 8.8 Hz, 2H), 3.30 (d,  $J$  = 6.1 Hz, 4H).  $^{13}\text{C}$  NMR (75 MHz,  $\text{CDCl}_3$ )  $\delta$  145.1, 136.4, 136.0, 130.2, 127.7, 124.3, 118.5, 117.8, 116.7, 112.0, 59.1, 36.8. HR-MS (FAB+) Calculated for  $\text{C}_{24}\text{H}_{29}\text{N}_2$ : 345.2331; found: 345.2339.

**Synthesis of 1,3-bis(2-allylphenyl)-4,5-divinylimidazolidin-2-one (3.12):** Crude  $N^3,N^4$ -bis(2-allylphenyl)hexa-1,5-diene-3,4-diamine was taken up in dry  $\text{CH}_2\text{Cl}_2$  (30 mL).  $\text{Et}_3\text{N}$  (0.73 mL, 5.2 mmol) and DMAP (10 mg) were added and the solution was cooled to  $0^\circ\text{C}$ . Diphosgene (0.46 mL, 3.82 mmol) was added and the solution was stirred for 2 h.

Excess diphosgene was then quenched by careful addition of H<sub>2</sub>O. The suspension was then washed with brine, dried with MgSO<sub>4</sub>, filtered and concentrated. The resulting pale yellow solid was washed with hexanes and dried. Silica gel chromatography afforded the desired product (4:1 hexanes:EtOAc). <sup>1</sup>H NMR (300 MHz, CDCl<sub>3</sub>) δ 7.40 – 7.10 (m, 8H), 6.09 – 5.89 (m, 2H), 5.89 – 5.68 (m, 2H), 5.23 – 5.02 (m, 8H), 4.35 (dd, J = 6.0, 1.9 Hz, 2H), 3.66 – 3.25 (m, 4H). <sup>13</sup>C NMR (75 MHz, CDCl<sub>3</sub>) δ 157.0, 138.9, 137.3, 136.4, 134.5, 130.5, 127.6, 127.0, 121.3, 116.4, 66.6, 36.0. HR-MS (FAB+) Calculated for C<sub>25</sub>H<sub>27</sub>N<sub>2</sub>O: 371.2123; found: 371.2119.

**Synthesis of (3.13):** A 100 mL r.b. flask was charged with **3.12** (0.69 g, 1.86 mmol) and a stirbar. The flask was flushed with argon, and dry CH<sub>2</sub>Cl<sub>2</sub> was added via cannula. An oven-dried 10 mL r.b. flask was cooled under argon and then charged with the catalyst (63 mg, 0.07 mmol), to which CH<sub>2</sub>Cl<sub>2</sub> (1 mL) was added via syringe. The catalyst solution was then added dropwise to the substrate solution. After 4 h at r.t., the amber solution was filtered through a pad of SiO<sub>2</sub>, which was washed with a 3:1 hexanes:ethyl acetate solution (200 mL) to afford the desired product. <sup>1</sup>H NMR (300 MHz, CDCl<sub>3</sub>) δ 7.51 (d, J = 7.9 Hz, 2H), 7.34 – 6.98 (m, 6H), 6.09 – 5.79 (m, 2H), 5.58 (dd, J = 11.4, 2.4 Hz, 2H), 4.15 – 3.75 (m, 4H), 3.06 (dd, J = 16.1, 8.7 Hz, 2H). <sup>13</sup>C NMR (75 MHz, CDCl<sub>3</sub>) δ 167.6, 139.2, 138.8, 138.3, 129.0, 127.8, 126.6, 126.2, 125.7, 77.7, 77.4, 77.2, 76.8, 63.1, 32.4. HR-MS (FAB+) Calculated for C<sub>21</sub>H<sub>18</sub>N<sub>2</sub>O: 314.1419; found: 314.1416.

**Synthesis of (3.14):** A 100 mL r.b. flask was charged with the tetracyclic urea (0.58 g, 1.86 mmol), MeOH (20 mL) and a stirbar. 10% Pd/C (0.1g, 0.09 mmol) was added and



the flask was flushed with argon. A balloon of H<sub>2</sub> was attached and the suspension was stirred until TLC indicated complete consumption of starting material. The suspension was then filtered through a plug of Celite and concentrated to afford the desired product as a beige solid. <sup>1</sup>H NMR (300 MHz, CDCl<sub>3</sub>) δ 7.47 (dd, J = 8.0, 1.2 Hz, 2H), 7.31 – 7.05 (m, 4H), 3.17 (d, J = 10.8 Hz, 2H), 2.99 – 2.72 (m, 2H), 2.03 (d, J = 12.3 Hz, 4H), 1.80 (d, J = 12.5 Hz, 2H), 1.47 – 1.26 (m, 2H). <sup>13</sup>C NMR (75 MHz, CDCl<sub>3</sub>) δ 156.6, 139.8, 138.7, 130.4, 127.2, 126.0, 125.9, 64.1, 38.8, 35.6, 24.9. HR-MS (FAB+) Calculated for C<sub>21</sub>H<sub>22</sub>N<sub>2</sub>O: 318.1732; found: 318.1742.

**Synthesis of (3.15):** A 10 mL 2-neck r.b. flask was charged with **3.14** (0.35 g, 1.10 mmol) and a stirbar. A reflux condenser was attached and the system was flushed with argon. Dry THF (15 mL) was added by syringe and LiAlH<sub>4</sub> (0.22 g, 5.5 mmol) was added portionwise via spatula. The suspension was then heated at reflux for 2 h. After cooling to r.t., excess LiAlH<sub>4</sub> was quenched by careful addition of H<sub>2</sub>O and 1 M NaOH. The slurry was filtered through a pad of Celite and extracted with Et<sub>2</sub>O. The combined organic layers were concentrated, and the resulting residue was treated with 5 M HCl and heated to 60 °C for 2 h. The solution was cooled to r.t. and the pH was adjusted to 12 using 1 normal NaOH. The desired product was then extracted with CH<sub>2</sub>Cl<sub>2</sub>, dried with Na<sub>2</sub>SO<sub>4</sub>, and concentrated to afford a pale beige solid. <sup>1</sup>H NMR (300 MHz, CDCl<sub>3</sub>) δ 7.17 – 7.03 (m, 4H), 6.93 – 6.80 (m, 4H), 2.97 – 2.61 (m, 6H), 2.04 – 1.77 (m, 6H), 1.63 – 1.44 (m, 2H). <sup>13</sup>C NMR (75 MHz, CDCl<sub>3</sub>) δ 148.6, 133.6, 130.8, 127.0, 121.3, 119.9, 61.9, 35.4, 34.6, 25.4. HR-MS (FAB+) Calculated for C<sub>20</sub>H<sub>25</sub>N<sub>2</sub>: 293.2018; found: 293.2018.

**Synthesis of (3.16)<sup>3</sup>:** A 10 mL r.b. flask was charged with a solution of the diamine (0.35 g, 1.2 mmol) in acetic acid (0.8 mL) and a stirbar. Pentafluorobenzaldehyde (0.4 g, 2 mmol) was added and the solution was stirred at r.t. overnight. The resulting precipitate was collected by filtration using an M frit and washed with cold methanol. <sup>1</sup>H NMR (600 MHz, CDCl<sub>3</sub>) δ 7.34 (d, J = 8.4 Hz, 1H), 7.21 (t, J = 7.8 Hz, 1H), 7.14 (t, J = 6 Hz, 1H), 7.13 (d, J = 6 Hz, 1H), 7.03 (s, 1H), 6.98 (d, J = 7.8 Hz, 1H), 6.93 (t, J = 7.2 Hz, 1H), 6.86 (d, J = 7.8 Hz, 1H), 6.72 (t, J = 7.2 Hz, 1H), 4.36 (t, J = 12.6 Hz, 1H), 3.25 (m, 1H), 2.78 (m, 2H), 2.71 (t, J = 15.6 Hz, 1H), 2.48 (dd, J = 4.2 Hz, 15.6 Hz, 1H), 2.04 (d, J = 12.6 Hz, 2H), 1.93 (m, 3H), 1.79 (m, 2H), 1.34 (m, 1H). <sup>13</sup>C NMR (125 MHz, CDCl<sub>3</sub>) δ 146.0 (d, 2C), 145.4, 143.7, 141.0 (d, 1C), 137.7 (d, 2C), 137.1, 131.3, 130.8, 129.1, 127.7, 127.1, 122.7, 119.2, 116.6, 116.4, 112.5, 69.4, 68.9, 67.5, 36.3, 34.4, 31.8, 28.6, 26.1, 24.9. <sup>19</sup>F NMR (470 MHz, CDCl<sub>3</sub>) δ -143.75 (dd, 2F), -155.30 (t, 1F), -162.67 (dt, 2F). HRMS (FAB+) calculated for C<sub>27</sub>H<sub>22</sub>N<sub>2</sub>F<sub>5</sub> 469.1703; found: 469.1709.

## FORMATION OF RHODIUM COMPLEXES:

**Synthesis of (3.17):** See below for the analogous procedure to the formation of (3.18).

For proton and carbon shifts, please see attached spectra. Proton NMR and 2D experiments indicated two rotational isomers at room temperature. Variable temperature experiments were conducted up to 60 °C and showed no exchange between the two species at that temperature. HRMS (FAB+) calculated for C<sub>29</sub>H<sub>34</sub>ClN<sub>2</sub>Rh 548.1466 found 548.1460

---

<sup>3</sup> Blum, A. P.; Ritter, T.; Grubbs, R. H. *Organometallics* **2007**, 26, 2122.

**Synthesis of (3.18):** In the glovebox, a 25 mL Schlenck flask equipped with a stirbar was charged with  $[\text{Rh}(\text{COD})\text{Cl}]_2$  (18 mg, 0.073 mmols) and the pentafluorophenyl adduct (34 mg, 0.072 mmols). To this was added 2 mL of benzene. The flask was sealed, removed from the glove box and heated at 100°C for 48 h. The reaction mixture was purified on silica gel (50% ether/hexanes) to afford a crystalline yellow solid. A single rotational isomer was identified in solution.  $^1\text{H}$  NMR (500 MHz,  $\text{CDCl}_3$ )  $\delta$  8.56 (d,  $J$  = 8.4 Hz, 1H), 7.74 (d,  $J$  = 7.8 Hz, 1H), 7.38 (t,  $J$  = 6.6 Hz, 1 H), 7.31 – 7.28 (m, 1H), 7.25 – 7.21 (m, 3H), 7.17 (d,  $J$  = 8.4 Hz, 1H), 4.68 – 4.63 (m, 1H), 4.61 – 4.57 (m, 1H), 3.66 (t,  $J$  = 15 Hz, 1H), 3.34 – 3.31 (m, 1H), 3.27 (t,  $J$  = 12 Hz, 2H), 2.86 (dd,  $J$  = 5.4, 18.6 Hz, 1H), 2.74 – 2.68 (m, 2H), 2.62 (t,  $J$  = 18 Hz, 1H), 2.00 – 1.95 (m, 3H), 1.86 (d,  $J$  = 21.6 Hz, 1H), 1.77 – 1.71 (m, 4H), 1.61 (s, 2H), 1.50 – 1.34 (m, 6H).  $^{13}\text{C}$  NMR (125 MHz,  $\text{CDCl}_3$ )  $\delta$  209.2 (d,  $J$  = 47.1 Hz, C–Rh), 142.5, 141.7, 140.9, 137.4, 130.8, 129.7, 129.2, 127.9, 127.8, 127.4, 127.2, 126.0, 99.6 (d,  $J$  = 6.3 Hz, 1C), 98.1 (d,  $J$  = 5.1 Hz, 1C), 71.2, 71.1, 70.7 (d,  $J$  = 15.6 Hz, 1C), 65.8 (d,  $J$  = 14.4 Hz, 1C), 38.2, 37.8, 36.0, 35.5, 33.3, 31.2, 29.5, 27.2, 24.7, 24.6. HRMS (FAB+) calculated for  $\text{C}_{29}\text{H}_{34}\text{ClN}_2\text{Rh}$  548.1544; found: 548.1530

## REFERENCES AND NOTES

- (1) (a) Arduengo, A. J.; Harlow, R. L.; Kline, M. *J. Am. Chem. Soc.* **1991**, *113*, 361–363. (b) Dixon, D. A.; Arduengo, A. J. *J. Phys. Chem.* **1991**, *95*, 4180–4182. (c) Diez–Gonzalez, S.; Marion, N.; Nolan, S. P. *Chem. Rev.* **2009**, *109*, 3612–3676. (d) Corberan, R.; Mas–Marza, E.; Peris, E. *Eur. J. Inorg. Chem.* **2009**, 1700–1716. (e) Lee, H. M.; Lee, C. C.; Cheng, P. Y. *Curr. Org. Chem.* **2007**, *11*, 1491–1524. (f) Herrmann, W. A.; Schutz, J.; Frey, G. D.; Herdtweck, E. *Organometallics* **2006**, *25*, 2437–2448.
- (2) (a) Schwab, P.; France, M. B.; Ziller, J. W.; Grubbs, R. H. *Angew. Chem. Int. Ed.* **1995**, *34*, 2039–2041. (b) Trnka, T. M.; Grubbs, R. H. *Acc. Chem. Res.* **2001**, *34*, 18–29. (c) Herrmann, W. A. *Angew. Chem. Int. Ed.* **2002**, *41*, 1290–1309. (d) Crudden, C. M.; Allen, D. P. *Coord. Chem. Rev.* **2004**, *248*, 2247–2273. (e) Snead, D. R.; Seo, H.; Hong, S. *Curr. Org. Chem.* **2008**, *12*, 1370–1387. (f) de Fremont, P.; Marion, N.; Nolan, S. P. *Coord. Chem. Rev.* **2009**, *253*, 862–892.
- (3) (a) Enders, D.; Balensiefer, T. *Acc. Chem. Res.* **2004**, *37*, 534–541. (b) Brown, M. K.; May, T. L.; Baxter, C. A.; Hoveyda, A. H. *Angew. Chem. Int. Ed.* **2007**, *46*, 1097–1100.
- (4) Berlin, J. M.; Campbell, K.; Ritter, T.; Funk, T. W.; Chlenov, A.; Grubbs, R. H. *Org. Lett.* **2007**, *9*, 1339–1342.
- (5) Vehlow, K.; Gessler, S.; Blechert, S. *Angew. Chem. Int. Ed.* **2007**, *46*, 8082–8085.
- (6) (a) Clavier, H.; Correa, A.; Cavallo, L.; Escudero–Adan, E. C.; Benet–Buchholz, J.; Slawin, A. M. Z.; Nolan, S. P. *Eur. J. Inorg. Chem.* **2009**, 1767–1773.

- (b) Ragone, F.; Poater, A.; Cavallo, L. *J. Am. Chem. Soc.* **2010**, *132*, 4249–4258.
- (7) Schanz, H. J.; Linseis, M. A.; Gilheany, D. G. *Tetrahedron–Asymmetry* **2003**, *14*, 2763–2769.
- (8) (a) Herrmann, W. A.; Baskakov, D.; Herdtweck, E.; Hoffmann, S. D.; Bunlaksanausorn, T.; Rampf, F.; Rodefied, L. *Organometallics*, **2006**, *25*, 2449–2456. (b) Baskakov, D.; Herrmann, W. A.; Herdtweck, E.; Hoffmann, S. D. *Organometallics* **2007**, *26*, 626–632.
- (9) Witiak, D. T.; Rotella, D. P.; Filippi, J. A.; Gallucci, J. *J. Med. Chem.* **1987**, *30*, 1327–1336.
- (10) Blum, A. P.; Ritter, T.; Grubbs, R. H. *Organometallics* **2007**, *26*, 2122–2124.

*Chapter 4*

## SELECTIVE DIENE METATHESIS

## INTRODUCTION

Selectivity in the olefin metathesis reaction encompasses many challenging and unique problems including enantioselectivity, diastereoselectivity and chemoselectivity.<sup>1</sup> When a compound contains multiple double bonds, selectivity for a specific olefinic fragment for metathesis is desirable. Specifically, there is interest in synthesizing conjugated dienes via cross-metathesis.<sup>2</sup> Discussed herein are chemoselective methods developed for reactivity at the terminal olefin of a conjugated diene utilizing ruthenium catalysts.

Conjugated dienes are found abundantly in a wide range of natural products and are also synthetically useful for various materials applications.<sup>3</sup> Among the reactions available for the formation of conjugated dienes, palladium-catalyzed cross-coupling reactions such as the Stille and Suzuki couplings have proven the most reliable.<sup>4</sup> While the use of olefin cross-metathesis for the synthesis of conjugated dienes is less explored, it is highly desirable since such a transformation would provide facile access to a wide range of currently inaccessible or difficult to synthesize substrates.

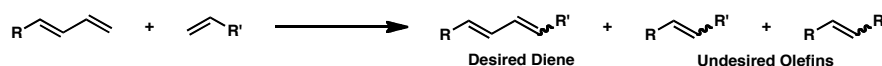


**Figure 4.1. Selectivity in Diene Cross-Metathesis.**

In order for olefin cross-metathesis to be a useful method for synthesizing conjugated dienes, issues of chemo- and diastereoselectivity must be overcome (figure 4.1). In the diene, there are two double bonds that both may potentially react in cross-metathesis. In order to form the desired conjugated diene, formation of the undesired olefins must be suppressed. Funk explored a novel method of imposing selectivity, by shielding the undesired olefin via electronic or steric deactivation utilizing the known

lowered reactivity of olefins containing electron-withdrawing or sterically demanding substituents.<sup>2,5</sup>

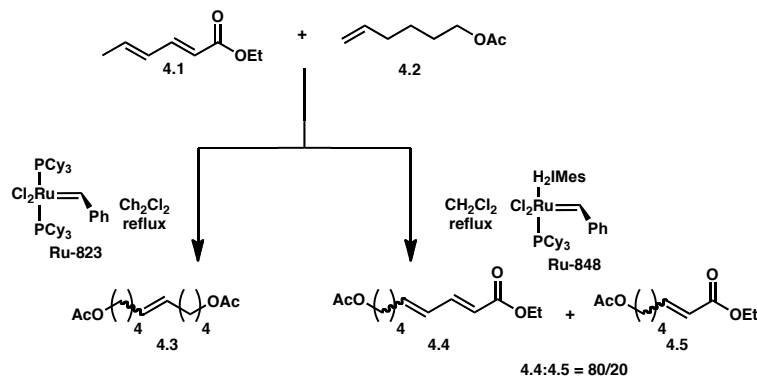


**Figure 4.2. Electronic Manipulation of Diene Selectivity in CM.**

Shown in figure 4.2 is the cross-metathesis of ethyl sorbate with 5-hexenyl acetate. When Grubbs first-generation catalyst was used, only homocoupled product formed from 4.2 was observed. A 4:1 ratio of the desired diene product 4.4 to the undesired  $\alpha,\beta$ -unsaturated ester 4.5 was obtained when Grubbs second-generation catalyst was used. Although this methodology showed some selectivity for the terminal double bond, reactivity at the undesired position still occurred.

Substrates, such as those shown in figure 4.3, were then screened to examine if varying the other electron-withdrawing substituents on the undesired olefinic fragment could enhance the selectivity for the desired versus undesired products.<sup>2</sup> The olefin where reactivity is desired is highlighted in red (figure 4.3).

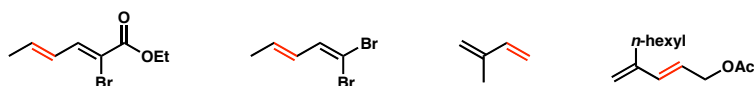


**Figure 4.3. Substrates Screened for Electronic and Steric Deactivation.**

This strategy provided the anticipated selectivity and good amounts of the desired diene. However, it requires specific functionalities to be embedded within potential



substrates, thus imposing constraints on the overall generality of this methodology.

Dienes without electronically dissymmetric double bonds still prove to be challenging olefin cross-metathesis substrates for forming the desired products.

Compound **4.6**, shown in figure 4.4 and known as codlemone, is an example of such a diene, which is unfunctionalized about the olefinic moieties.<sup>6</sup> Codlemone is among the known insect pheromones, which are of great industrial interest, as they would allow the agricultural industry to develop organic and non-toxic, “biorational” pesticides. The search for biologically tolerable and environmentally safe methods for controlling an insect population continues as an alternative to traditional chemical pesticides. Much attention is currently being paid to species-specific behavior modification methods.<sup>7</sup> With an ever-growing population, the world cannot afford the up to one-third loss of food produced that is being destroyed by insects.<sup>7d</sup>

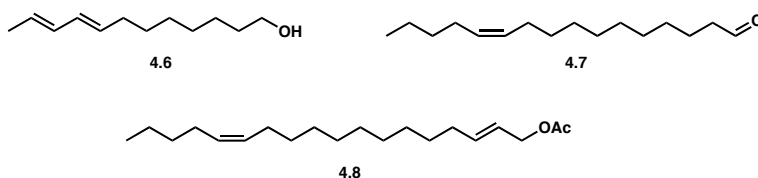


**Figure 4.4. Known Insect Pheromones.**

The use of insect pheromones as insecticide replacements is being developed as a sustainable and environmentally friendly method for controlling loss of crops. Since the male of a species will follow a gradient of pheromone secreted by the female as part of mating behaviors, farmers can spray copious amounts of the same natural product, thus erasing the gradient and confusing the male insect. If the male of the species cannot find the female, the mating cycle of the pest is disrupted and thus use of any additional insecticide is bypassed. Another method exploiting synthetic insect pheromones involves

mass trapping and extermination of an insect population—to date, an estimated 10 million hectares are protected via attract-and-kill techniques utilizing pheromones.<sup>7b</sup> Since pheromones are species-specific compounds that have shown efficacy at low concentrations, these methods do not harm beneficial species and allow for readily controllable insect management. Notably, the use of insect pheromones on food crops has not shown detectable amounts of residue on the resultant produce.<sup>7c</sup>

Codlemone specifically is a pheromone for the *lepidoptera tortricidae*, a family of insects commonly known as moths.<sup>8</sup> This family contains many agricultural pests such as the rose leaf roller, cherry fruitworm, and the codling moth. The codling moth has become a particular pest of note, often destroying large apple crops and in recent years, the moth has developed resistance to even the harshests of insecticides.<sup>7e,8c</sup> Although codlemone, the best-selling insect pheromone worldwide, is commercially available and several synthetic routes have been utilized for its production, none so far capitalize on the economical and facile nature of olefin metathesis.<sup>9</sup> Developing green and sustainable biorational pesticides relies on such facile and economical production of large quantities of the desired pheromones; in turn, developing these methods is imperative for consumer and agricultural worker safety, environmental safety and overall food security.

## MODEL SYSTEM FOR DIENE SELECTIVITY

The proposed model for diene selectivity does not rely on steric or electronic shielding of either olefin of the diene. Instead, an allyl ether functionality is incorporated into the diene to form **4.9** (figure 4.5). When substrate **4.9** is exposed to a ruthenium metathesis catalyst, it is proposed that the unhindered olefin will form the initial

alkylidene shown, **4.10**. Subsequent rapid intramolecular recombination and extrusion of 2,5-dihydrofuran would then lead to the desired ruthenium alkylidene, **4.11**. Addition of excess cross-partner, in the model case *cis*-diacetoxybutene was used, would then afford the desired diene product, **4.12**.

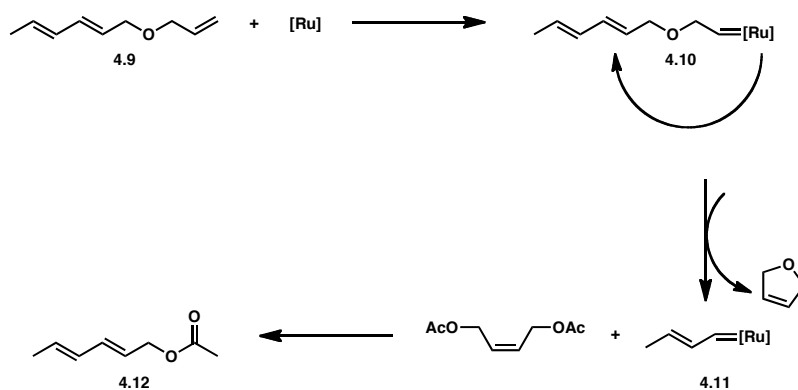


**Figure 4.5. Desired Reaction Pathway.**

It is reasonable that the above desired pathway will be favored over intramolecular ring closing and extrusion of the less thermodynamically stable seven-membered ring, as shown in figure 4.6, which would yield the undesired alkylidene **4.13**. If the undesired pathway is traversed, the diene functionality is lost in the seven-membered ring and addition of an excess of cross-partner leads to the undesired olefinic product, **4.14**.

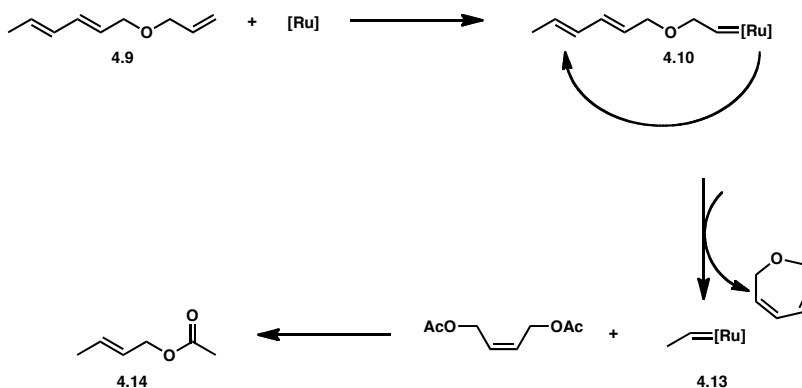


**Figure 4.6. Undesired Reaction Pathway.**

One-step synthesis of the diene substrate **4.9** involved allylation of the commercially available 2,4-hexadienol. In order to confirm the identity of the desired product, independent synthesis was undertaken and consisted of acylation of the same 1,4-hexadienol to give diene **4.12**. Other potential products such as the furan and undesired olefin were commercially available and their retention times were recorded on a gas chromatograph (GC). Response factors for the compounds of interest were established and area integrations from GC were converted to known amounts using an internal standard. Initial screening conditions are shown in table 4.1. Although both Grubbs first generation (Ru-823) and second generation (Ru-848) catalysts were screened, Ru-848 was shown to be too active, giving several side-products and low conversions to the desired diene. Thus we focused our attentions on Ru-823.

**Table 4.1. Initial Screening Conditions for Model System**

Catalyst	Mol%	Diene/Cross-Partner	Temperature	Solvent
[Ru-823]	2.5%	1:2	23°C	CH <sub>2</sub> Cl <sub>2</sub>
[Ru-823]	5.0%	1:2	23°C	CH <sub>2</sub> Cl <sub>2</sub>
[Ru-823]	2.5%	1:3	23°C	CH <sub>2</sub> Cl <sub>2</sub>
[Ru-823]	5.0%	1:3	23°C	CH <sub>2</sub> Cl <sub>2</sub>
[Ru-823]	2.5%	1:5	23°C	CH <sub>2</sub> Cl <sub>2</sub>
[Ru-823]	5.0%	1:5	23°C	CH <sub>2</sub> Cl <sub>2</sub>
[Ru-823]	2.5%	1:2	40°C	CH <sub>2</sub> Cl <sub>2</sub>
[Ru-823]	5.0%	1:2	40°C	CH <sub>2</sub> Cl <sub>2</sub>
[Ru-823]	2.5%	1:3	40°C	CH <sub>2</sub> Cl <sub>2</sub>
[Ru-823]	5.0%	1:3	40°C	CH <sub>2</sub> Cl <sub>2</sub>

An excess of the cross-partner, *cis*-diacetoxymethylbutene, was necessary to form the desired product. Shown in figure 4.7 is the conversion to diene, **4.12**, at room

temperature with varying catalyst concentration and equivalents of cross-partner.

Unfortunately, the conversion to the desired diene never exceeded 50%. The highest recorded diene conversion was 45% at 20 hours with a 1:5 ratio of substrate to cross-partner and a 2.5% molar loading of ruthenium catalyst.

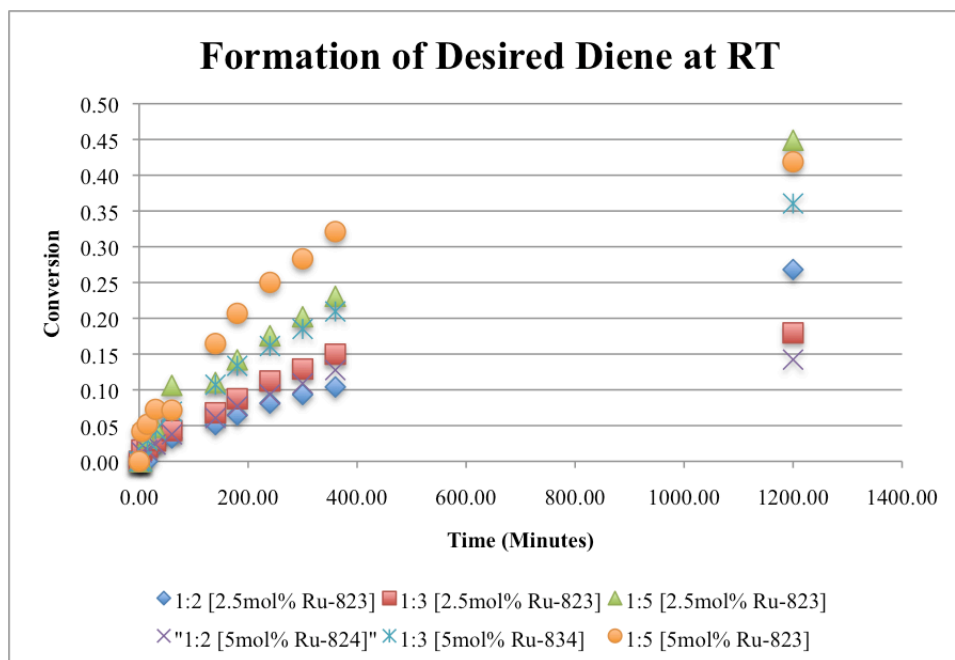


**Figure 4.7. Formation of Desired Diene at Room Temperature.**

Shown in figure 4.8 is the conversion to the undesired olefin, **4.14**, at room temperature. Although the initial conversion is low, after 20 hours a substantial amount of this byproduct appears. At less than 6 hours, the formation of undesired olefin is suppressed to below 5% conversion, though the highest corresponding conversion to the desired diene at this point is only 32% according to GC analysis.

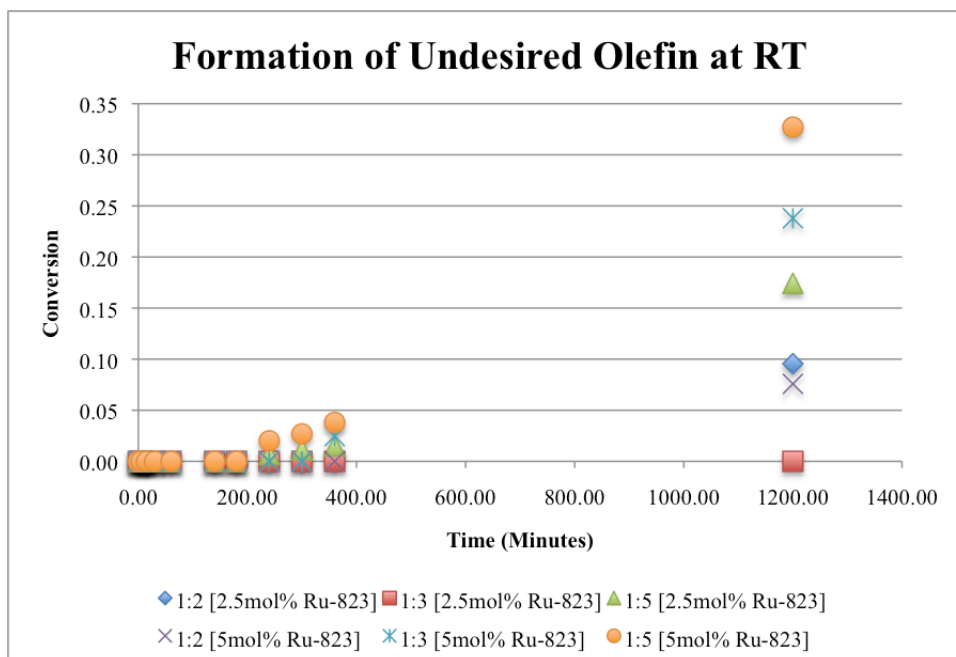


**Figure 4.8. Formation of Undesired Olefin at Room Temperature.**

At this time we chose to examine the reaction at elevated temperatures of 40°C. Here the conversion to desired diene reaches a maximum of 50% at 6 hours (figure 4.9). At 20 hours, the conversion to diene begins to erode, most likely due to secondary metathesis events or perhaps decomposition of the dienyl product.

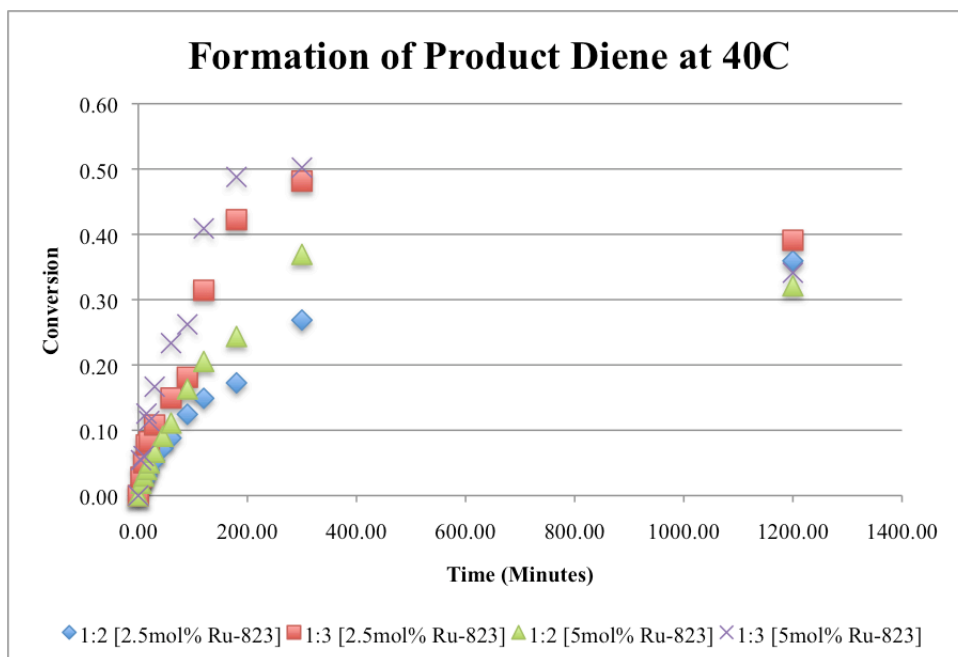


**Figure 4.9. Formation of Desired Diene at 40°C.**

While this was a promising conversion in a reasonable time span, analysis of the conversion to undesired olefin at the same time showed a parallel increase (figure 4.10).

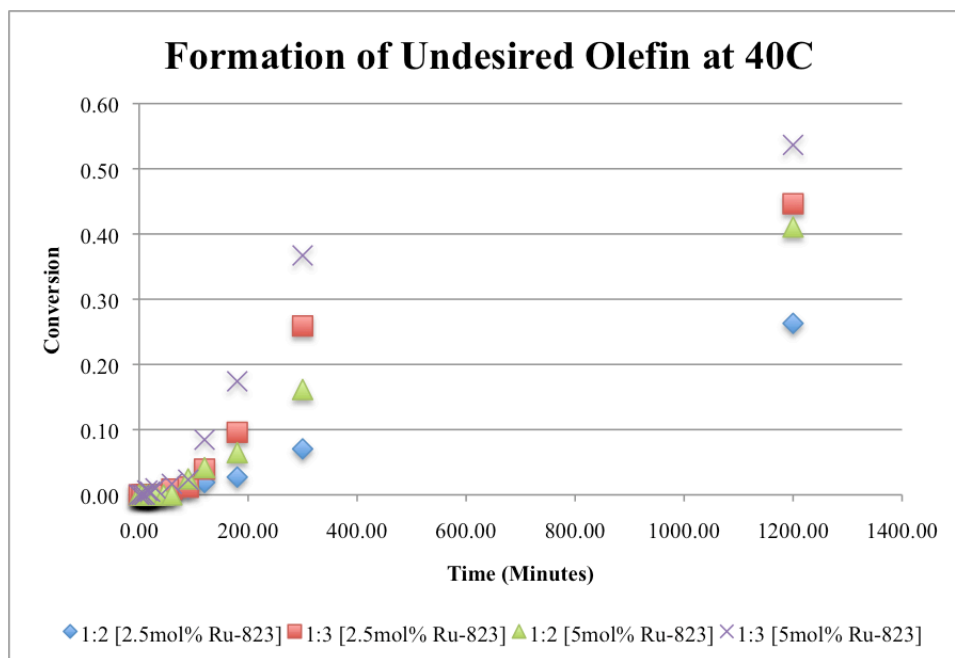


**Figure 4.10. Formation of Undesired Olefin at 40°C.**

Shown in table 4.2 are the most promising ratios of desired diene, **4.12**, to undesired olefin, **4.14**, in each reaction profile, and the time at which they were obtained. Unfortunately, the reactions which give the highest ratios also gave the lowest overall conversions. At room temperature, a ratio of 23:1 can be obtained, but only at 23% conversion to desired diene. Examining those reactions which obtained a 40% or higher conversion to the diene, showed that the selectivities were 5.1:1 and 4.2:1. Thus, the selectivities compare to those obtained utilizing selective olefin shielding methods. However, the overall conversions are lower.

**Table 4.2. Selectivity of Desired Diene over Undesired Olefin**

<b>Mol%</b>	<b>Diene/Cross-Partner</b>	<b>Temperature</b>	<b>Diene/Olefin</b>	<b>Time (hrs)</b>
2.5%	1:2	23°C	27:10	20
5.0%	1:2	23°C	14:8	20
2.5%	1:3	23°C	18:0	20
5.0%	1:3	23°C	21:2	6
2.5%	1:5	23°C	23:1	6
5.0%	1:5	23°C	32:4	6
2.5%	1:2	40°C	27:7	5
5.0%	1:2	40°C	37:16	5
2.5%	1:3	40°C	42:10	3
5.0%	1:3	40°C	41:8	2

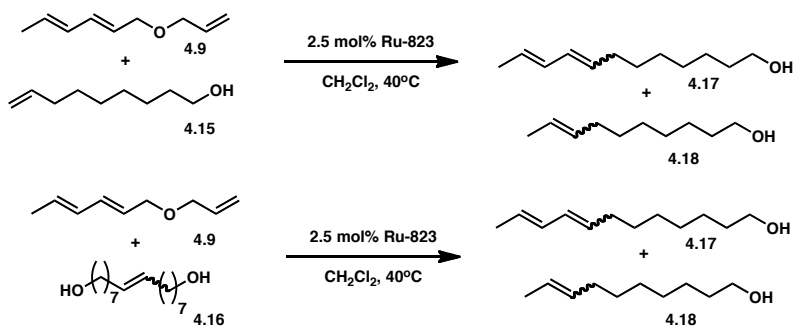
Although the conversions were less than expected, the selectivities for this model system were promising. Therefore we applied the optimized conditions to the synthesis of *E,E*-8,10-dodecanediol.



## APPLICATIONS IN PHEROMONE SYNTHESIS

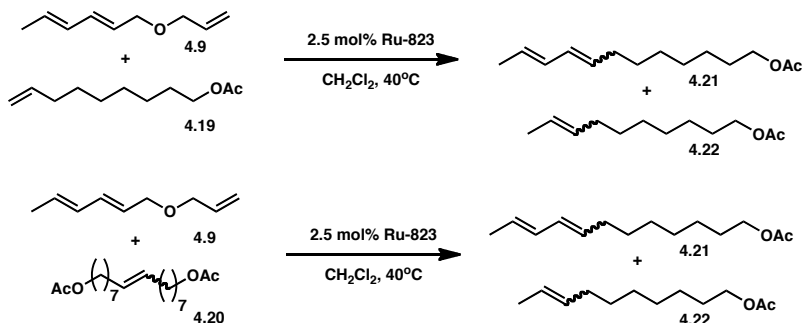
We began by attempting the cross-metathesis of substrate diene **4.9** with nonenyl alcohol **4.15**, as well as with the diol **4.16**, which was obtained from homodimerization of the commercially available nonenyl alcohol, **4.15** (scheme 4.1).

**Scheme 4.1. Attempts at Pheromone Synthesis.**



These reactions gave less than 10% conversion to the desired diene product, *E,E*-8,10-dodecanediol, **4.17**. Many unidentified side products, including the undesired olefin byproduct, **4.18**, were isolated. Increased loadings, from 2.5 mol% to 5.0 mol%, did not significantly increase conversion to the diene. Cross-metathesis of acetate **4.19** and the diacetate **4.20** gave slightly improved yields (10-15%) to both diene **4.21** and olefinic product **4.22**, but still yielded many unknown byproducts (scheme 4.2).

**Scheme 4.2. Further Attempts at Pheromone Synthesis.**



In the model system, the only observed side-products were the 5- and 7-membered ring extrusion products, and the undesired olefinic product. In this system,

several unidentified side-products were also formed, as the diene substrate was observed to convert to these products rapidly in the presence of ruthenium metathesis catalyst. One byproduct was isolated as the olefin isomerized product, however, attempts at suppressing olefin isomerization using 1,4-benzoquinone were unsuccessful, as were attempts at isolating and characterizing the other unknown side products.

## CONCLUSIONS

A method for the selective formation of conjugated dienes via cross-metathesis has been developed which does not require prefunctionalization of the substrate with protecting moieties. The highest ratios of desired diene product to undesired olefin byproduct obtained were 23:1 and 18:0, though the best selectivities (taking into account overall conversion) obtained were 5.1:1 and 4.2:1, where the conversion to the diene was greater than 40%.

Attempts were made to apply the optimized conditions from the model system toward synthesis of *E,E*-8,10-dodecanediene, otherwise known as codlemone, the sex pheromone of the codling moth. Although conversion to the desired diene product did not exceed 10%, several byproducts of the reaction were identified as either products of olefin isomerization or decomposition, which can potentially be controlled and reduced. Further investigations of the model system and the pheromone synthesis are ongoing in our lab. Importantly, this methodology represents a two-step route to the codlemone pheromone, which is currently only available via 6-8 step synthetic routes without the aid of cross-metathesis.<sup>9</sup>

## EXPERIMENTAL METHODS

### Materials and Methods

NMR spectra were measured on an Oxford 300 MHz spectrometer running Varian VNMR software unless otherwise noted. Resonances for NMR spectra are reported relative to Me<sub>4</sub>Si ( $\delta$  0.0) for <sup>1</sup>H and <sup>13</sup>C. Spectra are reported as follows: chemical shift ( $\delta$  ppm), multiplicity, coupling constant (Hz) and integration. High Resolution Mass Spectroscopy (HRMS) was obtained by the California Institute of Technology MS Facility. Air-sensitive metal-containing complexes were handled in a dry box under nitrogen or via standard Schlenck techniques under argon. Flash chromatography was conducted using silica gel 60 with the exception of ruthenium-containing complexes, which was conducted using TSI Scientific silica. Solvents were purified by passage through alumina.<sup>1</sup> Ruthenium starting materials were provided by Materia, Inc. All other reagents were purchased from Aldrich and used without prior purification unless otherwise noted.

Response factors for all compounds relative to tridecane were gathered on a gas chromatograph according to the procedure outlined in Ritter et al.<sup>2</sup>

**Synthesis of (4.9):** (2*E*, 4*E*)-hexa-2,4-dienol was purchased from Aldrich and distilled before use. A flame-dried, round-bottom flask was charged with the dienol (1.93 g, 20 mmol), NaH (1 g, 40 mmol) and dry THF (100 mL, 0.2 M in alcohol). The solution was refluxed for 30 minutes, then cooled to room temperature. Allyl bromide (4.2 mL, 50

<sup>1</sup> Pangborn, A. B.; Giardello, M. A.; Grubbs, R. H.; Rosen, R. K.; Timmers, F. J. *Organometallics* **1996**, *15*, 1518–1520.

<sup>2</sup> Ritter, T.; Hejl, A.; Wenzel, A. G.; Funk, T. W.; Grubbs, R. H. *Organometallics* **2006**, *25*, 5740–5745.

mmol) was added via syringe. The mixture was refluxed overnight, then cooled to room temperature and quenched with a saturated solution of ammonium chloride (50 mL), extracted with diethyl ether (3x50mL) and dried over magnesium sulfate. The allylated product was distilled under pressure and isolated as a clear oil.  $^1\text{H}$  NMR (300 MHz,  $\text{CDCl}_3$ )  $\delta$  6.16 (bt, 1 H), 6.00 (t (br), 1H), 5.93 – 5.80 (m, 1H), 5.71 – 5.53 (m, 1H), 5.23 (d,  $J$  = 16.5 Hz, 1H), 5.13 (d,  $J$  = 9.9 Hz, 1H), 3.96 – 3.90 (m, 4H), 1.71 (d,  $J$  = 6.6 Hz, 3H).  $^{13}\text{C}$  NMR (75 MHz,  $\text{CDCl}_3$ )  $\delta$  134.8, 133.1, 130.8, 126.6, 116.7, 70.8, 70.4, 18.0.

**Synthesis of (4.12):** (2*E*, 4*E*)-hexa-2,4-dienol was purchased from Aldrich and distilled before use. A flame-dried, round-bottom flask was charged with methylene chloride (10 mL), the dienol (2 g, 20.4 mmol), acetic anhydride (2 mL, 22.4 mmol), triethylamine (4.25 mL, 30.6 mmol) and a catalytic amount of 4-dimethylaminopyridine. The reaction was stirred open to air for 4 hours and quenched with a saturated solution of ammonium chloride (20 mL) and extracted with methylene chloride (3 x 20 mL) and dried over magnesium sulfate. The acylated product was distilled under pressure and isolated as a clear oil  $^1\text{H}$  NMR (300 MHz,  $\text{CDCl}_3$ )  $\delta$  6.24 – 6.14 (m, 1H), 5.97 (t,  $J$  = 15.3 Hz, 1H), 5.73 – 5.50 (m, 2H), 4.49 (d,  $J$  = 6.3 Hz, 2H), 1.98 (s, 3H), 1.69 (d,  $J$  = 6.9 Hz, 3H).  $^{13}\text{C}$  NMR (75 MHz,  $\text{CDCl}_3$ )  $\delta$  170.6, 134.7, 131.0, 130.5, 123.6, 64.8, 20.8, 18.0.

**Synthesis of (4.16):** A flame-dried, round-bottom flask was charged with the nonenyl alcohol **4.15** (2.2 g, 15.5 mmol), Ru-848 (400 mg, 0.5 mmol) and methylene chloride (50 mL). The reaction was stirred at reflux for 3 hours, cooled to room temperature and

purified by flash chromatography (5% EtOAc:hexanes).  $^1\text{H}$  NMR (300 MHz,  $\text{CDCl}_3$ )  $\delta$  5.82 – 5.69 (m, 1H), 3.55 (t,  $J$  = 5.7 Hz, 2H), 2.63 (bs, 1H), 2.02 – 1.91 (m, 2H), 1.58 – 1.49 (m, 2H), 1.28 (bs, 8H).  $^{13}\text{C}$  NMR (75 MHz,  $\text{CDCl}_3$ )  $\delta$  140.0, 114.2, 62.7, 33.7, 32.6, 29.5, 29.0, 28.8, 25.7.

**Synthesis of (4.19):** Nonenyl alcohol **4.15** was acylated in a procedure analogous to the synthesis of **4.12** and flashed in 5% EtOAc:Hexanes.  $^1\text{H}$  NMR (300 MHz,  $\text{CDCl}_3$ )  $\delta$  5.80 – 5.66 (m, 1H), 4.95 – 4.84 (m, 2H), 3.98 (t,  $J$  = 6.6 Hz, 2H), 1.97 (s, 3H), 1.58 – 1.52 (m, 2H), 1.26 (bs, 10H).

**Synthesis of (4.20):** Nonenyl acetate **4.19** was homodimerized in a procedure analogous to the synthesis of **4.16**.  $^1\text{H}$  NMR (300 MHz,  $\text{CDCl}_3$ )  $\delta$  5.29 – 5.25 (m, 1H), 3.94 (t,  $J$  = 7.5 Hz, 2H), 1.93 (s, 3H), 1.89 – 1.83 (m, 2H), 1.53 – 1.49 (m, 2H), 1.21 (bs, 8H).

**General Diene-Cross Metathesis Procedure:** A flame-dried 20 mL vial was charged with a stirbar, allylated diene **4.9** (67.1 mg, 0.5 mmol) and tridecane (0.5mmol). A solution of ruthenium catalyst (2.5 mol% or 5.0 mol%) was added in methylene chloride (2.5 mL) and allowed to stir for 5 minutes. An excess of the diacetate cross-partner (5, 3 or 2 equivalents) was than added (167.2 mg, 1.0 mmol). Aliquots (0.1 mL) were taken at the appropriate time points and quenched into a GC vial containing 3 molar ethylvinylether in methylene chloride and then subjected to GC analysis. Conversions are reported using the response factors gathered against tridecane.

## REFERENCES AND NOTES

- (1) (a) Grubbs, R. H. *Handbook of Metathesis*; Wiley-VCG: Weinheim, Germany, **2003** and references cited therein. (b) Ivin, K. J.; Mol, J. C. *Olefin Metathesis and Metathesis Polymerization*; Academic Press: San Diego, CA. **1997** and references cited therein. (c) Noels, A. F.; Demonceau, A. *J. Phys. Org. Chem.* **1998**, *11*, 602–609. (d) Grubbs, R. H. *Tetrahedron*, **2004**, *60*, 7117–7140. (e) Grubbs, R. H. *Angew. Chem. Int. Ed.* **2006**, *45*, 3760–3765. (f) Schrock, R. R. *Angew. Chem. Int. Ed.* **2006**, *45*, 3748–3759.
- (2) Funk, T. W.; Efskind, J.; Grubbs, R. H. *Org. Lett.* **2005**, *7*, 187–190.
- (3) (a) Diver, S. T.; Giessert, A. J. *Chem. Rev.* **2004**, *104*, 1317–1382. (b) Garbaccio, R. M.; Stachel, S. J.; Baeschlin, D. K.; Danishefsky, S. J. *J. Am. Chem. Soc.* **2001**, *123*, 10903–10908. (c) Dvorak, C. A.; Schmitz, W. D.; Poon, D. J.; Pryde, D. C.; Lawson, J. P.; Amos, R. A.; Meyers, A. I. *Angew. Chem. Int. Ed.* **2000**, *39*, 1664–1666. (d) Wagner, J.; Cabrejas, L. M. M.; Grossmith, C. E.; Papageorgiou, C.; Senia, F.; Wagner, D.; France, J.; Nolan, S. P. *J. Org. Chem.* **2000**, *65*, 9255–9260.
- (4) (a) Miyaura, N.; Satoh, M.; Suzuki, A. *Tetrahedron Lett.* **1986**, *27*, 3745–3748. (b) Uenishi, J.; Beau, J.-M.; Armstrong, W.; Kishi, Y. *J. Am. Chem. Soc.* **1987**, *109*, 4756–4758. (c) Zhang, F.; Peng, L.; Zhang, T.; Mei, T.; Liu, H.; Li, Y. *Synth. Commun.* **2003**, *33*, 3761–3770. (d) Fargeas, V.; Ane, A.; Dubreuil, D.; Lebreton, J. *Synlett*, **2009**, *20*, 3341–3345.
- (5) Chatterjee, A. K.; Choi, T.-L.; Sanders, D. P.; Grubbs, R. H. *J. Am. Chem. Soc.* **2003**, *37*, 11360–11370.

- (6) Backman, A.-C.; Anderson, P.; Bengtsson, M.; Lofqvist, J.; Unelisu, C. R.; Witzgall, P. *J. Comp. Physiol. A* **2000**, *186*, 513–519.
- (7) (a) Howse, P. E.; Stevens, I. D. R.; Jones, O. *Insect Pheromones and Their Use in Pest Management*; Chapman and Hall, London, **1998**. (b) Witzgall, P.; Kirsch, P.; Cork, A. *J. Chem. Ecol.* **2010**, *36*, 80–100. (c) Tinsworth, E. F. *Behavior Modifying Chemicals for Insect Management*; Marcel Dekker, New York, **1990**. (d) Ehrlich, P. R.; Ehrlich, A. H.; Daily, G. C. *Popul. Develop. Rev.* **1993**, *19*, 1–32. (e) Elzen, G. W.; Hardee, D. D. *Pest. Manag. Sci.* **2003**, *59*, 770–776. (f) Bergstrom, L. G. W.; *Chem. Comm.* **2008**, *34*, 3959–3979.
- (8) (a) Roelofs, W. L.; Comeau, A.; Hill, A.; Milicevic, G. *Science* **1971**, *174*, 297–299. (b) Bartell, R. J.; *Physiol. Entomol.* **1982**, *7*, 353–364. (c) Krupke, C. H.; Roitberg, B. D.; Judd, G. J. R. *Environ. Entomol.* **2002**, *31*, 181–197.
- (9) (a) Tellier, F.; Hammoud, A.; Ratovelomanana, V.; Linstrumelle, G.; Descoins, C. *Bioorg. Med. Chem. Lett.* **1993**, *3*, 1620–1632. (b) Tellier, F.; Sauvetre, R. *Tetrahedron Lett.* **1992**, *33*, 3643–3644.

## RGD POLYMERS AND RUTHENIUM REMOVAL



## INTRODUCTION

The advent of ruthenium-catalyzed olefin metathesis has led to the development of many novel and useful materials applications.<sup>1,2</sup> With the latest generation of ruthenium catalysts, broad functional group tolerance has engendered the polymerization of monomers containing complex fragments including peptides and carbohydrates, previously unrealizable feats.<sup>3</sup> Polymers with low polydispersity indices (PDIs) have been developed due to the rapid initiation kinetics of Grubbs 2<sup>nd</sup> generation bipyridine catalyst,  $[(H_2IMes)(py)_2(Cl)_2Ru=CHPh]$ .<sup>4</sup> In the broader context of synthetic biomaterials for tissue engineering and biomedical applications, metathesis has proven, and will continue to prove, a valuable and functional tool.

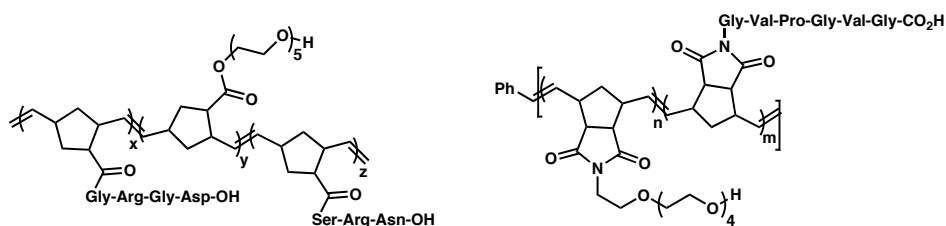


**Figure 5.1. Polynorbornenes Containing Peptidic Side Chains.**

Synthetic mimics of polypeptides formed via ring-opening metathesis polymerization (ROMP) are well preceded in the literature (figure 5.1).<sup>3</sup> Not only are ROMP polymerizations tolerant of the polar amino acids and provide well-defined molecular weights, ROMP with the appropriate initiator also affords all the benefits of a living polymerization. Thus, due to its functional group tolerance, ROMP has proven superior to traditional methods of polymerization, such as radical polymerizations, for the synthesis of polymers with bioactive oligopeptide sequences. Specifically, our group has developed elegant syntheses

of polynorbornenes containing the elastin mimic, valine-proline-glycine-valine-glycine (VPGVG) side chain, the glycine-arginine-glycine-aspartic acid (GRGD) sequence and the serine-arginine-asparagine (SRN) sequence for biological evaluation.<sup>3</sup>

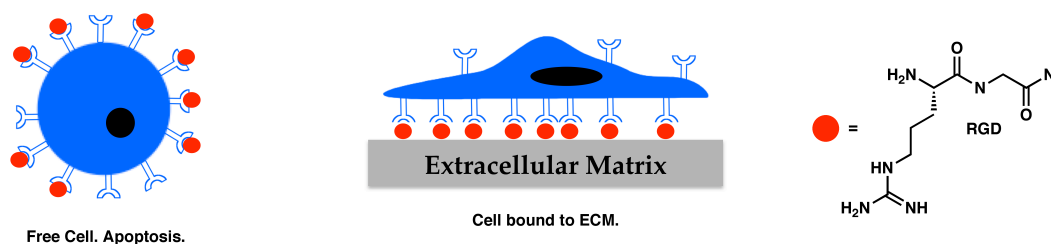


**Figure 5.2. Cell Adhesion and Cell Survival.**

The arginine-glycine-aspartic acid (RGD) sequence has been shown to participate in modulating cell adhesion, which is crucial to cell survival when cells are incorporated onto synthetic scaffolds (figure 5.2).<sup>5</sup> Specifically, RGD is the minimal sequence of fibronectin required for binding cell-surface integrins, and thus materials made from polynorbornenes with pendent RGDs promote cell survival. Polymers with RGDs have also shown efficacy in antimetastatic applications as cancer therapeutics.<sup>5d</sup> In the synthesis of scaffolds for which functionality involves cell adhesion, inclusion of the RGD sequence in some aspect of the polymeric scaffold is necessary.

In order to utilize ROMP for the efficient and facile synthesis of biopolymers, several considerations need to be taken into account. The monomers incorporated must promote biocompatibility; RGD can be incorporated for cell adhesion, but other aspects such as hydrophilicity and nontoxicity must also be considered. To encourage aqueous solubility, polyethylene glycol (PEG)

units can be incorporated either as a second monomer in a random copolymerization, or as part of the original RGD monomer.<sup>6</sup> Following polymerization, the resultant polymer product will contain ruthenium byproducts from the metathesis reaction, which necessitate the development of effective ruthenium-removal methods. Finally, the overall activity of a given polymer must be established with known cell-adhesion and cell-survival methodologies.

A current application being pursued in our lab is the synthesis of an RGD-containing hydrogel to form a bulk material that can then be used in semi-permanent contact lenses. In order to form a hydrogel with the desired properties, three monomers will need to be incorporated into a random copolymer, a monomer containing RGD, a monomer containing PEG, and a monomer to enable cross-linking and hydrogel formation (figure 5.3).

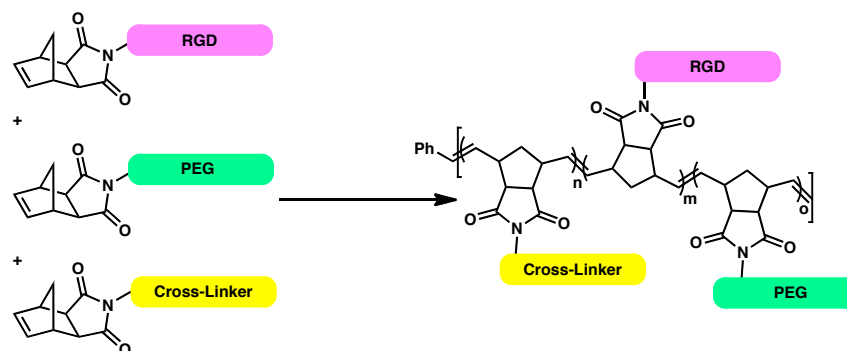


**Figure 5.3. Schematic for Desired RGD-Polymer.**

## **RUTHENIUM REMOVAL IN POLYNORBORNENES**

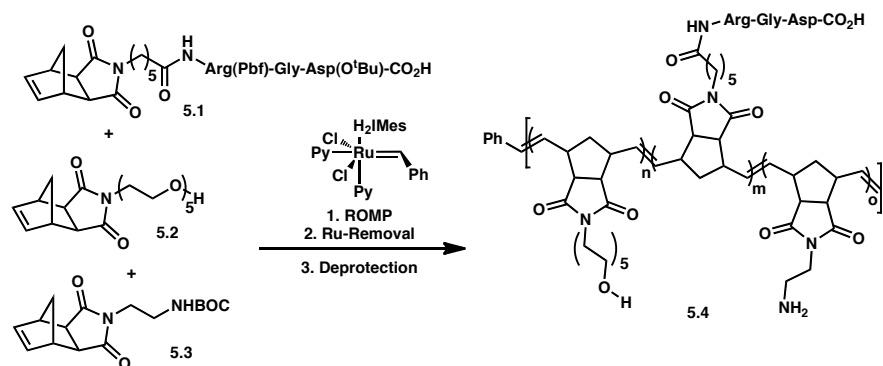
The polymers described herein are intended for biological use, thus the removal of ruthenium below the 10 parts per million (ppm) limit is important to maintain biological compatibility and nontoxicity as described by the FDA.<sup>7</sup>

Many methods have been developed and described for the removal of left over ruthenium content in both small molecule metathesis and polymer formation reactions. Compounds such as tris(hydroxymethyl)phosphine (THMP),  $\text{Pb}(\text{OAc})_4$ , DMSO, and methods such as catalyst modification or aqueous extraction have all been explored for their potential to rid desired products of undesired ruthenium.<sup>8,9,10</sup>

For the application of these polymer scaffolds as semipermanent contact lenses, the removal of the colored ruthenium byproduct will be especially important. Of the various methods for removing ruthenium from polymerization reactions, THMP has shown the most promise. Unlike cross-metathesis or other metathesis reactions, ROMP requires a specific ruthenium precursor, namely the bipyridine catalyst with its known rapid initiation kinetics, and thus catalyst modification is unavailable as a method for ruthenium removal.

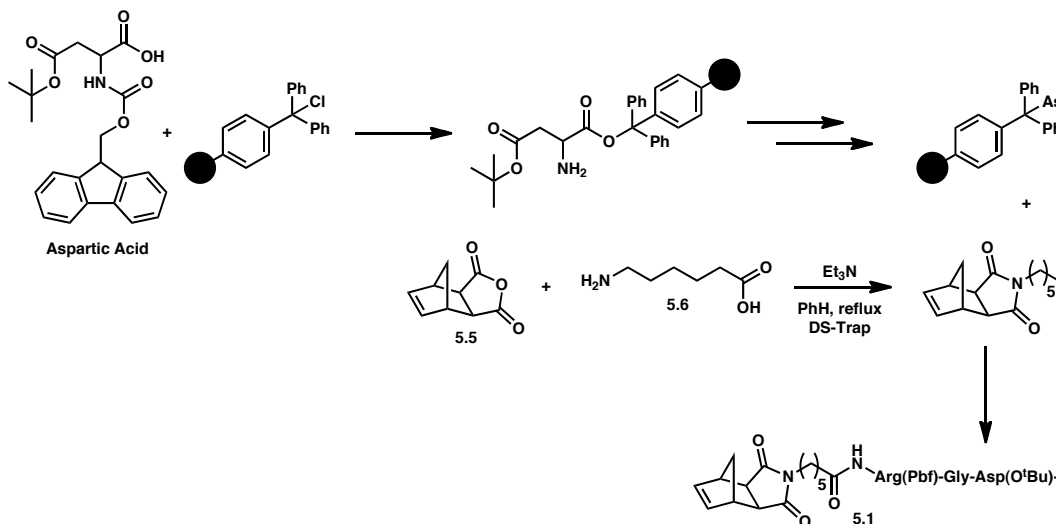
Tris(hydroxymethyl)phosphine is an air stable and water soluble phosphine which readily coordinates to ruthenium metal.<sup>8</sup> Addition of THMP to an organic solution of product mixture will result in coordination of the ruthenium, and removal can be achieved via simple aqueous extraction. Studies have been conducted on the varying amounts of THMP necessary to remove ruthenium from small-molecule ring-closing metathesis as well as simple ROMP reactions. In this chapter, we describe the attempts to remove ruthenium from RGD-containing polymers made via ROMP, which are intended for biological use as semipermanent contact lenses. The initial polymer structure studied, polymer **5.4**, is shown in scheme 5.1.

Scheme 5.1. Initial Polymer Designed for Hydrogel Formation.



In order to synthesize monomer **5.1**, standard solid phase peptide synthesis (SPPS) techniques were conducted using Fmoc-protected amino acids (scheme 5.2).<sup>11</sup> The norbornene anhydride **5.5** was condensed using a Dean-Stark trap, with the 6-amino-hexanoic acid **5.6**, to provide norbornene **5.7** that was utilized in the final SPPS coupling step. The monomer product **5.1** was then cleaved from the bead.

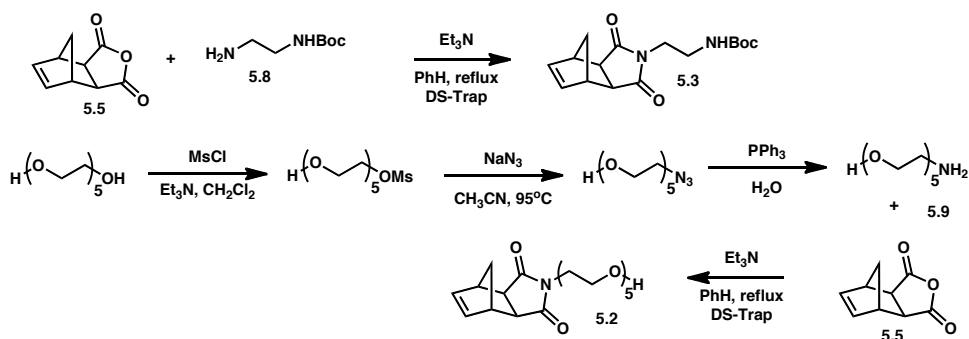
Scheme 5.2. Synthesis of Monomer 5.1.



Monomer **5.3** was obtained via a similar condensation reaction between the protected diamine and the norbornene anhydride (scheme 5.3). Synthesis of

monomer **5.2** began with mesylation of pentaethylene glycol. The mesylate was then transformed to the azide and reduced to the amine-alcohol **5.9**, which was finally condensed in a Dean-Stark trap with the norbornene anhydride **5.5** to provide monomer **5.2**.

**Scheme 5.3. Synthesis of Monomers 5.2 and 5.3.**



Monomers **5.1**, **5.2** and **5.3** were then randomly copolymerized using the bipyridine catalyst at room temperature with a ratio of 15:20:65 of monomers **5.1:5.2:5.3** with a total monomer to catalyst ratio of 100:1.<sup>4</sup>

With the polymers in hand, THMP in isopropanol with triethylamine was added in excess and stirred for 24 hours at 70°C. Ruthenium content after precipitation and deprotection was determined via inductive-coupled plasma mass spectrometry (ICP-MS). The ppm level of ruthenium in 4 mg samples of polymer are shown in figure 5.4.

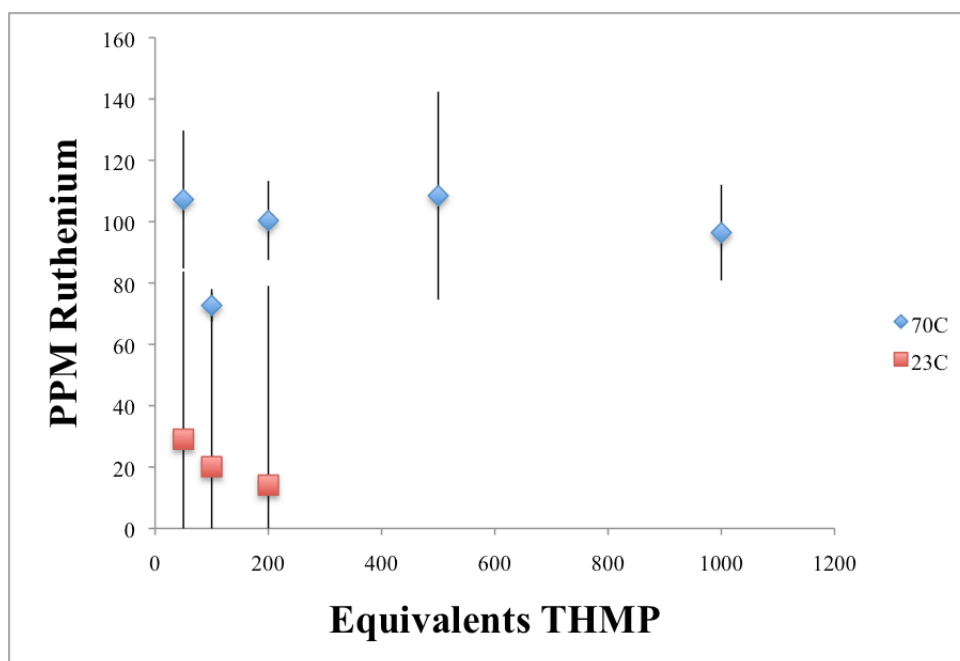


**Figure 5.4. Remnant Ruthenium Content at 70°C and 23°C.**

Although increasing the equivalents of THMP did not give lower ruthenium content, lowering the temperature did seem to give a lower final ruthenium level, though the error associated renders the temperature-dependent trend inconclusive. Qualitatively, the lower ruthenium content did show a significant color change for the sample, as shown in figure 5.5.

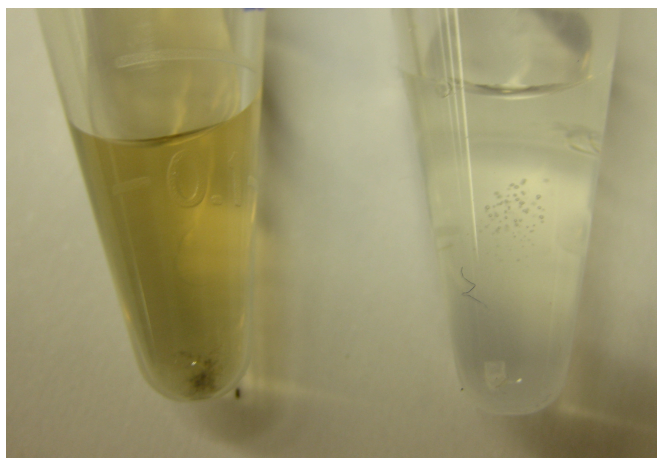


**Figure 5.5. Polymer Samples Without versus With Ruthenium Removal.**

Decreasing the monomer to catalyst ratio from 100:1 to 20:1 was investigated to see if shorter polymers allowed better access to embedded ruthenium byproducts, however, this did not achieve lower ppm levels for 4 mg samples of polymer. Instead, due to the increased overall ruthenium per polymer chain, the ppm levels of ruthenium actually increased drastically, as shown in Figure 5.6.

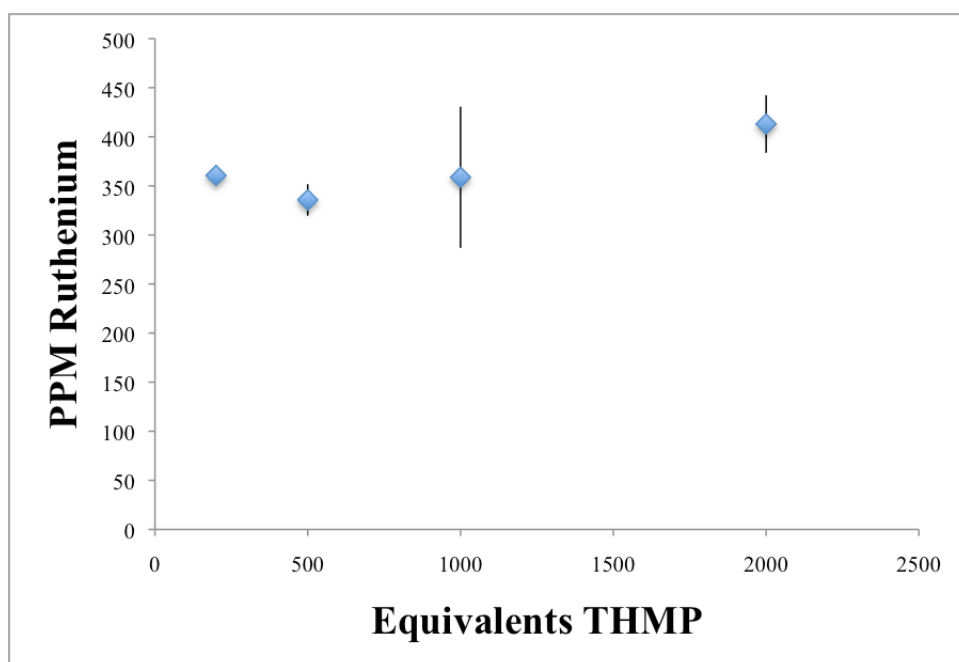


**Figure 5.6. Remnant Ruthenium Content at 70°C for 20:1 Ratio.**

At this point, various phosphines were explored and tris(*n*-butyl)phosphine (TBP) showed great promise in removing remnant ruthenium content. The procedure for removal was identical as with the THMP samples, and for 4 mg of the original polymer, ruthenium content was shown to be below 30 ppm regardless of the number of equivalents of TBP added (figure 5.7).



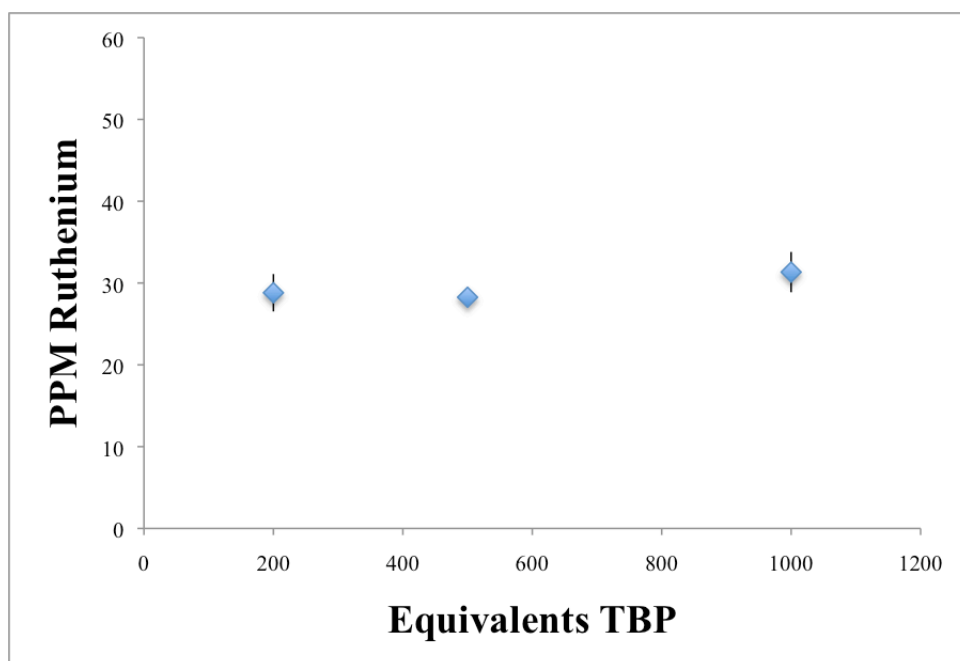
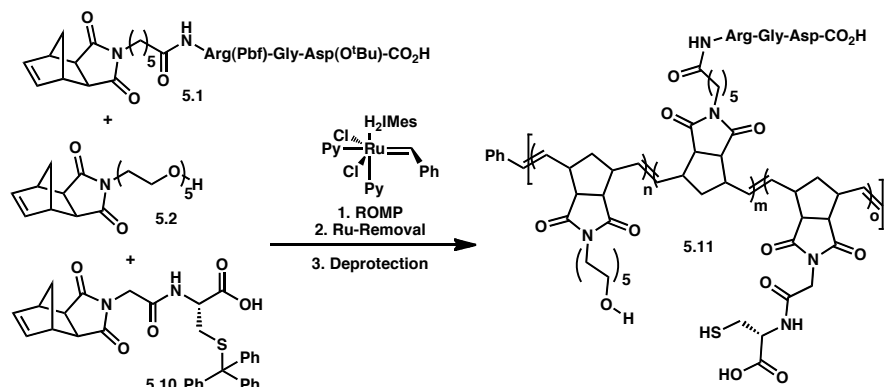


**Figure 5.7. Remnant Ruthenium Content at 70°C with TBP.**

## **NOVEL THIOL-MONOMERS FOR HYDROGEL FORMATION**

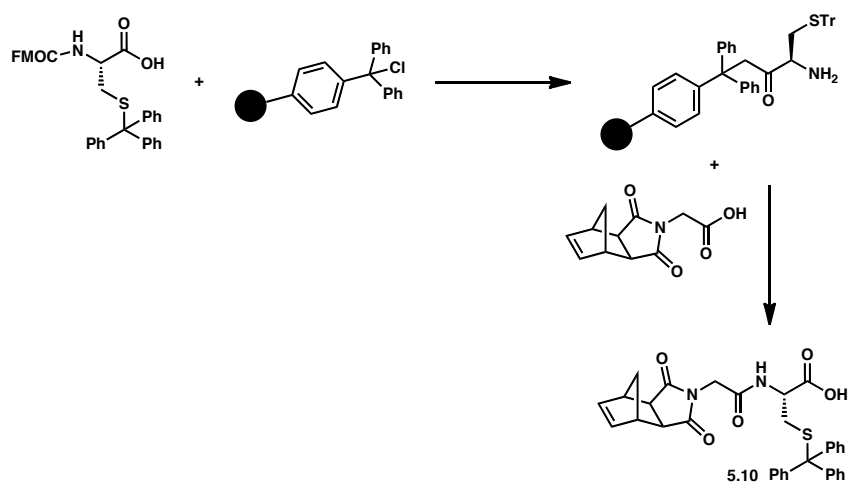
With remnant ruthenium content significantly lowered, we turned our attention towards forming bulk materials by cross-linking polymer **5.4** (scheme 5.1). Unfortunately, although cross-linking the free-amine with glutaraldehyde was successful, the final hydrogel material was a dark-brown color, despite the uncross-linked polymer was clear after ruthenium removal. We began to explore other methods of cross-linking and a novel cysteine-containing monomer was designed to allow for a free thiol to serve as the new cross-linking handle (scheme 5.4). One could imagine thiol-ene chemistry or a radical reaction to promote cross-linking throughout the polymer network to form the desired hydrogel.<sup>12</sup>

Scheme 5.4. Polymer with Protected Thiol Monomer for Cross-linking.

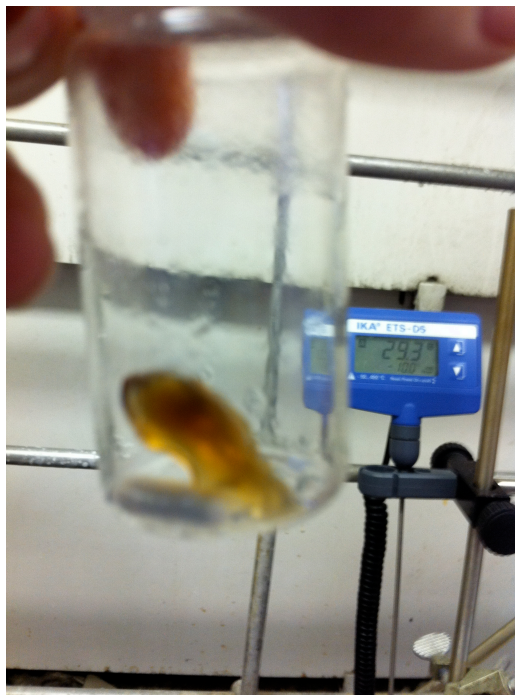


Synthesis of the thiol-containing monomer **5.10** again proceeded via SPPS techniques using the Fmoc-protected amino acid (scheme 5.5). The norbornene **5.10** was obtained and incorporated into random copolymers with monomers **5.1** and **5.2** as shown in figure 5.11. A 100:1 overall monomer to catalyst ratio was utilized, though the ratio of individual monomers was varied. The protected polymer was shown to have a PDI of 1.058 and an observed Mn of 26,580 that was standard for these RGD-containing norbornene polymers.

Scheme 5.5. Synthesis of Protected Cysteine Monomer.

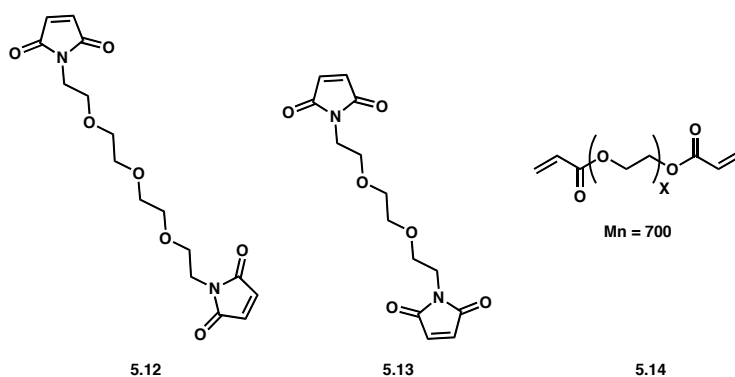


After deprotection, the free thiols in polymer **5.11** showed disulfide formation, often forming a hydrogel but in uncontrollable circumstances and ultimately was nonoptimal for formation of the contact lenses (figure 5.8).



**Figure 5.8. Uncontrolled Crosslinking of Polymer 5.11.**

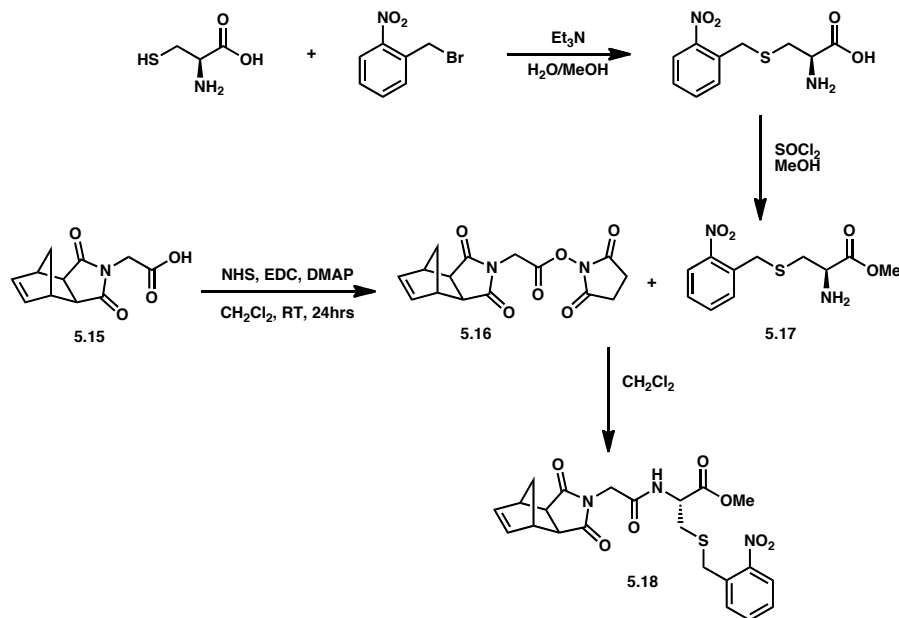
Addition of a 2% dithiothreitol (DTT) in water solution during dialysis and handling of the deprotected polymer reduced premature cross-linking. However, this prevented the desired thiol to maleimide cross-linking. Shown in figure 5.9 are the various cross-linkers attempted. Bis-maleimides **5.12** and **5.13** were attempted for uncatalyzed thiol-ene crosslinking, and diacrylate **5.14** was attempted with Vazo-44 for radical initiated thiol-ene chemistry.



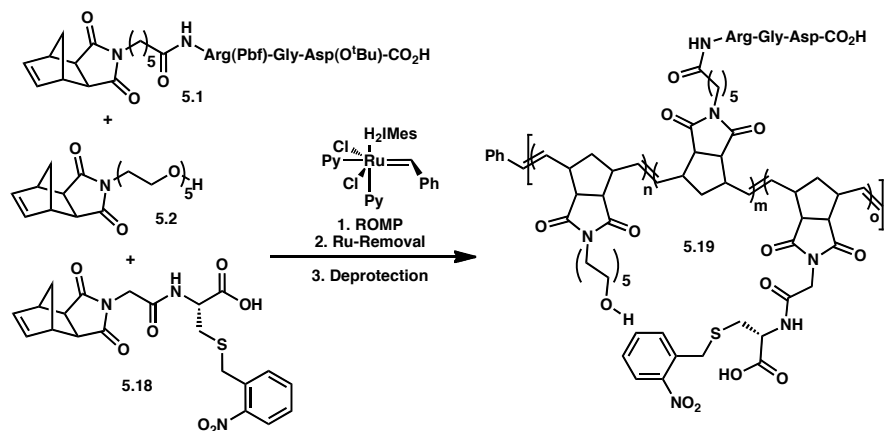
**Figure 5.9. Attempted Cross Linkers for Free Thiol.**

Controlled removal of DTT was found to be challenging, therefore a new thiol-containing monomer was designed, this time with a nitrobenzyl (NBz) protecting group that would prevent disulfide formation post-acid mediated deprotection of the other protecting groups. The nitrobenzyl group is unique in that it is photocleavable but stable in the presence of acid, unlike the other protecting groups used in the RGD-monomer.<sup>13</sup> Thus, the thiol group can be unmasked after deprotection of the RGD unit, under controllable conditions.

Synthesis of the NBz-protected cysteine monomer began with addition of nitrobenzyl bromide to the free cysteine to form the *S*-protected amino acid (scheme 5.6). Esterification of the carboxylic acid with thionyl chloride gave the cysteine derivative **5.17**. Norbornene **5.15** was transformed to the NHS ester under standard EDC-coupling conditions and then added to **5.17** as a solution in dichloromethane to form the final, desired NBz-protected thiol-containing monomer **5.18**.

Scheme 5.6. Synthesis of NBz-Protected Cysteine Monomer **5.18**.

This monomer was then incorporated into a random copolymer with norbornenes **5.1** and **5.2** as shown in scheme 5.7. Various monomer to monomer ratios were attempted, and a 15:75:10 ratio of monomers **5.1**:**5.2**:**5.18** was shown to be optimal for water solubility and handling purposes.

Scheme 5.7. Incorporation of NBz-Cysteine Monomer into Polymer **5.19**.

Photocleavage experiments were conducted on the final polymer **5.19** to promote sulfur to sulfur crosslinking, and although the solution of polymer did

appear more viscous, complete crosslinking was not observed and neither a thin film nor bulk materials were obtained. Cleavage of the NBz-group in the presence of bis-maleimide for thiol-ene crosslinking was also tested and found to be only marginally successful.

## CONCLUSIONS

Several polymers, **5.4**, **5.11** and **5.19**, containing the RGD peptide sequence were synthesized as random copolymers with two other monomer structures, one for water compatibility and one for cross-linking purposes. Ruthenium removal studies were conducted on polymer **5.4** using THMP and TBP in varying equivalents. The phosphine TBP was shown to be the best for removing ruthenium content to below 30 ppm consistently and with little variation with increasing equivalents.

Although a fully cross-linked hydrogel system has not yet been established, good progress toward various polymer architectures, which may provide the appropriate crosslinking handles, has been made and further studies will be conducted on their hydrogel potential in the application of semipermanent contact lenses.

## EXPERIMENTAL METHODS

### Materials and Methods

All reactions involving metal complexes were conducted under nitrogen or argon atmospheres using standard glove box or standard Schlenk techniques. Solvents were purified by passage through alumina.<sup>1</sup> Resonances for NMR spectra are reported relative to Me<sub>4</sub>Si ( $\delta$  0.0) for <sup>1</sup>H and <sup>13</sup>C. Spectra are reported as follows: chemical shift ( $\delta$  ppm), multiplicity, coupling constant (Hz) and integration.

Ruthenium starting materials were provided by Materia, Inc. All other reagents were purchased from Aldrich and used without prior purification.

**Synthesis of (5.1):** Standard SPPS protocols were followed. HR-MS (FAB+) Calculated for C<sub>44</sub>H<sub>64</sub>N<sub>7</sub>SO<sub>12</sub>: 914.4334; found: 914.4367.

### **Synthesis of 14-hydroxy-3,6,9,12-tetraoxatetradecyl methane sulfonate:**

Pentaethylene glycol (12.1 g, 50.1 mmol) was added to 500 mL of methylene chloride in a 3-neck 1L round-bottom flask. Triethylamine (7.1 mL, 50.1 mmol) was added and the flask was fitted with an addition funnel. Mesyl chloride (7.1 mL, 16.9 mmol) was added to the addition funnel along with another 125 mL of methylene chloride. The solution of mesyl chloride was added dropwise via the addition funnel over an hour. The reaction mixture was stirred at room temperature overnight. 100 mL of saturated sodium bicarbonate was added and

---

<sup>1</sup> Pangborn, A. B.; Giardello, M. A.; Grubbs, R. H.; Rosen, R. K.; Timmers, F. J. *Organometallics* **1996**, *15*, 1518–1520.

then the mixture was extracted with methylene chloride (3x200 mL), washed with brine and dried over sodium sulfate. The resultant mixture was flashed in 50% acetone:hexanes and isolated as an oil.  $^1\text{H}$  NMR (500 MHz,  $\text{CDCl}_3$ )  $\delta$  4.29 – 4.25 (m, 2H), 3.68 – 3.64 (m, 2H), 3.55 (bt,  $J = 13.8$  Hz, 16H), 2.99 (bs, 3H).

**Synthesis of 14-azido-3,6,9,12-tetraoxatetradecan-1-ol:** To a solution of the mesylate (4.4 g, 14 mmol) in dry acetonitrile (47 mL) was added solid sodium azide (1.37 g, 21 mmol). The reaction mixture was heated to refluxing overnight, then cooled to room temperature and filtered over a pad of Celite and washed with ethyl acetate. The crude product was flashed in 40% acetone:hexanes and isolated as an oil.  $^1\text{H}$  NMR (500 MHz,  $\text{CDCl}_3$ )  $\delta$  3.65 – 3.56 (m, 16H), 3.53 – 3.5 (m, 2H), 3.32 – 3.29 (m, 2H).

**Synthesis of 14-amino-3,6,9,12-tetraoxatetradecan-1-ol (5.9):** To a solution of the azide (3 g, 11.4 mmol) in toluene (30 mL) was added triphenylphosphine (3.3 g, 12.6 mmol) and water (0.4 mL, 23 mmol). The reaction mixture was stirred at room temperature overnight at which point the reaction was diluted with more water (20 mL) and the two layers were separated. The aqueous layer was concentrated to yield the product as an oil.  $^1\text{H}$  NMR (500 MHz,  $\text{CDCl}_3$ )  $\delta$  4.78 (bs, 2H), 3.65 (bs, 14H), 3.56 (bt,  $J = 6.5$  Hz, 2H), 3.52 (bt,  $J = 5.5$  Hz, 2H), 2.78 (bt,  $J = 5$  Hz, 2H).



**Synthesis of (5.2):** A 50 mL round-bottom flask was charged with anhydride **5.15** (865 mg, 5.3 mmol), amine **5.9** (1.3 g, 5.5 mmol) and toluene (9 mL, 1M). Triethylamine (0.763 mL, 1.1 mmol) was added and stirred. The flask was fitted with a reflux condenser and stirred at reflux overnight. The flask was then removed from heat and allowed to cool to room temperature. The solution was concentrated to a white solid and dissolved in 20 mL of EtOAc and washed with 0.2N HCl (2x10mL). The organic layer was then dried over sodium sulfate and filtered. This solution was then diluted with saturated aqueous sodium bicarbonate (11 mL) and extracted with methylene chloride (2x10 mL). The aqueous layer was acidified with 5 mL of 3N HCl to pH = 2 and a white precipitate was observed. This solution was then extracted with chloroform (4x7 mL). The organic layers were combined, dried over sodium sulfate and concentrated.  $^1\text{H}$  NMR (300 MHz,  $\text{CDCl}_3$ )  $\delta$  6.21 (s, 2H), 3.65 – 3.50 (m, 18H), 3.19 (s, 2H), 2.61 (s, 2H), 2.09 (s, 1H), 1.41 (d,  $J$  = 10 Hz, 1H), 1.27 (d,  $J$  = 10 Hz, 1H).

**Synthesis of (5.3):** A procedure analogous to the synthesis of **5.2** was followed.  $^1\text{H}$  NMR and  $^{13}\text{C}$  NMR agreed with published literature.

**Synthesis of (5.10):** Standard SPPS protocols were followed. HR-MS (FAB+) Calculated for  $\text{C}_{33}\text{H}_{29}\text{N}_2\text{SO}_5$ : 565.1797; found: 565.1799.

**Synthesis of nitrobenzylcysteine:** To a flame-dried 100 mL round-bottom flask was added a solution of nitrobenzylbromide (2 g, 9.2 mmol) in methanol (30 mL). A solution of free cysteine (1.27 g, 10 mmol) in water (30 mL) and triethylamine (1.412 mL, 9.2 mmol) was cooled to 0 °C and added dropwise to the round-bottom flask. The reaction mixture was stirred for 30 minutes at 0 °C and then another 30 minutes at room temperature. The formed crystals were then filtered over an M-frit. NMR was taken in 10% deuterated TFA in D<sub>2</sub>O. <sup>1</sup>H NMR and <sup>13</sup>C NMR agreed with published literature.

**Synthesis of (5.17):** A 50 mL round-bottom flask was charged with methanol (18 mL) and the nitrobenzylcysteine (700 mg, 2.73 mmol) and then cooled on ice. Redistilled thionyl chloride (2 mL, 3.25 mmol) was then added dropwise and stirred at room temperature overnight, wherein the solution becomes clear. Saturated sodium bicarbonate was then added and the solution was extracted with methylene chloride, washed with brine, dried over sodium sulfate and then concentrated. <sup>1</sup>H NMR (500 MHz, CDCl<sub>3</sub>) δ 7.95 – 7.91 (m, 1H), 7.55 (t, J = 9.5 Hz, 1H), 7.42 – 7.93 (m, 2H), 4.17 – 4.14 (m, 1H), 4.05 (d, J = 13.5 Hz, 1H), 3.96 (d, J = 13.5 Hz, 1H), 3.66 (s, 3H), 3.03 – 2.99 (m, 1H), 2.89 – 2.83 (m, 1H).

**Synthesis of (5.15):** A procedure analogous to the synthesis of **5.2** was followed. <sup>1</sup>H NMR (500 MHz, CDCl<sub>3</sub>) δ 6.23 (s, 2H), 4.21 (s, 2H), 3.25 (s, 2H), 2.70 (s, 2H), 1.54 (d, J = 10 Hz, 1H), 1.44 (d, J = 9.5 Hz, 1H).

**Synthesis of (5.16):** A 50 mL round-bottom flask was charged with norbornene **5.15** (500 mg, 2.3 mmol), solid NHS (390 mg, 3.4 mmol), EDC (650 mg, 3.4 mmol) and methylene chloride (20 mL). A catalytic amount of dimethylaminopyridine was added and the reaction was stirred at room temperature overnight. The crude mixture was flashed with 1:1 EtOAc:hexanes.  $^1\text{H}$  NMR (300 MHz,  $\text{CDCl}_3$ )  $\delta$  6.30 (s, 2H), 4.55 (s, 2H), 3.31 (s, 2H), 2.82 (s, 4H), 2.77 (s, 2H), 1.54 (d,  $J = 11$  Hz, 1H), 1.50 (d,  $J = 10$  Hz, 1H).

**Synthesis of (5.18):** A 100 mL round-bottom flask was charged with norbornene **5.16** (1.2 g, 3.7 mmol), protected cysteine **5.17** (1 g, 3.7 mmol) and methylene chloride (37 mL). The reaction was stirred for 2 hours at room temperature. LC-MS confirmed the identity of the product.  $^1\text{H}$  NMR (300 MHz,  $\text{CDCl}_3$ )  $\delta$  7.97 (d,  $J = 9$  Hz, 1H), 7.54 (t,  $J = 8.5$  Hz, 1H), 7.43 – 7.40 (m, 2H), 6.28 (s, 2H), 4.80 – 4.76 (m, 1H), 4.27 – 4.13 (m, 4H), 3.72 (s, 3H), 3.29 (s, 2H), 2.96 – 2.87 (m, 2H), 2.72 (s, 2H), 1.77 (d,  $J = 11$  Hz, 1H), 1.51 (d,  $J = 11.5$  Hz, 1H). HR-MS (FAB+) Calculated for  $\text{C}_{19}\text{H}_{28}\text{O}_9\text{N}_3\text{S}$ : 474.1536; found: 474.1559.

#### **General Procedure for Ring-Opening Metathesis Polymerization (ROMP):**

To an oven-dried, 20 mL vial was added a stir bar, monomer **5.1** (34.3 mg, 0.0375 mmol), monomer **5.2** (61.3 mg) and monomer **5.10** (28.3 mg, 0.05 mmol). Dry methylene chloride (3 mL) and methanol (1 mL) were added. A solution of 1.8 mg bispyridine catalyst in methylene chloride (1 mL) was added and stirred for 30 minutes at room temperature. The reaction was quenched with 1 mL of 3M ethyl

vinyl ether and stirred for an additional 1 hour. If ruthenium removal procedures were to be conducted, they would begin here (see below). The reaction mixture was then precipitated into 40 mL of diethyl ether and centrifuged. A solution of 95% trifluoroacetic acid: 2.5% water: 2.5% triisopropylsilane was added for deprotection of the polymer and stirred for 4 hours. This solution was then precipitated into 40 mL of diethyl ether and centrifuged 3 times. A 10% solution of the deprotected polymer in water (with or without DTT) was made and stored for crosslinking purposes.

**General Procedure for Ruthenium Removal:** A standard polymerization was followed and after quenching for 1 hour, the reaction mixture was split into vials each containing 1 gram of catalyst. A varying (50-1000) equivalent of THMP or TBP in isopropanol was added along with 2 times the equivalents of triethylamine. The reaction was allowed to stir overnight either at room temperature or 70 °C. After 24 hours, the reaction was precipitated into diethyl ether and then followed the standard deprotection protocols (see above). The final polymer samples were made into 10% solutions in water and 4 mg, 6 mg and 8 mg samples were subjected to ICP-MS.

## REFERENCES AND NOTES

- (1) (a) Grubbs, R. H. *Handbook of Metathesis*; Wiley-VCH: Weinheim, Germany, **2003** and references cited therein. (b) Ivin, K. J.; Mol, J. C. *Olefin Metathesis and Metathesis Polymerization*; Academic Press: San Diego, CA. **1997** and references cited therein. (c) Noels, A. F.; Demonceau, A. *J. Phys. Org. Chem.* **1998**, *11*, 602–609. (d) Grubbs, R. H. *Tetrahedron*, **2004**, *60*, 7117–7140. (e) Grubbs, R. H. *Angew. Chem. Int. Ed.* **2006**, *45*, 3760–3765. (f) Schrock, R. R. *Angew. Chem. Int. Ed.* **2006**, *45*, 3748–3759.
- (2) (a) Rybak, A.; Fokou, P. A.; Meier, M. A. R. *Eur. J. Lipid Sci. Tech.* **2008**, *110*, 797–804. (b) Elias, X.; Pleixats, R.; Man, M. W. C. *Adv. Synth. Cat.* **2007**, *349*, 1701–1713. (c) Bielawski, C. W.; Grubbs, R. H. *Prog. Polym. Sci.* **2007**, *32*, 1–29. (d) Frenzel, U.; Nuyken, O. *J. Polym. Sci., Part A: Polym. Chem.* **2002**, *40*, 2895–2916.
- (3) (a) Maynard, H. D.; Okada, S. Y.; Grubbs, R. H. *Macromolecules* **2000**, *33*, 6239–6248. (b) Maynard, H. D.; Okada, S. Y.; Grubbs, R. H. *J. Am. Chem. Soc.* **2001**, *123*, 1275–1279. (c) Blackwell, H. E.; Grubbs, R. H. *Angew. Chem. Int. Ed.* **1998**, *37*, 3281–3284. (d) Conrad, R. M.; Grubbs, R. H. *Angew. Chem. Int. Ed.* **2009**, *48*, 8328–8330.
- (4) Sanford, M. S.; Love, J. A.; Grubbs, R. H. *Organometallics* **2001**, *20*, 5314–5318.
- (5) (a) Ruoslahti, E.; Pierschbacher, M. D. *Science* **1987**, *238*, 491–497. (b) Ruoslahti, E. *Annu. Rev. Cell Dev. Bio.* **1996**, *12*, 697–715.

- (c) Pierschbacher, M. D.; Polarek, J. W.; Craig, W. S.; Tschopp, J. F.; Sipes, N. J.; Harper, J. R. *J. Cell Biochem.* **1994**, *56*, 150–154.
- (d) Akiyama, S. K.; Olden, K.; Yamada, K. M. *Cancer Metastasis Rev.* **1995**, *14*, 173–189. (e) Schottelius, M.; Laufer, B.; Kessler, H.; Wester, H. J. *Acc. Chem. Res.* **2009**, *42*, 969–980.
- (6) Knop, K.; Hoogenboom, R.; Fischer, D.; Schubert, U. S. *Angew. Chem. Int. Ed.* **2010**, *49*, 6288–6308.
- (7) (a) Zaidi, K. *Pharmacopeial Forum* **2008**, *34*, 1345–1348. (b) Criteria given in the EMEA Guideline on the Specification Limits for Residues of Metal Catalysts, available at: [www.emea.europa.eu/pdfs/human/swp/444600.pdf](http://www.emea.europa.eu/pdfs/human/swp/444600.pdf)
- (8) (a) Maynard, H. D.; Grubbs, R. H. *Tetrahedron Lett.* **1999**, *40*, 4137–4140. (b) Ellis, J. W.; Harrison, K. N.; Hoye, P. A. T.; Orpen, A. G.; Pringle, P. G.; Smith, M. B. *Inorg. Chem.* **1992**, *31*, 3026–3033.
- (c) Lambeth, R. H.; Pederson, S. J.; Baranoski, M.; Rawlett, A. M. *J. Polym. Sci., Part A: Polym. Chem.* **2010**, *48*, 5752–5757.
- (9) (a) Knight, D. W.; Morgan, I. R.; Proctor, A. J. *Tetrahedron Lett.* **2010**, *51*, 638–640. (b) Paquette, L. A.; Schloss, J. D.; Efremov, I.; Fabris, F.; Gallou, F.; Mendez–Andino, J.; Yang, J. *Org. Lett.* **2000**, *2*, 1259–1261.
- (10) Michrowska, A.; Gulajski, L.; Kaczmarska, Z.; Mennecke, K.; Kirschning, A.; Grela, K. *Green Chem.* **2006**, *8*, 685–688.

- (11) (a) Mitchell, A. R. *Biopolymers* **2008**, *90*, 175–184. (b) Amblard, M.; Fehrentz, J. A.; Martinez, J.; Subra, G. *Mol. Biotech.* **2006**, *33*, 239–254. (c) Merrifield, R. B. *J. Am. Chem. Soc.* **1963**, *85*, 2149–2154.
- (12) Hoyle, C. E.; Lowe, A. B.; Bowman, C. N. *Chem. Soc. Rev.* **2010**, *39*, 1355–1387.
- (13) Muttenthaler, M.; Ramos, Y. G.; Feytens, D.; de Araujo, A. D.; Alewood, P. F. *Biopolymers* **2010**, *94*, 423–432.

*Appendix A*

## BIMETALLIC RUTHENIUM FISCHER-CARBENE COMPLEXES



## INTRODUCTION

The olefin metathesis reaction has gained considerable momentum as a synthetic tool in the past decade.<sup>1,2</sup> Moreover, the advent of the well-defined ruthenium olefin metathesis catalysts **A.1** and **A.2** has allowed for an unprecedented ease of use due to their high activity, air stability and functional group tolerance (figure A.1).<sup>3</sup>

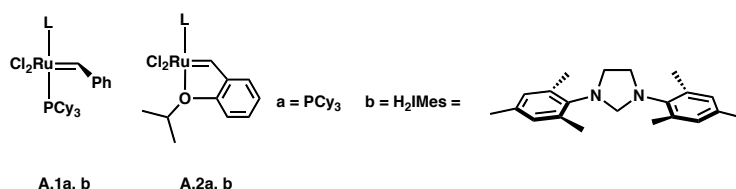
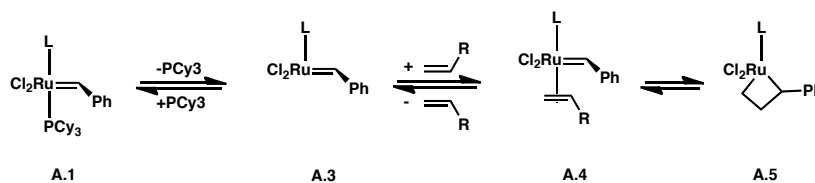


**Figure A.1. Commercially Available Ruthenium Catalysts.**

Although the general features of the mechanism of ruthenium-mediated olefin metathesis are well understood, reactive intermediates along the pathway to metallacyclobutane formation and breakdown have not been isolated.<sup>4</sup> Model complexes however, have been isolated and characterized.<sup>5</sup> In order to design and construct catalysts with greater stability and efficiency, a better understanding of the exact structure of the intermediates, as well as their modes of decomposition, must be obtained.

Early mechanistic analysis of **A.1a** and **A.1b** revealed a dissociative mechanism, wherein initiation proceeds with loss of a phosphine ligand.<sup>4b</sup> The exposed 14-electron species **A.3** is thus the active species that enters into the catalytic cycle (scheme A.1).

**Scheme A.1. Initial Steps of Olefin Metathesis Mechanism.**



Based on this paradigm, elegant studies from the Piers lab have yielded the phosphonium alkylidene species **A.6**, which has shown remarkable initiation in olefin metathesis (figure A.2).<sup>6</sup> Piers was able to prepare and stabilize the 14-electron **A.6** via steric encumbrance by the bulky phosphonium. Phosphonium alkylidene **A.6** was then used to generate and characterize the related ruthenacyclobutane.<sup>6b</sup> Although **A.6** is a direct analogue of intermediate **A.3**, 14-electron benzylidene species with either phosphine or *N*-heterocyclic carbene (NHC) L-type ligands such as **A.3b** have not yet been realized.

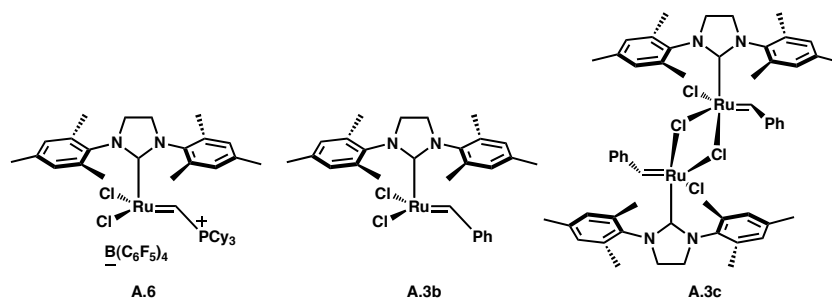
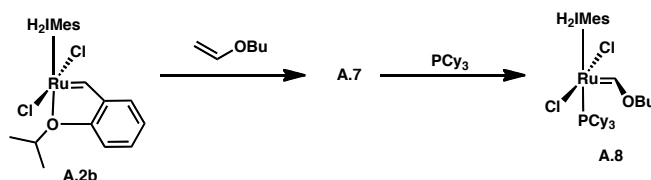


**Figure A.2. Phosphonium Alkylidene and Potential Intermediates.**

Several results have led us to believe that the short-lived intermediate **A.3b** could easily dimerize to form **A.3c**, where the chloride ligands bridge the two metal centers and yield a stabilized 16-electron species. In recent work from our lab, vinyl ethers were used to study the initiation behavior of phosphine-free systems.<sup>7</sup> The addition of vinyl ethers, after one turnover of productive metathesis, should yield a metathesis-inactive Fischer carbene species. Hejl found that addition of *n*-butyl vinyl ether to **A.2b** gave an unknown complex, **A.7** (scheme A.2). The characteristic green color of **A.2b** disappeared upon addition of excess vinyl ether to give a yellow compound in solution, with two new benzylidene resonances in the proton NMR between 13 and 14 ppm. These resonances were consistent with Fischer carbene formation, and a dimeric ruthenium species was

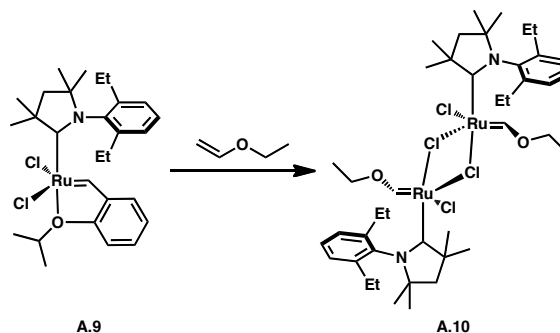
invoked, however, definite structures were not obtained. Addition of excess phosphine to **A.7** generated the known Fischer carbene complex, **A.8**.

**Scheme A.2. Initiation Study with Butyl Vinyl Ether.**



Further evidence toward the existence of bimetallic ruthenium species was obtained in studies of catalysts bearing cyclic(alkyl)(amino)carbenes (CAACs).<sup>8</sup> Anderson was able to characterize **A.10** by single crystal X-ray spectroscopy providing more evidence for the intermediacy of this type.

**Scheme A.3. Addition of Ethyl Vinyl Ether to A.9.**



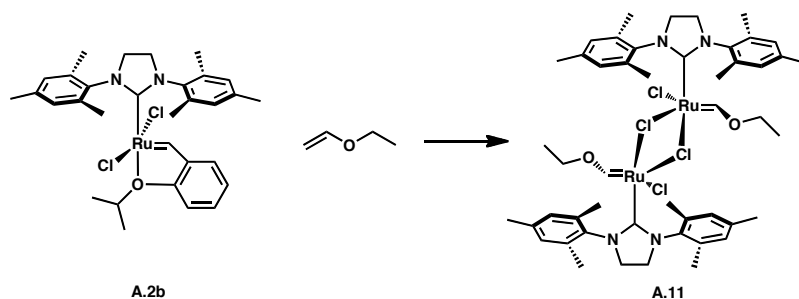
Therefore it was reasonable to assume that **A.7** had an analogous bimetallic structure. The initial goal of this project was to isolate and characterize **A.7** in the solid state in order to gain structural information on this type of intermediate. We believe that **A.7** serves as the Fischer carbene structural analog for **A.3c**, which could potentially be generated in the catalytic cycle of olefin metathesis. We hoped to then gain insight from studies of **A.7** and systems similar to **A.7** that could be applied toward the synthesis and characterization of **A.3c**. In a phosphine-free system, complex **A.3c** could potentially

enter into the catalytic cycle of olefin metathesis directly, thus bypassing the initial dissociation step.

## CRYSTAL STRUCTURE OF BIMETALLIC RUTHENIUM SPECIES

Initial attempts to grow single crystals with common solvent mixtures failed to give samples of adequate quality. However, slow vapor diffusion of isooctane into a benzene solution of **A.11** yielded orange crystals suitable for X-ray characterization (scheme A.4). Figure A.3 shows the crystal structure.

**Scheme A.4. Addition of Ethyl Vinyl Ether to A.2b.**



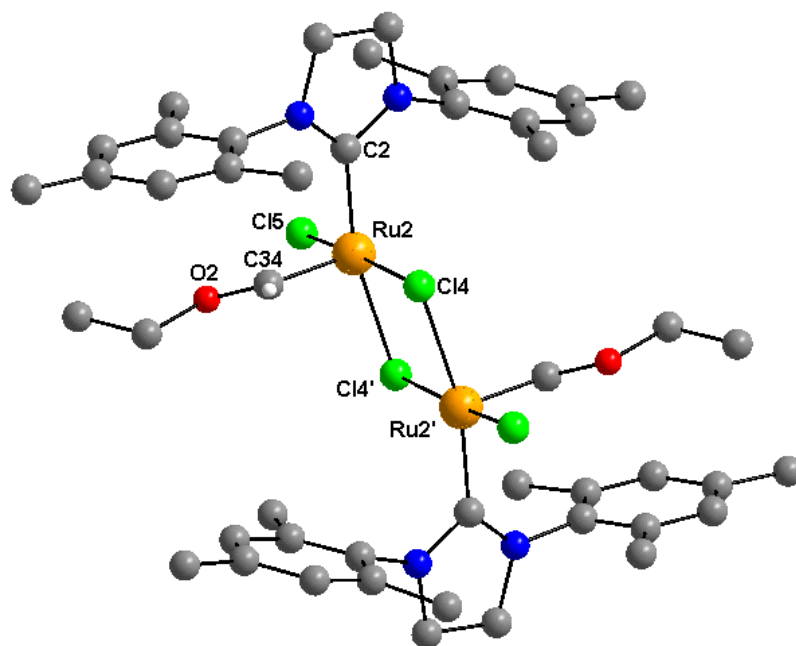


Figure A.3. Crystal Structure of Bimetallic Species A.11.

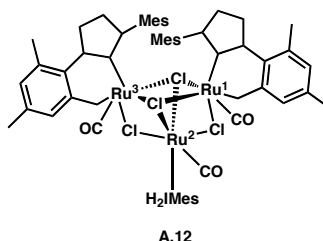
Table A.1 gives relevant data gathered from the crystal structure.

Table A.1. Selected Bond Lengths [Å] and Angles [°] for A.11

Selected Distances (Å)	Selected Angles (°)
Ru(2)-Cl(4) = 2.4212	Cl(5)-Ru(2)-Cl(4) = 171.983
Ru(2)-Cl(4)' = 2.4561	Cl(5)-Ru(2)-Cl(4)' = 89.56
Ru(2)-Cl(5) = 2.3455	Cl(4)-Ru(2)-Cl(4)' = 83.155
Ru(2)-Ru(2)' = 3.6486	Cl(5)-Ru(2)-C(34) = 95.708
Ru(2)-C(34) = 1.8618	
Ru(2)-C(2) = 2.0077	

We were surprised to note that although the bulk of the material was the bimetallic ruthenium species **A.11**, there was a small amount of a secondary complex

formed. X-ray analysis of this minor material showed the trimetallic species **A.12** shown in figure A.4.



**Figure A.4. Trimetallic Ruthenium Complex.**

Despite some amount of disorder in the crystal structure, the structure was of sufficient quality to establish connectivity. Two of the ruthenium atoms have undergone C–H activation of the NHC ligand. C–H activation of the available methyl group in ruthenium catalysts bearing NHC ligands has been well-established as a mode of decomposition.<sup>9</sup> The metal-carbonyls are most likely products of ethyl vinyl ether decomposition. Figure A.5 shows the crystal structure obtained, with intact mesityl groups omitted for clarity.

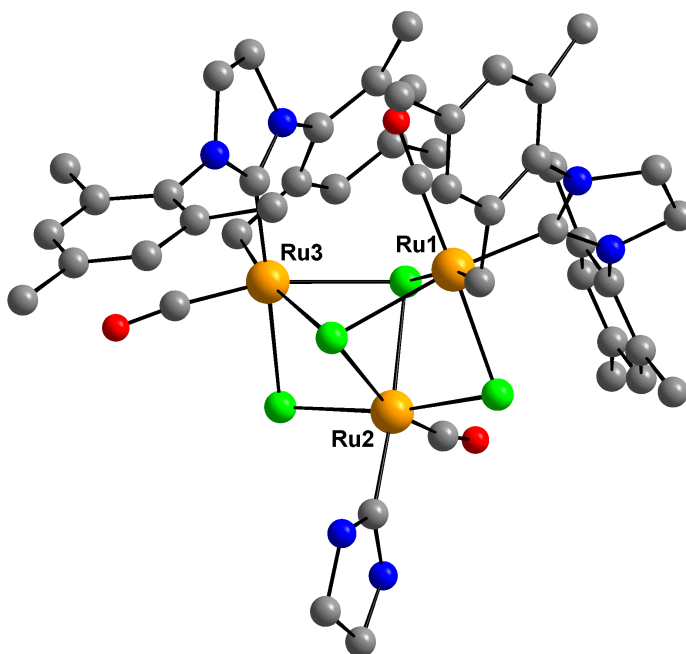
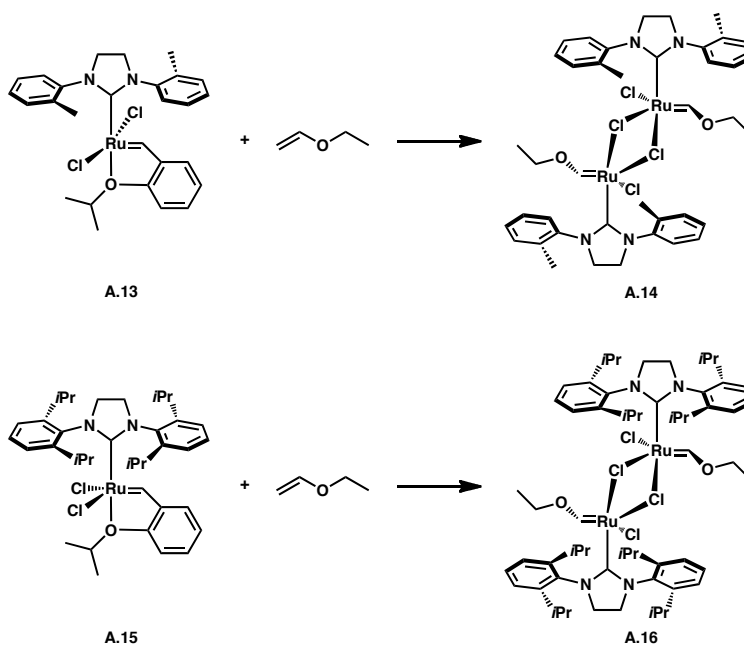


**Figure A.5.** Crystal Structure of Trimetallic Species **A.12**.

It is possible that **A.12** arises from attack by a 14-electron ruthenium species onto a partial decomposition product of bridged bimetallic species **A.11**. In the crystal structure of **A.12**, Ru(1) and Ru(3) are shown to be equivalent, each has three chloride interactions. Ru(2) is inequivalent, and appears to be in bonding distance with four chlorides. We are as yet unsure of the nature of this compound, though the preliminary X-ray data is quite intriguing.

Initial attempts were also made to examine the potential of catalysts **A.13** and **A.15** to form bimetallic Fischer carbene species (scheme A.5). However, all attempts to grow X-ray quality crystals have failed to date. Further investigation of concentration and solvent system for both vapor and layer diffusion need to be conducted in these systems.

Scheme A.5. Attempts at Bimetallic Crystallization of A.13 and A.15.



## CONCLUSIONS

A bimetallic ruthenium Fischer carbene species that serves as a structural model for intermediates relevant to olefin metathesis was synthesized and characterized in the solid state. An unexpected trimeric ruthenium species was also isolated and characterized via X-ray crystallography. The presented data is preliminary, and full characterization of both **A.11** and **A.12** is ongoing.



## EXPERIMENTAL METHODS

### Materials and Methods

NMR spectra were measured on an Oxford 300 MHz spectrometer running Varian VNMR software unless otherwise noted. Air-sensitive metal-containing complexes were handled in a dry box under nitrogen or via standard Schlenck techniques under argon. Ruthenium starting materials were provided by Materia, Inc. All other reagents were purchased from Aldrich and used without prior purification.

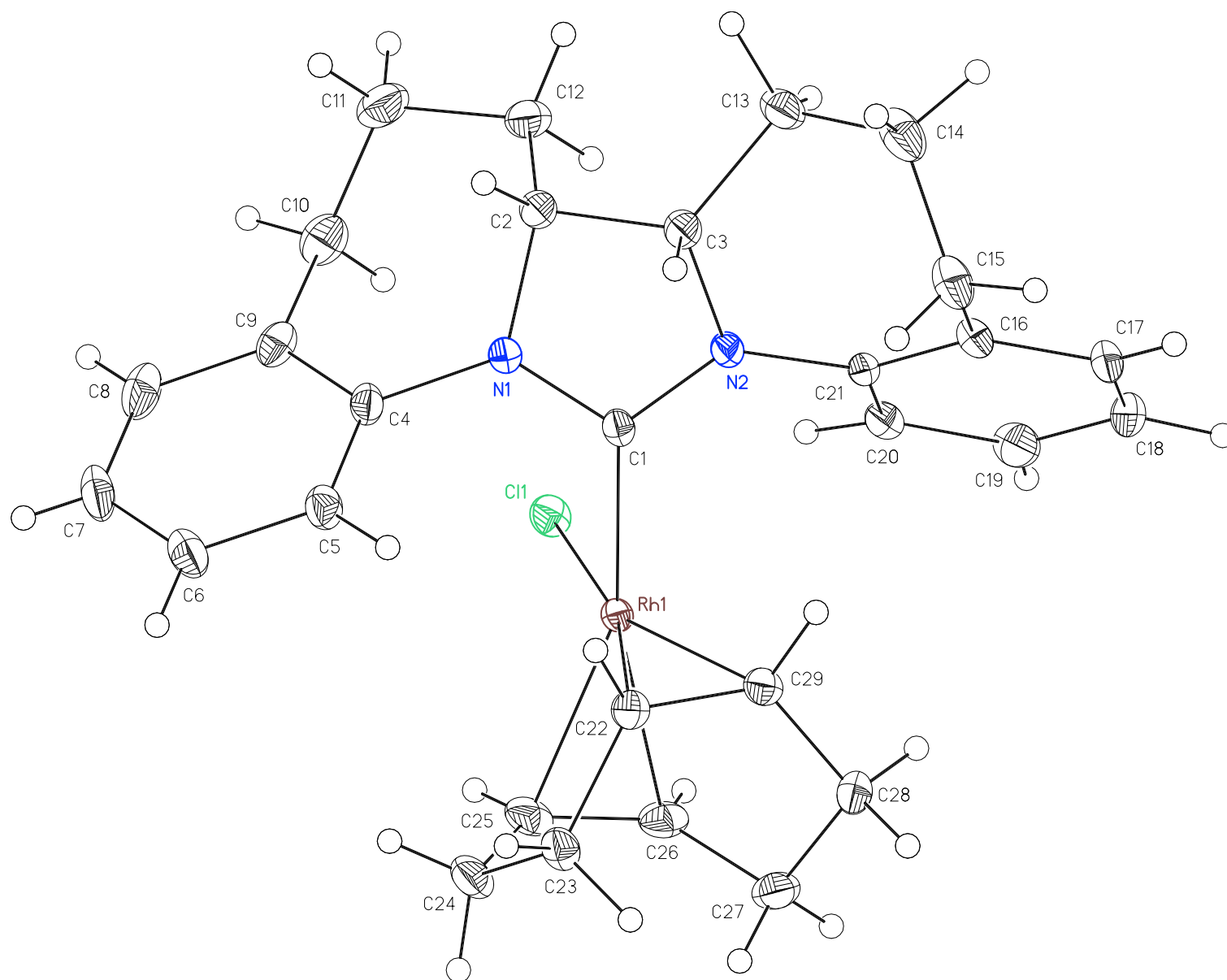
**General Procedure for Synthesis of Bimetallic Species:** An oven-dried 4-dram vial was charged with ruthenium complex **A.2b** and taken into a glove box. Dry benzene was added, followed by ethyl vinyl ether (30 equiv.). After 30 minutes, a color change was noted from green to orange, and the small vial was placed inside a larger, 20-dram vial filled with isooctane. Crystals were grown via vapor diffusion. The crystals were moderately air-stable.

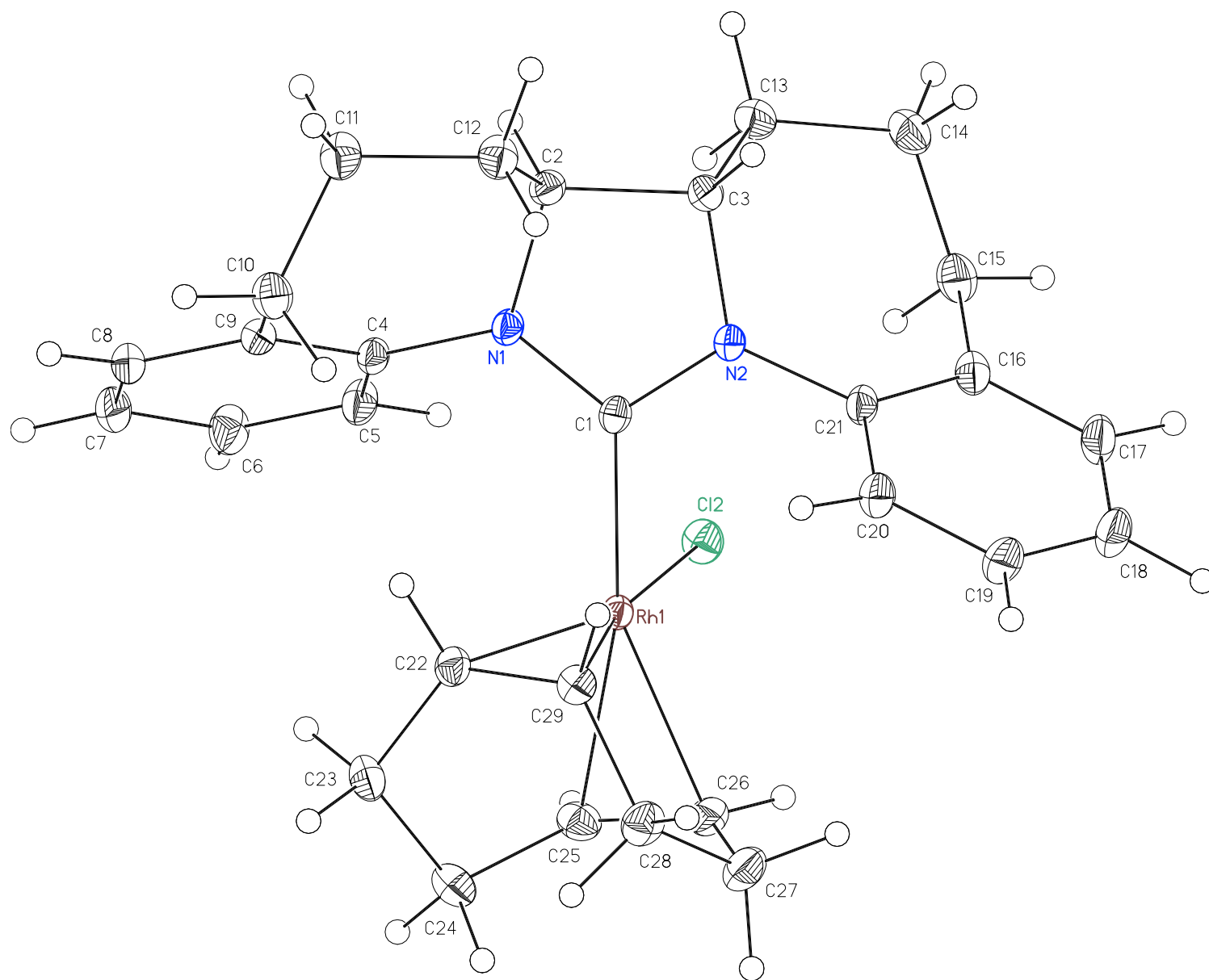
**X-ray Crystallography Procedures:** X-ray quality crystals were grown as indicated. The crystals were mounted on a glass fiber with Paratone-N oil. X-ray diffraction studies were carried out in the Beckman Institute Crystallographic Facility on a Bruker Smart 1000 CCD diffractometer. Structures were determined using direct methods with standard Fourier techniques employing the Bruker AXS software package. In some cases, Patterson maps were used in place of the direct methods procedure.

## REFERENCES AND NOTES

- (1) (a) Grubbs, R. H. *Handbook of Metathesis*; Wiley-VCH: Weinheim, Germany, **2003** and references cited therein. (b) Ivin, K. J.; Mol, J. C. *Olefin Metathesis and Metathesis Polymerization*; Academic Press: San Diego, CA. **1997** and references cited therein. (c) Noels, A. F.; Demonceau, A. *J. Phys. Org. Chem.* **1998**, *11*, 602–609. (d) Grubbs, R. H. *Tetrahedron*, **2004**, *60*, 7117–7140. (e) Grubbs, R. H. *Angew. Chem. Int. Ed.* **2006**, *45*, 3760–3765. (f) Schrock, R. R. *Angew. Chem. Int. Ed.* **2006**, *45*, 3748–3759.
- (2) (a) Stewart, I. C.; Ung, T.; Pletnov, A. A.; Berlin, J. M.; Grubbs, R. H.; Schrodi, Y. *Org. Lett.* **2007**, *9*, 1589–1592. (b) Chung, C. K.; Grubbs, R. H. *Org. Lett.* **2008**, *10*, 2693–2696. (c) Seiders, T. J.; Ward, D. W.; Grubbs, R. H. *Org. Lett.* **2001**, *3*, 3225–3228. (d) Bielawski, C. W.; Benitez, D.; Grubbs, R. H. *Science*, **2002**, *297*, 2041–2043. (e) Endo, K.; Grubbs, R. H. *J. Am. Chem. Soc.* **2011**, *133*, 8525–8527. (f) Keitz, B. K.; Endo, K.; Herbert, M. B.; Grubbs, R. H. *J. Am. Chem. Soc.* **2011**, *133*, 9686–9688.
- (3) (a) Nguyen, S. T.; Johnson, L. K.; Grubbs, R. H. *J. Am. Chem. Soc.* **1992**, *114*, 3974–3975. (b) Schwab, P.; France, M. B.; Ziller, J. W.; Grubbs, R. H. *Angew. Chem. Int. Ed.* **1995**, *34*, 2039–2040. (c) Scholl, M.; Trnka, T. M.; Morgan, J. P.; Grubbs, R. H. *Tet. Lett.* **1999**, *40*, 2247–2250. (d) Scholl, M.; Ding, S.; Lee, C. W.; Grubbs, R. H. *Org. Lett.* **1999**, *1*, 953–956. (e) Garber, S. B.; Kingsbury, J. S.; Gray, B. L.; Hoveyda, A. H. *J. Am. Chem. Soc.* **2000**, *122*, 8168–8179.
- (4) (a) Herisson, J.-L.; Chauvin, Y. *Makromol. Chem.* **1971**, *141*, 161–176. (b) Dias, E. L.; Nguyen, S. T.; Grubbs, R. H. *J. Am. Chem. Soc.* **1997**, *119*, 3887–3897.

- (c) Sanford, M. S.; Love, J. A.; Grubbs, R. H. *Organometallics*, **2001**, *20*, 5314–5318.
- (5) (a) Anderson, D. A.; Hickstein, D. D.; O’Leary, D. J.; Grubbs, R. H. *J. Am. Chem. Soc.* **2006**, *128*, 8386–8387.
- (6) (a) Romero, P. E.; Piers, W. E. *J. Am. Chem. Soc.* **2007**, *129*, 1698–1704.  
(b) Romero, P. E.; Pier, W. E. *J. Am. Chem. Soc.* **2005**, *127*, 5032–5033. (c) van der Eide, E. F.; Romero, P. E.; Piers, W. E. *J. Am. Chem. Soc.* **2008**, *130*, 4485–4491. (d) Leitao, E. M.; van der Eide, E. F.; Romero, P. E.; Piers, W. E.; McDonald, R. *J. Am. Chem. Soc.* **2010**, *132*, 2784–2794. (e) Rowley, C. N.; van der Eide, E. F.; Piers, W. E.; Woo, T. K. *Organometallics*, **2008**, *27*, 6043–6045.
- (7) Hejl, A., California Institute of Technology, 2007.
- (8) Anderson, D. R., California Institute of Technology, 2007.
- (9) Hong, S. H.; Chlenov, A.; Day, M. W.; Grubbs, R. H. *Angew. Chem. Int. Ed.* **2007**, *46*, 5148–5151.





*Appendix B*

## CRYSTALLOGRAPHIC DATA

CALIFORNIA INSTITUTE OF TECHNOLOGY  
BECKMAN INSTITUTE  
X-RAY CRYSTALLOGRAPHY LABORATORY



Date 24 July 2008

**Crystal Structure Analysis of:**

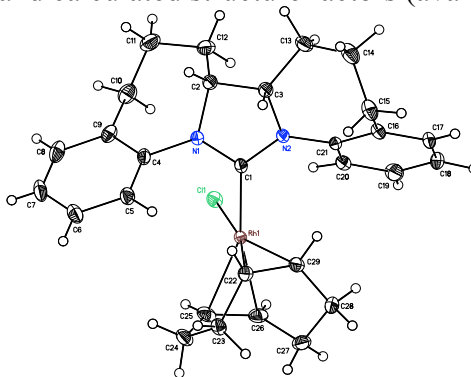
**ICS05**

(shown below)

<b>For</b>	Investigator: Ian Stewart	ext. 6885
	Advisor: R. H. Grubbs	ext. 6003
	Account Number:	RHG.METAL-1-NIH.METAL2
<b>By</b>	Michael W. Day	116 Beckman ext. 2734 e-mail: mikeday@caltech.edu

Contents

Table 1. Crystal data
Figures Minimum overlap
Table 2. Atomic Coordinates
Table 3. Selected bond distances and angles
Table 4. Full bond distances and angles
Table 5. Anisotropic displacement parameters
Table 6. Hydrogen atomic coordinates
Table 7. Observed and calculated structure factors (available upon request)



ICS05

**Note:** The crystallographic data have been deposited in the Cambridge Database (CCDC) and has been placed on hold pending further instructions from me. The deposition number is 696088. Ideally the CCDC would like the publication to contain a footnote of the type: "Crystallographic data have been deposited at the CCDC, 12 Union Road, Cambridge CB2 1EZ, UK and copies can be obtained on request, free of charge, by quoting the publication citation and the deposition number 696088."



**Table 1. Crystal data and structure refinement for ICS05 (CCDC 696088).**

Empirical formula	C <sub>29</sub> H <sub>34</sub> N <sub>2</sub> ClRh
Formula weight	548.94
Crystallization Solvent	Toluene/hexane
Crystal Habit	Fragment
Crystal size	0.13 x 0.11 x 0.11 mm <sup>3</sup>
Crystal color	Light yellow



### Data Collection

Type of diffractometer	Bruker KAPPA APEX II
Wavelength	0.71073 Å MoK $\alpha$
Data Collection Temperature	100(2) K
$\theta$ range for 9945 reflections used in lattice determination	2.39 to 37.76°
Unit cell dimensions	a = 17.2031(7) Å b = 11.6106(5) Å c = 12.3438(5) Å $\beta$ = 98.397(2)°
Volume	2439.10(18) Å <sup>3</sup>
Z	4
Crystal system	Monoclinic
Space group	Cc
Density (calculated)	1.495 Mg/m <sup>3</sup>
F(000)	1136
Data collection program	Bruker APEX2 v2.1-0
$\theta$ range for data collection	2.12 to 37.83°
Completeness to $\theta$ = 37.83°	92.2 %
Index ranges	-28 ≤ h ≤ 23, -19 ≤ k ≤ 19, -21 ≤ l ≤ 20
Data collection scan type	scans; 11 settings
Data reduction program	Bruker SAINT-Plus v7.34A
Reflections collected	27779
Independent reflections	8931 [R <sub>int</sub> = 0.0420]
Absorption coefficient	0.830 mm <sup>-1</sup>
Absorption correction	None
Max. and min. transmission	0.9142 and 0.8998

**Table 1 (cont.)****Structure solution and Refinement**

Structure solution program	SHELXS-97 (Sheldrick, 2008)
Primary solution method	Direct methods
Secondary solution method	Difference Fourier map
Hydrogen placement	Difference Fourier map
Structure refinement program	SHELXL-97 (Sheldrick, 2008)
Refinement method	Full matrix least-squares on $F^2$
Data / restraints / parameters	8931 / 2 / 434
Treatment of hydrogen atoms	Unrestrained
Goodness-of-fit on $F^2$	1.618
Final R indices [ $I > 2\sigma(I)$ , 7983 reflections]	$R1 = 0.0323$ , $wR2 = 0.0499$
R indices (all data)	$R1 = 0.0391$ , $wR2 = 0.0504$
Type of weighting scheme used	Sigma
Weighting scheme used	$w = 1/\sigma^2(F_o^2)$
Max shift/error	0.002
Average shift/error	0.000
Absolute structure determination	Anomalous differences
Absolute structure parameter	-0.013(15)
Largest diff. peak and hole	2.588 and -1.995 e.Å <sup>-3</sup>

**Special Refinement Details**

Crystals were mounted on a glass fiber using Paratone oil then placed on the diffractometer under a nitrogen stream at 100K.

Refinement of  $F^2$  against ALL reflections. The weighted R-factor ( $wR$ ) and goodness of fit ( $S$ ) are based on  $F^2$ , conventional R-factors ( $R$ ) are based on  $F$ , with  $F$  set to zero for negative  $F^2$ . The threshold expression of  $F^2 > 2\sigma(F^2)$  is used only for calculating R-factors(gt) etc. and is not relevant to the choice of reflections for refinement. R-factors based on  $F^2$  are statistically about twice as large as those based on  $F$ , and R-factors based on ALL data will be even larger.

All esds (except the esd in the dihedral angle between two l.s. planes) are estimated using the full covariance matrix. The cell esds are taken into account individually in the estimation of esds in distances, angles and torsion angles; correlations between esds in cell parameters are only used when they are defined by crystal symmetry. An approximate (isotropic) treatment of cell esds is used for estimating esds involving l.s. planes.